**Circuits and Systems**
Mekelweg 4,
2628 CD Delft
The Netherlands
http://ens.ewi.tudelft.nl/

**CAS-2015-4328930**

# M.Sc. Thesis

# Sensor Selection and Bit Allocation in WSNs with Realistic Digital Communication Channels

**Hongrun Zhang**

## Abstract

For energy management in wireless sensor networks, only the sensors with most informative measurements are activated to operate. How to select sensors that make good tradeoff between performance and energy consumption is what many researchers are focusing on. Existing solutions assume analog data model, i.e., the data from sensors collected by a center node, called fusion center, are analog measurements. In practical application, due to limitations of energy of sensors and bandwidth of wireless channel, original measurements are usually compressed before being transmitted to the fusion center. In addition, transmitted signals are usually distorted by wireless channel effects, therefore it is possible that the received data are corrupted with errors.

In this thesis, we consider two compressive techniques: one-bit quantization and multi-bit quantization. In one-bit quantization, an indicator message is generated in a sensor according to whether the original measurement is larger than a threshold or not. In multi-bit quantization, the original measurements are quantized to multiple bits and only the most significant bits are reserved. The indicators or the most significant bits are then transmitted through realistic wireless channel to the fusion center for it to process. By these ways, the transmitted signals are digital, and they may flip into opposite values by the effects of wireless channels. For one-bit quantization case, we develop a sensor selection approach, based on convex programming. For multi-bit quantization, we extend the sensor selection to bit allocation and propose a novel algorithm to determine the number of bits to transmit for each sensor, which is also based on convex programming. In both cases we consider the effects of wireless channels, which are characterized as bit error rate. Particularly, for the multi-bit quantization, numerical results show that the bit allocation can further reduce the cost that we defined compared with existing solutions where transmitted data are assumed to be analog.

# Sensor Selection and Bit Allocation in WSNs with Realistic Digital Communication Channels

## Quantization And Bit Errors

---

Thesis

submitted in partial fulfillment of the
requirements for the degree of

Master of Science

in

Telecommunication

by

Hongrun Zhang
born in Shantou, China

This work was performed in:

Circuits and Systems Group
Department of Microelectronics & Computer Engineering
Faculty of Electrical Engineering, Mathematics and Computer Science
Delft University of Technology

**Delft University of Technology**

Delft University of Technology
Department of
Microelectronics & Computer Engineering

The undersigned hereby certify that they have read and recommend to the Faculty of Electrical Engineering, Mathematics and Computer Science for acceptance a thesis entitled **"Sensor Selection and Bit Allocation in WSNs with Realistic Digital Communication Channels"** by **Hongrun Zhang** in partial fulfillment of the requirements for the degree of **Master of Science**.

Dated: 26-11-2015

Chairman:

prof.dr.ir. Geert Leus

Advisors:

prof.dr.ir. Geert Leus

dr. Andrea Simonetto

Committee Members:

dr.ir. Richard Heusdens

dr.ir. Jac Romme

# Abstract

For energy management in wireless sensor networks, only the sensors with most informative measurements are activated to operate. How to select sensors that make good tradeoff between performance and energy consumption is what many researchers are focusing on. Existing solutions assume analog data model, i.e., the data from sensors collected by a center node, called fusion center, are analog measurements. In practical application, due to limitations of energy of sensors and bandwidth of wireless channel, original measurements are usually compressed before being transmitted to the fusion center. In addition, transmitted signals are usually distorted by wireless channel effects, therefore it is possible that the received data are corrupted with errors.

In this thesis, we consider two compressive techniques: one-bit quantization and multi-bit quantization. In one-bit quantization, an indicator message is generated in a sensor according to whether the original measurement is larger than a threshold or not. In multi-bit quantization, the original measurements are quantized to multiple bits and only the most significant bits are reserved. The indicators or the most significant bits are then transmitted through realistic wireless channel to the fusion center for it to process. By these ways, the transmitted signals are digital, and they may flip into opposite values by the effects of wireless channels. For one-bit quantization case, we develop a sensor selection approach, based on convex programming. For multi-bit quantization, we extend the sensor selection to bit allocation and propose a novel algorithm to determine the number of bits to transmit for each sensor, which is also based on convex programming. In both cases we consider the effects of wireless channels, which are characterized as bit error rate. Particularly, for the multi-bit quantization, numerical results show that the bit allocation can further reduce the cost that we defined compared with existing solutions where transmitted data are assumed to be analog.

# Acknowledgments

Great gratitude to prof.dr.ir. Geert Leus and dr. Andrea Simonetto for their precious help, advices and time for my thesis. Thank also the committee members, dr.ir. Richard Heusdens and dr.ir. Jac Romme, and the nice people in Circuits and System group. To my parents.

Hongrun Zhang
Delft, The Netherlands
26-11-2015

# Contents

# List of Figures

# List of Tables

# 1 Introduction

Wireless sensor networks (WSNs) are of great importance in nowadays industrial applications, like object localization, environment monitoring, mobile target tracking, to name a few. One crucially important issue in WSNs is energy management [14, 38]. Since in many applications, sensors are usually deployed in hazardous or forbidden areas, it is usually not an option to maintain the sensors during their operation period. At the same time, sensors are usually self-powered by the batteries embedded in them, and the amount of power in the batteries is limited. Therefore, many researches have designed efficient energy management schemes for a WSN to prolong its longevity. One popular scheme is sensor selection, i.e., only the most informative sensors are activated to operate.

The main concept of sensor selection problems is to make a tradeoff between the performance and the number of activated sensors − basically, the more sensors are activated the higher the performance that will be achieved, but the energy consumption will be higher at the same time, and visa versa. Based on this idea, two patterns of sensor selection were proposed. The first one optimizes the performance and restricts the number of selected sensors under a certain value, while the second one minimizes the number of selected sensors and constrains the performance to a predescribed level. These two patterns have no fundamental differences, and the choice between them depends on practical applications.

To develop sensor selection schemes, one needs to specify the performance metric, which depends on the specific problem. For example, if the function of a WSN is for detection, the performance metric can be the detection or false alarm rate [7], or if it is for estimation, the mean square error (MSE) is often the performance metric. In this thesis, we focus on the estimation aspect. Except for the MSE which is the trace of the error covariance matrix, other metrics are also adopted, like the maximum eigenvalue of the error covariance matrix, the determinant of the error covariance matrix, or the largest diagonal element of the error covariance matrix. All these metrics are based on the error covariance matrix and have their geometrical meanings in error control, which we will briefly explain in the following. However, for many cases the error covariance matrices have no closed-form, like for some non-linear models for example. Therefore many papers focus on finding proxy metrics that do not depend on the error covariance matrix but are related to it. The authors in [9] propose to replace the error covariance matrix by the Cramer-Rao lower bound (CRLB). By this, the metrics become the trace, the minimum eigenvalue and the determinant of the CRLB, etc. Particularly, when prior knowledge about the unknown parameter is available, the Bayesian CRLB is a better choice, and this is what we adopt to develop our approaches in this thesis. For the minimum eigenvalue and trace of the CRLB, we can also find the corresponding geometrical meaning in error control. Other performance metrics are also proposed for sensor selection, like frame potential [30], mutual information [15, 20], etc.

Sensor selection is basically a combinational problem, i.e., the best sub-set of sensors are selected that meet the requirements. A simple and naive way to solve sensor selection problems is by exhaustive search: all combinations of sensors are considered and the optimal one is chosen. By this tactic we can always find the best sub-set. However, this is an intractable approach if the number of sensors is large. Alternatively, convex relaxation and greedy algorithms are adopted. Convex relaxation aims to relax the corresponding optimization problems to convex problems such that they can be solved efficiently by typical convex optimization tools. Although it is easy to implement, convex relaxation in general makes no guarantees on the distance between the solution by convex relaxation and the optimal solution by exhaustive search. In some cases this distance can be upper bounded, but usually under restrictive assumptions. Greedy algorithms are computationally more efficient approach for sensor selection. Basically, they select sensors one by one each round, in a way that the new selected one greedily maximizes a metric. If the metric for greedy selection can be proved to be normalized monotone sub-modular, then the value of the metric determined by the subset of sensors by the greedy selection can be guaranteed within a certain range to the optimal value. However, it is difficult to find such metrics that are normalized monotone sub-modular and also related to the error covariance matrix.

## 1.1 Motivation and Problem Description

Existing works on sensor selection problems assume an analog data model, i.e., the measurements used to estimate the unknown parameter are analog. This assumption is impractical, because energy and bandwidth are limited in WSN. Therefore the original measurements are usually quantized before transmitted over realistic wireless channels. In addition, the uncertainties considered in existing works only reflect the measurement noise. In practice, the data transmitted over wireless channels may be affected by channel effects and errors will be brought in the received data. If we consider only the measurement noise and select a sub-set of sensors with the most informative measurements, a sub-set of sensors with a low channel quality may be selected, such that the final estimate by the measurements of these sensors has a low quality as well.

In this thesis we consider two quantization schems: one-bit quantization and multi-bit quantization. In one-bit quantization the transmitted data from a sensor is an indicator that specifies whether the measurement of the sensor is larger than a prescribed threshold or not. In multi-bit quantization, a simple quantization scheme is introduced to quantize the bounded measurements to multiple bits.

Over imperfect wireless channels, the transmitted bits may be received and decoded incorrectly. In one-bit quantization with imperfect wireless channels, the sensor selection problem is specified as how to select the minimum number of sensors to transmit one bit information to the fusion center and to guarantee a certain level of estimation performance. In multi-bit quantization, the sensor selection problem is generalized as how to determine the number of bits of each sensor that the corresponding cost such that we defined is minimized and at the same time the performance requirement is satisfied. The work in this thesis aims at solving these two challenging combinational problems, via convex relaxation.

## 1.2 Outline and Contribution

The contributions of this thesis are highlighted here. We propose to take the effects of wireless channel into account in sensor selection problem with linear model. The effects are generalized as bit error rate. We derive the Bayesian Fisher information matrices for the one-bit quantization and multi-bit quantization, and based on the derived Bayesian Fisher information matrices we first develop a sensor selection approach for the one-bit case. Then we extend the sensor selection approach to bit allocation in multi-bit cases and propose a novel bit allocation algorithm for it.

The content of this thesis is organized as follows:

- **Chapter 2: Related Work on Sensor Selection**
  In this chapter, the related works about sensor selection are presented and discussed. Several aspects of sensor selection are investigated: data models, noise models, optimization approaches and performance metrics.

- **Chapter 3: Wireless Sensor Networks with One-Bit Quantization**
  We begin our own work in this chapter. First, the framework and data model of the WSN are presented, and the one-bit quantization scheme is introduced. Then we briefly discuss the effect of realistic wireless channel and model it as bit error rate. The likelihood function of the received data through the realistic channel at the fusion center is derived, and by exploiting it we achieve the maximum a posteriori estimator and the Bayesian Cramer-Rao lower bound(or the Bayesian Fisher information). Next, for sensor selection, the performance metrics are discussed and we adopt the minimum eigenvalue of the Bayesian Fisher information as the performance metric to determine which sub-set of sensors should transmit one-bit data to the fusion center. The approach to solve this problem is the convex relaxation method. We then investigate the possibility that the selected sensors by convex relaxation are the same as an exhaustive search would select and propose an equivalence theorem under some conditions. Finally simulation results are presented and discussed.

- **Chapter 4: Wireless sensor network with Multi-Bit Quantization**
  In this chapter, a multi-bit quantization scheme is adopted to quantize the measurements to multiple bits. We then derive the likelihood function with and without the bit errors, as well as the corresponding Fisher information matrices and the MAP estimator. In addition, the aggregated error is defined, and the Bayesian mean square error of the least square error estimator is derived. Numerical simulation results are presented, which discuss the effect on the local measurement of the bit error rate and number of bits used to perform the quantization. We then propose a bit allocation algorithm based on convex relaxation exploiting the derived Bayesian Fisher information.

- **Chapter 5: Conclusion and Future Work**
  The conclusion of this thesis is drawn and future potential works are listed.

# Related Work on Sensor Selection

# 2

In this chapter, we review the state of art of sensor selection.

## 2.1 Linear Case

### 2.1.1 Basic Model

Many anthors solve sensor selection problems in the scenario of wireless sensor network (WSN). For the linear case, each sensor acquires scalar measurements linearly constituted by a unknown parameter $\boldsymbol{\theta} \in \mathbb{R}^D$ and measurement noise,

$$y_n = \boldsymbol{h}_n^T \boldsymbol{\theta} + w_n, \tag{2.1}$$

where $\boldsymbol{h}_n$ is the regressor, and one of the specific meanings of it is to be explained in Section 3.1.1, and $w_n$ is the measurement noise. The main function of such WSN is to collect measurements from the sensors and exploit them to obtain an accurate estimate of the unknown parameter $\boldsymbol{\theta}$.

Due to energy or bandwidth limitations, it is wise to activate subset of sensors with highly informative measurements, for the sake of management of resource of the whole WSN and prolongation of the longevity of sensors. To this end, it is important to design a criterion to select the best subset of sensors. Many criteria are based on the error covariance matrix,

$$\boldsymbol{\mathcal{C}} := \mathbb{E}\left\{ \left(\hat{\boldsymbol{\theta}} - \boldsymbol{\theta}\right) \left(\hat{\boldsymbol{\theta}} - \boldsymbol{\theta}\right)^T \right\}, \tag{2.2}$$

where $\hat{\boldsymbol{\theta}}$ is an estimate of $\boldsymbol{\theta}$. If Least Squares estimate is used, i.e., $\hat{\boldsymbol{\theta}} = \left(\boldsymbol{H}\boldsymbol{H}^T\right)^{-1} \boldsymbol{H}\boldsymbol{y}$, with $\boldsymbol{H} := [\ \boldsymbol{h}_1, \boldsymbol{h}_2, ..., \boldsymbol{h}_N\ ]$ and $\boldsymbol{y} := [y_1, y_2, ..., y_N]^T$, $\boldsymbol{\mathcal{C}}$ can be explicitly written as,

$$\boldsymbol{\mathcal{C}} = \left(\boldsymbol{H}\boldsymbol{\mathcal{C}}_w^{-1}\boldsymbol{H}^T\right)^{-1} \tag{2.3}$$

where $\boldsymbol{\mathcal{C}}_w$ is the covariance matrix of the noise $\boldsymbol{w} := [w_1, w_2, ..., w_N]^T$. Notice that this $\boldsymbol{\mathcal{C}}$ involves all sensors. To distinguish, we denote the error covariance matrix of subset of sensors as $\boldsymbol{\mathcal{C}}(\boldsymbol{z})$, where $\boldsymbol{z} \in \mathbb{R}^N$ is the selection vector and the $n$-th element of it $z_n$ indicates whether sensor $n$ is selected($z_n = 1$) or not($z_n = 0$). The specific expressions of $\boldsymbol{\mathcal{C}}(\boldsymbol{z})$ are different with different forms of the noise covariance, i.e., whether the elements of $\boldsymbol{w}$ are correlated or not. Anyway, $\boldsymbol{\mathcal{C}}(\boldsymbol{z})$ of all cases can be derived based on (2.3). We will discuss further about the specific expressions of $\boldsymbol{\mathcal{C}}(\boldsymbol{z})$ under different cases of $\boldsymbol{w}$ later.

Also notice that the metric $\boldsymbol{\mathcal{C}}(\boldsymbol{z})$ used to construct the criterion to select sensors is a matrix that we cannot exploit directly, therefore a cost function $f(\boldsymbol{\mathcal{C}}(\boldsymbol{z}))$ is used instead. Now we can come to the illustration of the essential sensor selection problem. Sensor

selection problems aim at making a good tradeoff between the performance metric $\boldsymbol{\mathcal{C}}(\boldsymbol{z})$ and the total number of sensor activated. Typically, there exist two patterns of sensor selection. The first one is to restrict the number of activated sensors to be below a certain value and minimize $f(\boldsymbol{\mathcal{C}}(\boldsymbol{z}))$,

$$\begin{aligned} \boldsymbol{z}^* = \arg\min_{\boldsymbol{z}} \quad & f(\boldsymbol{\mathcal{C}}((\boldsymbol{z}))) \\ \text{s.t.} \quad & \|\boldsymbol{z}\|_0 \leq K, \end{aligned} \tag{2.4}$$

where $\|\boldsymbol{z}\|_0$ denotes the number of non-zero elements of $\boldsymbol{z}$, and $K$ is a constant. Another pattern works opposite to the first one that it restricts the performance metric to be smaller than a threshold and minimize the number of activated sensors,

$$\begin{aligned} \boldsymbol{z}^* = \arg\min_{\boldsymbol{z}} \quad & \|\boldsymbol{z}\|_0 \\ \text{s.t.} \quad & f(\boldsymbol{\mathcal{C}}(\boldsymbol{z})) \leq T, \end{aligned} \tag{2.5}$$

where $T$ is a constant threshold. These two types have their own focusing biases. The first one emphasizes more on the performance metric, while the second one values more on the sparsity of selected sensor, that the smaller number of sensors to activate is the goal. These two patterns have no fundamental differences in terms of the techniques to solve the corresponding optimization problems. In fact, these two optimizations problems are usually solved by two techniques, convex relaxations and greedy algorithms. These two patterns both restrict one aspect and try to optimize the other aspect. In Section 3.3.1, we propose a third pattern by which we can adjust the weight of number of sensors and the performance metric by parameter $\mu$.

Many papers that delve in sensor selection problems vary on the choices of the scalarization function $f(\boldsymbol{\mathcal{C}}(\boldsymbol{z}))$. Typical choices are the E-optimal design, A-optimal design and D-optimal design, which have different geometrical meanings.

### 2.1.2 Typical Choices of the Scalarization Functions

The error covariance matrix has explicit relation to the accuracy of the estimation. One accuracy metric is defined as the $\eta$-confidence ellipsoid for $\boldsymbol{\theta} - \hat{\boldsymbol{\theta}}$ [18, 3],

$$\epsilon_\beta := \{\boldsymbol{a} | \boldsymbol{a}^T \boldsymbol{\mathcal{C}}(\boldsymbol{z}) \boldsymbol{a} \leq \beta(\eta)\} \tag{2.6}$$

i.e., the estimation error $\boldsymbol{\theta} - \hat{\boldsymbol{\theta}}$ lies in the space $\epsilon_\beta$ with probability $\eta$, where $\beta(\eta)$ is a function depending on $\eta$. Typical scalarization functions are relates to this ellipsoid:

- E-optimal design: $f(\boldsymbol{\mathcal{C}}(\boldsymbol{z})) = \lambda_{\max}\{\boldsymbol{\mathcal{C}}(\boldsymbol{z})\}$, the maximum eigenvalue of the $\boldsymbol{\mathcal{C}}(\boldsymbol{z})$, or the norm of $\boldsymbol{\mathcal{C}}(\boldsymbol{z})$, $\|\boldsymbol{\mathcal{C}}(\boldsymbol{z})\|_2$. Minimization of $\lambda_{\max}\{\boldsymbol{\mathcal{C}}(\boldsymbol{z})\}$ is equivalent to minimizing the diameter of the confidence ellipsoid.
- A-optimal design: $f(\boldsymbol{\mathcal{C}}(\boldsymbol{z})) = \mathbb{T}\mathrm{r}\{\boldsymbol{\mathcal{C}}(\boldsymbol{z})\}$, the trace of the error covariance matrix, or equivalently the mean square error of the estimate.
- D-optimal design: $f(\boldsymbol{\mathcal{C}}(\boldsymbol{z})) = \log\det\{\boldsymbol{\mathcal{C}}(\boldsymbol{z})\}$, the log-determinant of the error covariance matrix, and minimizing it consequently minimizes the volume of the confidence ellipsoid [18].

### 2.1.3 Convex Relaxation for the Scalarization Functions with Uncorrelated Noise

Suppose that the elements of the noise vector $\boldsymbol{w}$ are zero-mean and uncorrelated, i.e., the covariance matrix of $\boldsymbol{w}$ is a diagonal matrix, $\boldsymbol{\mathcal{C}}_w = \text{diag}[\sigma_1^2, \sigma_2^2, ..., \sigma_N^2]$. Due to the diagonal property of the noise covariance matrix, the error covariance matrix in term of the selection vector $\boldsymbol{z}$ can be written as,

$$\boldsymbol{\mathcal{C}}(\boldsymbol{z}) = \left( \sum_{n=1}^{N} z_n \sigma_n^{-2} \boldsymbol{h}_n \boldsymbol{h}_n^T \right)^{-1}. \tag{2.7}$$

Based on this expression, we can re-cast the optimization problems of sensor selection into convex programming, using the three scalarization functions described above, and the re-casting optimization problems are listed as below, where the set $\boldsymbol{\mathcal{Z}} = \left\{ \boldsymbol{z} | \|\boldsymbol{z}\|_1 \leq K, \boldsymbol{z} \in [0,1]^N \right\}$. The detailed illustrations of the following formulations can be found in [19].

- E-optimal design:

$$\begin{aligned} \{\boldsymbol{z}^*, t^*\} = \arg\min_{\boldsymbol{z} \in \boldsymbol{\mathcal{Z}}, t} \quad & -t \\ \text{s.t.} \quad & \sum_{n=1}^{N} z_n \sigma_n^{-2} \boldsymbol{h}_n \boldsymbol{h}_n^T \succeq t \boldsymbol{I}_D. \end{aligned} \tag{2.8}$$

  Here we introduce an auxiliary scalar parameter $t$.

- A-optimal design:

$$\begin{aligned} \{\boldsymbol{z}^*, \boldsymbol{t}^*\} = \arg\min_{\boldsymbol{z} \in \boldsymbol{\mathcal{Z}}, \boldsymbol{t}} \quad & \|\boldsymbol{t}\|_1 \\ \text{s.t.} \quad & \begin{bmatrix} z_n \sigma_n^{-2} \boldsymbol{h}_n \boldsymbol{h}_n^T & \boldsymbol{e}_j \\ \boldsymbol{e}_j^T & t_j \end{bmatrix} \succeq 0, \quad j = 1, 2, ..., D. \end{aligned} \tag{2.9}$$

  An auxiliary vector is introduced, $\boldsymbol{t} = [t_1, t_2, ..., t_N]^T \in \mathbb{R}^D$.

- D-optimal design:

$$\{\boldsymbol{z}^*, t^*\} = \arg\min_{\boldsymbol{z} \in \boldsymbol{\mathcal{Z}}, t} \quad -\log\det\{z_n \sigma_n^{-2} \boldsymbol{h}_n \boldsymbol{h}_n^T\}. \tag{2.10}$$

Notice that in the three optimization problems, the selection vector $\boldsymbol{z}$ is relaxed, that the value of an element of it be chosen in the interval $[0, 1]$, instead of the binary value $\{0, 1\}$, therefore we need to transform the solutions of the above problems to be binary vectors. One approach is to set the $K$ elements of solution $\boldsymbol{z}^*$ with largest values to be 1 and the rest to be zero [18], or alternatively use the random rounding algorithm [9]. However, one knows little about the gap of the optimal solution (by exhaustive searching) and the ones of the above relaxed optimization problems. In [16] the authors proves the equivalence of the optimal solution and the one of the A-optimal design under

certain conditions, and we propose the equivalence theorem for the E-optimal design in Section 3.2.3.

The above convex relaxed optimization problems are to solve the first type of sensor selections problem in 2.4, and it is not difficult to use the similar approaches to reach the convex relaxed optimization problem for the second type of sensor selection problem of 2.5.

### 2.1.4 Convex Relaxation with Correlated Noise

When the noise $w_n$ are mutually correlated, the noise covariance matrix is not a diagonal matrix, therefore we cannot write $\boldsymbol{\mathcal{C}}(\boldsymbol{z})$ as in equation (2.7), and the problem is more complicated. In this part we discuss the existing works to deal with the sensor selection problem for the correlated noise, using the A-optimal design scalarization function, i.e.,

$$\{\boldsymbol{z}^*, t^*\} = \underset{\boldsymbol{z}\in\boldsymbol{\mathcal{Z}}}{\arg\min} \quad f(\boldsymbol{\mathcal{C}}(\boldsymbol{z})) = \mathbb{T}\mathrm{r}\left\{\left(\boldsymbol{H}\boldsymbol{\mathcal{C}}_w^{-1}\boldsymbol{H}^T\right)^{-1}\right\}. \tag{2.11}$$

To simplify the problem, it is reasonable to assume the structure of the noise covariance as,

$$\boldsymbol{\mathcal{C}}_w = \alpha\boldsymbol{I}_N + \boldsymbol{S}. \tag{2.12}$$

With this we can express the inverse of the error covariance matrix with respect to the selection vector $\boldsymbol{z}$ as [22],

$$\left(\boldsymbol{\mathcal{C}}(\boldsymbol{z})\right)^{-1} = \boldsymbol{H}\boldsymbol{S}^{-1}\boldsymbol{H}^T - \boldsymbol{H}\boldsymbol{S}^{-1}\left(\boldsymbol{S}^{-1} + \alpha^{-1}\mathrm{diag}(\boldsymbol{z})\right)^{-1}\boldsymbol{S}^{-1}\boldsymbol{H}^T. \tag{2.13}$$

One good point to express $\boldsymbol{\mathcal{C}}(\boldsymbol{z})$ in this way is that, there is only one term containing the selection vector $\boldsymbol{z}$. However, it is still intractable to exploit the above expression to form a convex optimization problem. To address this issue, [22] proposes a two-fold relaxation approach by introducing two auxiliary matrices, and the consequently optimization problem is as below,

$$\begin{aligned} \{\boldsymbol{z}^*\} = \underset{\boldsymbol{z}\in\mathcal{Z},\boldsymbol{A},\boldsymbol{V}}{\arg\min} \quad & \mathbb{T}\mathrm{r}\{\boldsymbol{A}\} \\ \text{s.t.} \quad & \boldsymbol{B} - \boldsymbol{V} \succeq \boldsymbol{A}^{-1} \\ & \boldsymbol{V} \succeq \boldsymbol{H}\boldsymbol{S}^{-1}\left(\boldsymbol{S}^{-1} + \alpha^{-1}\mathrm{diag}(\boldsymbol{z})\right)^{-1}\boldsymbol{S}^{-1}\boldsymbol{H}^T, \end{aligned} \tag{2.14}$$

where $\boldsymbol{B} = \boldsymbol{H}\boldsymbol{S}^{-1}\boldsymbol{H}^T$ is constant w.r.t. $\boldsymbol{z}$. It can be shown that the above optimization problem is equivalent to the original one that minimize the trace of the error covariance under the constraint of number of activated sensors, i.e., it is explicit to see that one can convert the original optimization problem by introducing an auxiliary parameter $\boldsymbol{A}$ and minimizing the trace of it if we restrict $\boldsymbol{\mathcal{C}}(\boldsymbol{z}) \preceq \boldsymbol{A}$. Also notice that minimizing the trace of $\boldsymbol{A}$ will at the same time force the right term in (2.13), $\boldsymbol{H}\boldsymbol{S}^{-1}\left(\boldsymbol{S}^{-1} + \alpha^{-1}\mathrm{diag}(\boldsymbol{z})\right)^{-1}$, to reach its lower bound, therefore we can relax the constraint by introducing another

auxiliary $\boldsymbol{V}$, and we reach the equivalent optimization of (2.14). The constraint set in (2.14) can be re-cast as the SDP form,

$$\begin{aligned} \left[\begin{array}{cc} \boldsymbol{B}-\boldsymbol{V} & \boldsymbol{I}_D \\ \boldsymbol{I}_D & \boldsymbol{A} \end{array}\right] &\succeq 0 \\ \left[\begin{array}{cc} \boldsymbol{V} & \boldsymbol{H}\boldsymbol{S}^{-1} \\ \boldsymbol{S}^{-1}\boldsymbol{H}^T & \boldsymbol{S}^{-1}+\alpha^{-1}\mathrm{diag}(\boldsymbol{z}) \end{array}\right] &\succeq 0. \end{aligned} \tag{2.15}$$

Consequently, the optimization problem in (2.14) is a convex optimization and can be solved by typical convex optimization tools. Details about the optimization problem (2.14) can be found in [22]

Notice that the above approach is to solve the general case for correlated noise. When the noise $w_n$ are weakly correlated, i.e., the noise covariance matrix has small off-diagonal elements compared to the diagonal elements, the error covariance matrix with respect to $\boldsymbol{z}$ can be approximated as [34, 17, 16, 23],

$$\boldsymbol{\mathcal{C}}(\boldsymbol{z}) = \left(\boldsymbol{H}\boldsymbol{z}\boldsymbol{z}^T \odot \left(\boldsymbol{\mathcal{C}}_w\right)^{-1}\boldsymbol{H}^T\right)^{-1}, \tag{2.16}$$

where $\odot$ is the Hadamark product (element-wise product). To use this expression to form a computable convex optimization problem, a typical approach is to introduce an auxiliary matrix $\boldsymbol{Z}$ to replace the term $\boldsymbol{z}\boldsymbol{z}^T$,

$$\begin{aligned} \boldsymbol{z}^* = \arg\min_{\boldsymbol{z}\in\mathcal{Z}} \quad & \mathrm{Tr}\left\{\left(\boldsymbol{H}\boldsymbol{Z} \odot \left(\boldsymbol{\mathcal{C}}_w\right)^{-1}\boldsymbol{H}^T\right)^{-1}\right\} \\ \text{s.t.} \quad & \boldsymbol{Z} \succeq \boldsymbol{z}\boldsymbol{z}^T \\ & 0 \le \{\boldsymbol{Z}\}_{i,j} \le 1, i, j = 1, 2, ..., N. \end{aligned} \tag{2.17}$$

### 2.1.5 Greedy Selection Approach With Uncorrelated Noise

Beside convex relaxations, another prevalent approach for sensor selection is by greedy selection. The algorithm goes in an iteration manner. The main idea of greedy selection is summarized below. Basically, one needs to define a metric whose value is affected by the subset of sensors involved. Two sets of sensors exist initially, one is a empty set (set $\mathcal{A}$) and the other is a set containing all sensors(set $\mathcal{B}$). In each iteration, one sensor is selected to be moved from set $\mathcal{B}$ to set $\mathcal{A}$, according to the rule that the new selected sensor together with the existing sensors in set $\mathcal{A}$ will contribute the largest to increase the value of the metric. To be more specific, let us define the metric as $f(\mathcal{S})$, where $\mathcal{S}$ is a set of sensors, and let $s$ denote a individual sensors, then in each iteration a sensor in set $\mathcal{B}$ is selected by,

$$\arg\max_{s\in\mathcal{B}} \; f(\mathcal{A}+s) \tag{2.18}$$

The iterations finish when the number of sensors in set $\mathcal{A}$ equals to $K$. The greedy algorithm can also proceed from the opposite direction, i.e., $\mathcal{A}$ is initialized as containing all sensors and in each iteration we deduct one sensor that minimizes the metric the least.

Compared with the convex relaxation approaches, one significant advantage of greedy selection is that the latter is more computationally efficient, i.e., the computational complexities for convex relaxation and greedy selection are $\mathrm{O}(N^3D^2)$ and $\mathrm{O}(ND^3)$, respectively. The former one is cubic in the number of of all sensors $N$ and square in the dimension of $\boldsymbol{\theta}$, $D$, while the latter is linear in $N$ and cubic in $D$. However, note that in most case the number of sensors in a WSN is usually much large than the dimension of $\boldsymbol{\theta}$, therefore $N$ is the dominating part in the complexity analysis. Furthermore, [37] proposes a more efficient greedy algorithm whose complexity is $\mathrm{O}(ND^2)$.

Another aspect to discuss about greedy selection is its guarantee of the distance to the optimal solution if the metric $f(.)$ is a normalized monotone sub-modular function with respect to the selected sensors. Let $\mathcal{A}^*$ be the optimal subset, and $\mathcal{A}$ be the subset by greedy selection, if $f(.)$ is normalized monotone sub-modular function then we have,

$$f(\mathcal{A}) \geq (1-e)f(\mathcal{A}^*), \tag{2.19}$$

where $e$ is the Euler's number. For the definition of normalized monotone sub-modular function, readers can refer to [28, 30]. The key step to apply greedy selection is to form a normalized monotone sub-modular metric. Anyway, even the distance of the value of $f(\mathcal{A})$ to the $f(\mathcal{A}^*)$ can be guaranteed within a certain range, we cannot say that the greedy selection is better than convex relaxation in term of performance. In addition, for many cases it is hard to find out a suitable normalized monotone sub-modular metric, and that one is also related to the error covariance matrix. One such metric, for example, is based on the frame potential [30], defined as,

$$\mathrm{FP}(\boldsymbol{H}) = \sum_{i,j} \boldsymbol{h}_i^T \boldsymbol{h}_j. \quad i,j = 1,2,...,N. \tag{2.20}$$

The work in [30] shows that minimizing the frame potential for the selected sensors indirectly minimizes the mean square error, which is the trace of the error covariance. Intuitively, selecting subset of sensors with minimum value of corresponding frame potential can be seen as choosing sensors with most orthogonal $\boldsymbol{h}_n$. In [30] authors also propose an metric comprised by the frame potential that can be shown to be normalized monotone sub-modular, such that when applying greedy algorithm we can obtain an near optimal solution in term of minimizing the mean square error, which is computationally efficient compared with convex relaxation. However, it must be emphasized that the model in [30] requires the variances of $w_n$ to be identical, so that the distinction of sensors' measurements results from the regressors $\boldsymbol{h}_n$, or in other words, that approach is invalid when we consider non-identical noise variances.

## 2.2 Non-Linear Case

In above discussion, we considered the a measurement model where the scalar local measurement $y_n$ is linear in the unknown parameter $\boldsymbol{\theta}$. In many cases, $y_n$ is not linear

with respect to $\boldsymbol{\theta}$, i.e.,

$$y_n = h_n(\boldsymbol{\theta}) + w_n, \tag{2.21}$$

where $h_n$ is a non-linear function of $\boldsymbol{\theta}$. Since the estimates for $\boldsymbol{\theta}$ are usually complicated, there exists no closed-form expression for the error covariance matrix, and the metrics for sensor selection in linear case described above are not valid here. A popular proxy for the error covariance matrix is the Cramer-Rao Lower bound. For the E-optimal and A-optimal design listed above, if we substitute the error covariance matrix by the Cramer-Rao Lower bound, which is the inverse matrix of the Fisher information, we can guarantee the mean square error to be below certain level statistically, which will be presented in detail in Section 3.2.1.

For the case when noises $w_n$ are uncorrelated and zero-mean, exploiting the additive property of Fisher information, the Fisher information can be decomposed by the summation of the local Fisher information, i.e., the Fisher information with respect to the selection vector can be expressed as,

$$\boldsymbol{\mathcal{F}}(\boldsymbol{z}) = \sum_{n=1}^{N} z_n \boldsymbol{\mathcal{F}}(\boldsymbol{z})^{(n)}, \tag{2.22}$$

where $\boldsymbol{\mathcal{F}}(\boldsymbol{z})^{(n)}$ is the local Fisher information for sensor $n$. Details about the description of $\boldsymbol{\mathcal{F}}(\boldsymbol{z})$ can be found in Section 3.1.4. Based on this expression, it is easy to form a convex optimization problem for sensor selection [9]. It should be emphasized that $\boldsymbol{\mathcal{F}}(\boldsymbol{z})$ contains the unknown parameter $\boldsymbol{\theta}$, therefore we cannot exploit this expression directly for sensor selection because the value of $\boldsymbol{\theta}$ is not available in advance. To address this problem, [9] proposes to restrict the possible values of $\boldsymbol{\theta}$ to be a finite set according to the prior knowledge of $\boldsymbol{\theta}$, and to consider all the possible discrete values at the same time, or just replace $\boldsymbol{\theta}$ by the previous estimate of it as that in [8]. In this thesis, we adopt the Bayesian Cramer-Rao Lower bound instead of regular Cramer-Rao Lower bound, which exploits the prior information about $\boldsymbol{\theta}$ and it contains no $\boldsymbol{\theta}$ in the expression.

When the noise are correlated, the problem is more complicated because we cannot separate the Fisher information by the summation of local Fisher information. In [23], the authors consider the case when the noises are joint Gaussian distributed, and the Fisher information can be written as,

$$\boldsymbol{\mathcal{F}} = \nabla_{\boldsymbol{\theta}}^T \boldsymbol{h}(\boldsymbol{\theta})\ \boldsymbol{C}_w^{-1}\ \nabla_{\boldsymbol{\theta}} \boldsymbol{h}(\boldsymbol{\theta}) \tag{2.23}$$

where $\boldsymbol{h}(\boldsymbol{\theta}) = [h_1(\boldsymbol{\theta}), h_2(\boldsymbol{\theta}), ..., h_N(\boldsymbol{\theta})]$. This expression has the same structure as the error covariance matrix of uncorrelated noise described above, therefore it can be handled by the same approaches.

### 2.2.1 Other Proxies For The Non-Linear Case

Except substituting error covariance matrix by the Cramer-Rao lower bound, other proxies or approaches are also developed.

The authors in [31] propose to linearize the non-linear term $h_n(\boldsymbol{\theta})$ by Taylor expansion to the first order. To implement this idea, we first need to get an estimate of the unknown parameter $\hat{\boldsymbol{\theta}}$, and approximate the measurement leveraging this estimate,

$$y_n \approx h_n(\hat{\boldsymbol{\theta}}) + \nabla_{\boldsymbol{\theta}}^T h_n(\hat{\boldsymbol{\theta}})(\boldsymbol{\theta} - \hat{\boldsymbol{\theta}}) + w_n \tag{2.24}$$

By such approximation, the measurement model becomes linear with respect to $\boldsymbol{\theta}$, therefore it can be handled by typical approaches for linear cases. It must be emphasized that accuracy of the linearization procedure heavily depends on the accuracy of the estimate $\hat{\boldsymbol{\theta}}$. If $\hat{\boldsymbol{\theta}}$ is not a good estimate, large bias of the approximation in (2.24) will occur.

Another performance metric is the mutual information [15, 20], which can be obtained as [10],

$$\mathcal{I}(\boldsymbol{y}, \boldsymbol{\theta}) = \mathcal{H}(\boldsymbol{y}) - \mathcal{H}(\boldsymbol{y}|\boldsymbol{\theta}), \tag{2.25}$$

where $\mathcal{H}(y)$ is the amount of uncertainty or information of $\boldsymbol{y}$ and $\mathcal{H}(\boldsymbol{y}|\boldsymbol{\theta})$ is the amount of uncertainty or information of $\boldsymbol{y}$ after knowing $\boldsymbol{\theta}$. Intuitively, from equation (2.25) we can see the mutual information indicates how close $\boldsymbol{y}$ and $\boldsymbol{\theta}$ are related to each other, and the local mutual information $\mathcal{I}(y_n, \boldsymbol{\theta})$ can reveal how informative a sensor is. If the noise $w_n$ are uncorrelated, the global mutual information $\mathcal{I}(\boldsymbol{y}, \boldsymbol{\theta})$ can be decomposed as the summation of local mutual informations,

$$\mathcal{I}(\boldsymbol{y}, \boldsymbol{\theta}) = \sum_{n=1}^{N} \mathcal{I}(y_n, \boldsymbol{\theta}), \tag{2.26}$$

which has the same form of the Fisher information, hence it can be handled conveniently in sensor selection.

## 2.3 Conclusion

In this chapter, the state of art about sensor selection for WSN is presented. Many researchers propose and investigate approaches to solve the sensor selection problem under different scenarios. However, there is one issue on the data model that has not been investigated-the effects of wireless channel. In our following work we delve in solving sensor selection and bit allocation algorithm considering wireless channel effects. Traditional bit allocation schemes are usually based on greedy allocation [29]. Related to our approach is the work in [25]. There the the authors propose to apply convex tools to allocate a limited number of bits such that the inverse log-determinant of the posterior Fisher information is minimized. In our approach, we restrict the performance metric expressed by selection vectors to be larger than a pre-designed threshold, and minimize the global cost that we defined and this metric is related to the number o bits of the sensors. Our approach is not limited to the inverse of the log-det and in fact more general.

# Wireless Sensor Networks with One-Bit Quantization

# 3

In this section, we present the wireless sensor network framework and adopt the one-bit quantization scheme to compress the original measurement to transmit over the wireless channel. The impact of the wireless channel on the transmitted data is characterized by the bit error rate. Then we provide the maximum a posteriori estimator and derive the Bayesian Cramer-Rao lower bound. Next we adopt the minimum eigenvalue of the Bayesian Cramer-Rao lower bound as the performance metric for sensor selection by convex relaxation. Further, the possibility that the solution of convex relaxation being optimal is investigated and the corresponding equivalence theorem is proposed.

## 3.1 One-bit Quantization

### 3.1.1 Framework Description

Consider a wireless sensor network (WSN) comprised of a set of sensors with a fusion center. Suppose there are $N$ sensors and let the sensors be indexed from 1 to $N$, with the fusion center indexed as 0. The WSN aims at performing surveillance of multiple signal sources [21]. Suppose there are $D$ signal sources, and the $d$-th signal source $\theta_d$ is measured by the $n$-th sensor as $h_{n,d}\ \theta_d$. The value of $h_{n,d}$ depends on the distance between the corresponding sensor and signal source. Since the locations of the sources are fixed, it is assumed that $h_{n,d}$ is known to the sensor. The local measurement of each sensor is consequently the superposition of the receiving signals from all sources plus noise,

$$y_n = \sum_{d=1}^{D} h_{n,d}\theta_d + w_n \ = \boldsymbol{h}_n^T\boldsymbol{\theta} + w_n, \quad n = 1, 2, ...N, \tag{3.1}$$

where $\boldsymbol{h}_n := [h_{n,1}, h_{n,2}, ..., h_{n,D}]^T$, $\boldsymbol{\theta} := [\theta_1, \theta_2, ..., \theta_D]^T$, and $w_n$ is the measuring noise for sensor $n$. Before further discussion, we make the following assumptions:

**Assumption 1.** The noise $w_n$ is spatially uncorrelated with zero mean and variance $\sigma_n^2$, and its pdf, denoted as $f_n(w_n)$, is known by the fusion center.

Assumption 1 implies that the covariance matrix of $\boldsymbol{w} := [w_1, w_2, ..., w_N]^T$ is a diagonal matrix.

**Assumption 2.** The unknown parameter $\boldsymbol{\theta}$ is also a random parameter. The fusion center knows its a priori pdf $p(\boldsymbol{\theta})$.

The assumption on the regularity is needed to simply the analysis and the development of the algorithms. It is not restrictive in practice since, e.g., a zero mean Gaussian pdf verifies it.

In each round of measurements, the sensors transmit messages $m_n = \Phi(y_n)$ to the fusion center, and at the fusion center, an estimate of $\boldsymbol{\theta}$ is generated based on the received messages. If the bandwidth is infinite, sensors can transmit the original measurements, that is, $m_n = y_n$. However, due to bandwidth limitations in reality, they are not allowed to do so. Instead, message $m_n$ is generally a simplified version of the original measurement. One technique that has been investigated in many works is the one-bit quantization [33, 2, 42]. In one-bit quantization, the messages are a bit $b_n$ that is generated by the following principle,

$$b_n = \begin{cases} 1, & \text{if } y_n \in [\tau_n, +\infty) \\ 0, & \text{if } y_n \in (-\infty, \tau_n) \end{cases} \tag{3.2}$$

i.e, we set a threshold $\tau_n$ so that if $y_n$ is larger than it $b_n$ is 1, otherwise it is 0.

Figure 3.1.1 depicts the framework.

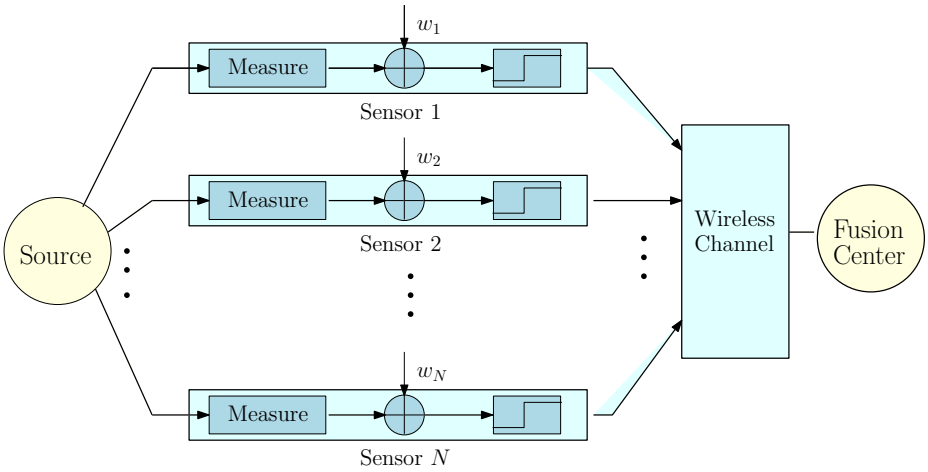


Figure 3.1: Illustration of the WSN. In each sensor, the original measurements added with noise are quantized before transmission.

### 3.1.2 Imperfect Wireless Channel

Due to the imperfection of the real wireless channel, the transmitted message $b_n$ can be corrupted due to wireless propagation phenomena. Let $c_n$ be the reception of $b_n$ at the fusion center. Corruptions result in incorrectness of $c_n$. In other words, $c_n$ maybe flipped to the opposite value of $b_n$, i.e, $c_n$ is decoded as 1 while $b_n$ is 0, or vice versa. To characterize the bit errors, we introduce the bit error rate $\text{Pe}_n$, which specifies the probability of incorrect decoding of one bit transmitted from sensor $n$ to the fusion center. The rate $\text{Pe}_n$ is usually the combined result of three factors, namely, the signal to noise ratio (SNR) $S_n/N_n$, the modulation scheme and the error correct coding, where

$S_n$ and $N_n$ are the received signal and noise power, respectively [39]. Generally, $\mathrm{Pe}_n$ can be approximated as,

$$\mathrm{Pe}_n = \mathrm{erfc}\left(\sqrt{k\frac{S_n}{N_n}}\right) \tag{3.3}$$

where erfc(.) is the complementary error function and $k$ is a constant determined by the modulation and coding type [39] [13].

Note the received signal power $S_n$ is an intricate parameter to be predetermined, which is the consequence of multiple effects. It is an attenuated version of the transmitted signal power due to the propagation in a wireless channel. Generally, three effects contribute to the attenuation of the received signal power. They are path-loss resulting from partial receiving of the whole transmitted power, shadowing due to obstacles in the propagation path and multi-path fading resulting from reflections. Considering all the three effects, the received signal power (in dBm) can be modeled as,

$$S_n = S_n^{'} + K_n - 10\gamma \log \frac{d_n}{d_0} - \mathcal{A}_n - \mathcal{B}_n, \tag{3.4}$$

where $S_n^{'}$ is the transmitted signal power, $K_n$ is an unit-less constant, $\gamma$ is the path-loss exponent, and $d_n$ is the Euclidean distance between sensor $n$ and the fusion center. $\mathcal{A}_n$ and $\mathcal{B}_n$ then characterize the shadowing effect and multi-path fading. Specification of this model can be found in [32].

In practice, $\mathrm{Pe}_n$ is usually detected during the training period. In this thesis, we assume it is known to the fusion center.

### 3.1.3 Maximum A Posteriori Estimation

In this part we derive the maximum a posteriori (MAP) estimate $\hat{\boldsymbol{\theta}}_{\mathrm{MAP}}$. Since the received data are the indicators, in general it is difficult to find an closed-form estimator. Since MAP also involves the prior knowledge of $\boldsymbol{\theta}$ in consideration, therefore MAP is a good choice for this case. The reason to choose MAP also results from that it is simple to implement, i.e., it maximizes the joint likelihood over $\boldsymbol{\theta}$. To obtain a MAP estimate, it is a prerequisite to derive the expression of the joint likelihood function $p(\boldsymbol{c}, \boldsymbol{\theta})$, where $\boldsymbol{c} := [c_1, c_2, ..., c_N]^T$ is the stacked vector of the received messages. We can see that for the transmitted bit $b_n$ the probability that $b_n = 1$ given $\boldsymbol{\theta}$ is,

$$g_n := \mathbb{P}\mathrm{r}(b_n = 1|\boldsymbol{\theta}) = 1 - \mathrm{F}_n(\tau_n - \boldsymbol{h}_n^T\boldsymbol{\theta}) \tag{3.5}$$

where $\mathrm{F}_n(t)$ is the cumulative density function (CDF) of $f_n(w)$, $\mathrm{F}_n(t) = \int_{-\infty}^{t} f_n(w)\mathrm{d}w$. As for the probability of $c_n = 1$, by the total probability rule we have,

$$\begin{aligned} s_n := \mathbb{P}\mathrm{r}(c_n = 1|\boldsymbol{\theta}) =& (1 - \mathrm{Pe}_n)g_n + \mathrm{Pe}_n(1 - g_n) \\ =& (1 - \mathrm{Pe}_n)(1 - \mathrm{F}_n(\tau_n - \boldsymbol{h}_n^T\boldsymbol{\theta})) + \mathrm{Pe}_n\mathrm{F}_n(\tau_n - \boldsymbol{h}_n^T\boldsymbol{\theta}). \end{aligned} \tag{3.6}$$

The joint likelihood can then be expressed as,

$$p(\boldsymbol{c}, \boldsymbol{\theta}) = p(\boldsymbol{c}|\boldsymbol{\theta})p(\boldsymbol{\theta}) = p(\boldsymbol{\theta}) \prod_{n=1}^{N} s_n^{c_n} (1 - s_n)^{1-c_n}. \tag{3.7}$$

By Bayes' rule, the MAP can finally be obtained by [12],

$$\hat{\boldsymbol{\theta}}_{\text{MAP}} = \arg\max_{\boldsymbol{\theta}} p(\boldsymbol{\theta}|\boldsymbol{c}) = \arg\max_{\boldsymbol{\theta}} p(\boldsymbol{c}|\boldsymbol{\theta})p(\boldsymbol{\theta}), \tag{3.8}$$

where in the second equation $\boldsymbol{c}$ is seen as a realized parameter. The estimate $\hat{\boldsymbol{\theta}}_{\text{MAP}}$ can also be obtained by the logarithm likelihood,

$$\begin{aligned} \hat{\boldsymbol{\theta}}_{\text{MAP}} =& \arg\max_{\boldsymbol{\theta}} \ \ln p(\boldsymbol{c}|\boldsymbol{\theta})p(\boldsymbol{\theta}) \\ =& \arg\max_{\boldsymbol{\theta}} \ \ln p(\boldsymbol{\theta}) + \sum_{n=1}^{N} c_n \ln s_n + (1 - c_n) \ln (1 - s_n). \end{aligned} \tag{3.9}$$

Notice that it is hard to achieve a closed-form solution for (3.9), due to the complicated expression of $p(\boldsymbol{\theta})$ and $s_n$ w.r.t. $\boldsymbol{\theta}$. Fortunately, it can be shown that $\ln p(\boldsymbol{c}|\boldsymbol{\theta})p(\boldsymbol{\theta})$ is concave if $p(\boldsymbol{\theta})$ and the pdf of the noise $f_n(w)$ are both log-concave. The proof is similar to that in [33]. Giving the concavity, we can solve (3.9) with typical convex optimization techniques, steepest descent gradient (SDG) [11], sub-gradient methods, or Newton's method, to name a few.

### 3.1.4 Bayesian Cramer-Rao Lower Bound

Now we derive the Bayesian Cramer-Rao lower bound, which is the lower bound for the Bayesian error covariance matrices for any estimators, and hence its trace is the lower bound for the MAP. The error covariance matrix is defined as follows,

$$\boldsymbol{\mathcal{C}}_{\text{B}}(\boldsymbol{\theta}) \triangleq \mathbb{E}_{\boldsymbol{\theta},\boldsymbol{c}}\{(\hat{\boldsymbol{\theta}} - \boldsymbol{\theta})(\hat{\boldsymbol{\theta}} - \boldsymbol{\theta})^T\} \tag{3.10}$$

The expectation is taken over $\boldsymbol{\theta}$ and $\boldsymbol{c}$. The Bayesian Cramer-Rao lower bound (B-CRB) provides lower bound on Bayesian error covariance matrix,

$$\boldsymbol{\mathcal{B}}_{\text{B}}(\boldsymbol{\theta}) \preceq \boldsymbol{\mathcal{C}}_{\text{B}}(\boldsymbol{\theta}). \tag{3.11}$$

The B-CRB can be obtained by the inverse of the corresponding Bayesian Fisher Information matrix (B-FIM), $\boldsymbol{\mathcal{B}}_{\text{B}} = \big( \boldsymbol{\mathcal{F}}_{\text{B}} \big)^{-1}$ , and the expression of the B-FIM is given by [36],

$$\boldsymbol{\mathcal{F}}_{\text{B}} = \mathbb{E}_{\boldsymbol{\theta},\boldsymbol{c}} \left\{ \nabla_{\boldsymbol{\theta}} \ln p(\boldsymbol{c}|\boldsymbol{\theta}) \nabla_{\boldsymbol{\theta}}^T \ln p(\boldsymbol{c}|\boldsymbol{\theta}) \right\} + \mathbb{E}_{\boldsymbol{\theta}} \left\{ \nabla_{\boldsymbol{\theta}} \ln p(\boldsymbol{\theta}) \nabla_{\boldsymbol{\theta}}^T \ln p(\boldsymbol{\theta}) \right\} \tag{3.12}$$

The gradient of the conditional likelihood can be computed as,

$$\begin{aligned}\nabla_{\boldsymbol{\theta}} \ln p(\boldsymbol{c}|\boldsymbol{\theta}) &= \sum_{n=1}^{N} \left( \frac{c_n}{s_n} - \frac{1-c_n}{1-s_n} \right) \nabla_{\boldsymbol{\theta}} s_n \\ &\overset{(1)}{=} \sum_{n=1}^{N} \frac{c_n - s_n}{s_n(1-s_n)} (1-2\mathrm{Pe}_n) f_n(\tau_n - \boldsymbol{h}_n^T \boldsymbol{\theta}) \boldsymbol{h}_n \end{aligned} \tag{3.13}$$

where the equality (1) is based on the expression of $s_n$ in (3.6). Under the regularity condition and given the independent measurements we then have,

$$\begin{aligned}\boldsymbol{\mathcal{F}}_{\mathrm{B}} =& \mathbb{E}_{\boldsymbol{\theta},\boldsymbol{c}} \left\{ \nabla_{\boldsymbol{\theta}} \ln p(\boldsymbol{c}|\boldsymbol{\theta}) \nabla_{\boldsymbol{\theta}}^T \ln p(\boldsymbol{c}|\boldsymbol{\theta}) \right\} + \mathbb{E}_{\boldsymbol{\theta},\boldsymbol{c}} \left\{ \nabla_{\boldsymbol{\theta}} \ln p(\boldsymbol{\theta}) \nabla_{\boldsymbol{\theta}}^T \ln p(\boldsymbol{\theta}) \right\} \\ =& \sum_{n=1}^{N} \mathbb{E}_{\boldsymbol{\theta},c_n} \left\{ \frac{(c_n - s_n)^2 (1-2\mathrm{Pe}_n)^2}{s_n^2 (1-s_n)^2} f_n^2(\tau_n - \boldsymbol{h}_n^T \boldsymbol{\theta}) \right\} \boldsymbol{h}_n \boldsymbol{h}_n^T \\ &+ \mathbb{E}_{\boldsymbol{\theta}} \left\{ \nabla_{\boldsymbol{\theta}} \ln p(\boldsymbol{\theta}) \nabla_{\boldsymbol{\theta}}^T \ln p(\boldsymbol{\theta}) \right\}. \end{aligned} \tag{3.14}$$

It can be simplified as,

$$\begin{aligned}\boldsymbol{\mathcal{F}}_{\mathrm{B}} =& \sum_{n=1}^{N} \mathbb{E}_{\boldsymbol{\theta}} \left\{ \mathbb{E}_{\boldsymbol{c}} \left\{ \frac{(c_n - s_n)^2}{s_n^2 (1-s_n)^2} \right\} (1-2\mathrm{Pe}_n)^2 f_n^2(\tau_n - \boldsymbol{h}_n^T \boldsymbol{\theta}) \right\} \boldsymbol{h}_n \boldsymbol{h}_n^T \\ &+ \mathbb{E}_{\boldsymbol{\theta}} \left\{ \nabla_{\boldsymbol{\theta}} \ln p(\boldsymbol{\theta}) \nabla_{\boldsymbol{\theta}}^T \ln p(\boldsymbol{\theta}) \right\} \\ =& \sum_{n=1}^{N} \mathbb{E}_{\boldsymbol{\theta}} \left\{ \left[ \frac{\mathbb{E}_{\boldsymbol{c}}\{c_n^2 + s_n^2 - 2 s_n c_n\}}{s_n^2 (1-s_n)^2} \right] (1-2\mathrm{Pe}_n)^2 f_n^2(\tau_n - \boldsymbol{h}_n^T \boldsymbol{\theta}) \right\} \boldsymbol{h}_n \boldsymbol{h}_n^T \\ &+ \mathbb{E}_{\boldsymbol{\theta}} \left\{ \nabla_{\boldsymbol{\theta}} \ln p(\boldsymbol{\theta}) \nabla_{\boldsymbol{\theta}}^T \ln p(\boldsymbol{\theta}) \right\} \\ \overset{(1)}{=}& \sum_{n=1}^{N} \mathbb{E}_{\boldsymbol{\theta}} \left\{ \frac{(1-2\mathrm{Pe}_n)^2}{s_n(1-s_n)} f_n^2(\tau_n - \boldsymbol{h}_n^T \boldsymbol{\theta}) \right\} \boldsymbol{h}_n \boldsymbol{h}_n^T \\ &+ \mathbb{E}_{\boldsymbol{\theta}} \left\{ \nabla_{\boldsymbol{\theta}} \ln p(\boldsymbol{\theta}) \nabla_{\boldsymbol{\theta}}^T \ln p(\boldsymbol{\theta}) \right\} \\ \overset{(2)}{=}& : \sum_{n=1}^{N} \boldsymbol{\mathcal{F}}_{\mathrm{B}}^{(n)} + \boldsymbol{\mathcal{F}}_{\boldsymbol{\theta}}, \end{aligned} \tag{3.15}$$

Equality (1) is based on the fact that $c_n$ is binary such that $\mathbb{E}\{c_n\} = \mathbb{E}\{c_n^2\} = s_n$. Equality (2) is from the definitions,

$$\boldsymbol{\mathcal{F}}_B^{(n)} := \mathbb{E}_{\boldsymbol{\theta}} \left\{ \frac{(1-2\mathrm{Pe}_n)^2}{s_n(1-s_n)} f_n^2(\tau_n - \boldsymbol{h}_n^T \boldsymbol{\theta}) \right\} \boldsymbol{h}_n \boldsymbol{h}_n^T \tag{3.16a}$$

$$\boldsymbol{\mathcal{F}}_{\boldsymbol{\theta}} := \mathbb{E}_{\boldsymbol{\theta}} \left\{ \nabla_{\boldsymbol{\theta}} \ln p(\boldsymbol{\theta}) \nabla_{\boldsymbol{\theta}}^T \ln p(\boldsymbol{\theta}) \right\} \tag{3.16b}$$

The B-CRB is then $\mathcal{B}_B = \left( \sum_{n=1}^{N} \boldsymbol{\mathcal{F}}_B^{(n)} + \boldsymbol{\mathcal{F}}_{\boldsymbol{\theta}} \right)^{-1}$.

## 3.2 Sensor Selection for One Bit Quantization

Observing the measurement model (3.1), we can see that the measurement of each sensor $y_n$ contributes differently in estimating the exact value of $\boldsymbol{\theta}$. The reasons for this phenomenon can be summarized by the following three factors:

- The regressor $\boldsymbol{h}_n$ determines how much information about $\boldsymbol{\theta}$ can be revealed from the measurement $y_n$. Explicitly, only the non-zero elements can convey the information of the corresponding element of $\boldsymbol{\theta}$. An extreme example is that when $\boldsymbol{h}_n$ is an all-zero vector, $y_n$ will only contain the measurement of noise.
- The measurement noise brings uncertainty to the measurement. Noise with a high variance will degrade severely the quality of the measurement.
- Each sensor has a different channel quality to the fusion center, which is characterized by the bit error rate $\mathrm{Pe}_n$. If we incorporate the measurement from a bad channel (high $\mathrm{Pe}_n$) instead of one of a good channel, a larger estimation error of $\hat{\boldsymbol{\theta}}$ will be brought.

Given the considerations above, it is wise to select a sub-set of sensors to operate and transmit measurements to the fusion center. By this strategy, not only can we avoid highly noisy measurements, but more importantly, the precious resources of the WSN can be efficiently managed, like the energy in the battery of the sensors, bandwidth and the computational complexity in the fusion center to compute $\hat{\boldsymbol{\theta}}$.

A primary problem to implement the sensor selection strategy is how to select the subset of sensors. Considering the estimation performance and resource reservation, we follow two principles in designing the one-bit sensor selection scheme:

- The number of sensors should be as small as possible, for the purpose of resources management in WSN.
- The measurements of the selected sensors should result in a limited estimation error.

Based on these two principles, we introduce some performance measure metrics in the following and formulate the convex optimization problem to find out the optimal subset of sensors based on the metrics selected.

### 3.2.1 Performance Criterion

An explicit performance metric is the mean square error, that is the trace of the error covariance matrix, or the Bayesian mean square error if prior information about the unknown parameter $\boldsymbol{\theta}$ is available. The performance criterion is then that the mean square error or Bayesian mean square error should be smaller than a threshold. However, under the one-bit quantization scheme, we adopt the MAP estimate and we cannot find out the closed form expression of the error covariance matrix. Therefore instead of adopting the mean square error or the Bayesian mean square error, we

introduce two proxy performance metrics that are related to the mean square error. The two metrics are based on the Cramer-Rao lower bound or Fisher information.

Prior to the description of the metrics, we define a binary vector $\boldsymbol{z} := [z_1, z_2, ..., z_N]^T$ to indicate whether a particular sensor is selected to be activated or not, i.e., $z_n = 1$ implies sensor $n$ is selected and vice versa. We can then express the global Fisher information as,

$$\boldsymbol{\mathcal{F}}(\boldsymbol{z}) = \sum_{n=1}^{N} z_n \, \boldsymbol{\mathcal{F}}^{(n)}, \tag{3.17}$$

where $\boldsymbol{\mathcal{F}}^{(n)}$ is the local Fisher information of sensor $n$. The first performance metric is the minimum eigenvalue of the global Fisher information, denoted as $\lambda_{\min}\{\boldsymbol{\mathcal{F}}(\boldsymbol{z})\}$, and the performance criterion is that we require it to be larger than a threshold $T_f$,

$$\lambda_{\min}\{\boldsymbol{\mathcal{F}}(\boldsymbol{z})\} \geq T_f, \tag{3.18}$$

The threshold $T_f$ can be chosen as,

$$T_f = \frac{D}{R_e^2} \frac{1}{1 - \mathrm{P_c}}. \tag{3.19}$$

In this way, we can guarantee that [40],

$$\mathbb{P}\mathrm{r}(\|\hat{\boldsymbol{\theta}} - \boldsymbol{\theta}\|_2 \leq R_e) \geq \mathrm{P_c}, \tag{3.20}$$

i.e., the probability that the estimation error $\|\hat{\boldsymbol{\theta}} - \boldsymbol{\theta}\|_2$ being smaller than $R_e$ is larger than $\mathrm{P_c}$. With this, we can control the tolerance of the estimation error by adjusting the the error radius $R_e$ and the reliability parameter $\mathrm{P_c}$, which are related to the threshold by (3.19).

Another performance metric is the trace of the Cramer-Rao lower bound, $\mathbb{T}\mathrm{r}\{(\boldsymbol{\mathcal{F}}(\boldsymbol{z}))^{-1}\}$. The corresponding performance criterion is that it should be smaller than a threshold,

$$\mathbb{T}\mathrm{r}\{(\boldsymbol{\mathcal{F}}(\boldsymbol{z}))^{-1}\} \leq T_c \tag{3.21}$$

In fact, for this metric, if we set $T_c = (1 - \mathrm{P}_c)R_e^2$, then (3.20) is also valid [6].

Note that the two criterions based on $\lambda_{\min}\{\boldsymbol{\mathcal{F}}(\boldsymbol{z})\}$ and $\mathbb{T}\mathrm{r}\{(\boldsymbol{\mathcal{F}}(\boldsymbol{z}))^{-1}\}$ are equivalent in terms of controlling the estimation error. However, the criterion based on $\lambda_{\min}\{\boldsymbol{\mathcal{F}}(\boldsymbol{z})\}$ is more computationally efficient [9]. Therefore we adopt the criterion based on $\lambda_{\min}\{\boldsymbol{\mathcal{F}}(\boldsymbol{z})\}$ for our sensor selection.

Since under Assumption 2, we know the prior pdf of $\boldsymbol{\theta}$, we can substitute the Fisher Information by the Bayesian Fisher information $\boldsymbol{\mathcal{F}}_{\mathrm{B}}(\boldsymbol{z}) = \sum_{n=1}^{N} z_n \, \boldsymbol{\mathcal{F}}_B^{(n)} + \boldsymbol{\mathcal{F}}_{\boldsymbol{\theta}}$, and the metric becomes $\lambda_{\min}\{\boldsymbol{\mathcal{F}}_B(\boldsymbol{z})\}$.

### 3.2.2 Sensor Selection with One-bit Quantization

In this part we describe the sensor selection problem, under the assumption that the bit error rate vector $\mathbf{Pe} := \left[\mathrm{Pe}_1, \mathrm{Pe}_2, ..., \mathrm{Pe}_N\right]^T$ is known to the fusion center. We adopt the performance criterion that the minimum eigenvalue of $\mathcal{F}_{\mathrm{B}}(\boldsymbol{z})$ is larger than or equal to $T_f$,

$$\lambda_{\min}\{\boldsymbol{\mathcal{F}}_B(\boldsymbol{z})\} \geq T_f \tag{3.22}$$

This means that each eigenvalue of $\boldsymbol{\mathcal{F}}_{\mathrm{B}}(\boldsymbol{z})$ should be larger than or equal to $T_f$, or all the eigenvalues of $\boldsymbol{\mathcal{F}}_B(\boldsymbol{z}) - T_f \boldsymbol{I}_D$ are larger than or equals to zero, which further implies that $\boldsymbol{\mathcal{F}}_B(\boldsymbol{z}) - T_f \boldsymbol{I}_D$ is a positive semi-definite matrix,

$$\boldsymbol{\mathcal{F}}_{\mathrm{B}}(\boldsymbol{z}) - T_f \boldsymbol{I}_D \succeq 0. \tag{3.23}$$

We require the number of sensors selected to be activated to be as small as possible, therefore we can consequently formulate the following optimization problem to compute the optimal $\boldsymbol{z}$,

$$\boldsymbol{z}^* = \underset{\boldsymbol{z}\in\{0,1\}^N}{\arg\min} \qquad \|\boldsymbol{z}\|_0 \tag{3.24a}$$

$$\text{s.t.} \qquad \sum_{n=1}^{N} z_n \boldsymbol{\mathcal{F}}_B^{(n)} + \boldsymbol{\mathcal{F}}_{\boldsymbol{\theta}} - T_f \boldsymbol{I}_D \succeq 0, \tag{3.24b}$$

where the $\ell_0$ norm $\|\boldsymbol{z}\|_0$ represents the number of non-zero elements of $\boldsymbol{z}$. Note that the constraint in (3.24b) is a linear matrix inequality (LMI) in semidefinite programming, thus it is convex in $\boldsymbol{z}$. However the objective function is not convex, which prevents us to solve the optimization problem (3.24) efficiently. To address this problem, a prevailing technique is to relax the $\ell_0$ norm to $\ell_1$ norm, i.e. $\|\boldsymbol{z}\|_0 \to \|\boldsymbol{z}\|_1 = \mathbf{1}_N^T \boldsymbol{z}$, where $\mathbf{1}_N$ is the all-one vector with dimention $N$. At the same time allowing the domain of $\boldsymbol{z}$ to be chosen from $[0,1]^N$. The relaxed optimization problem is then given by,

$$\hat{\boldsymbol{z}} = \underset{\boldsymbol{z}\in[0,1]^N}{\arg\min} \qquad \|\boldsymbol{z}\|_1 \tag{3.25a}$$

$$\text{s.t.} \qquad \sum_{n=1}^{N} z_n \boldsymbol{\mathcal{F}}_B^{(n)} + \boldsymbol{\mathcal{F}}_{\boldsymbol{\theta}} - T_f \boldsymbol{I}_D \succeq 0. \tag{3.25b}$$

Thanks to its convexity, this optimization problem can be solved effectively. Since the solution of (3.25) is not a binary vector, we need to transform it to decide which sensors should be selected. One straightforward way to do this is to select sensors one by one according to $\hat{\boldsymbol{z}}$ in the solution of (3.25). Specifically, given the solution of (3.25), each time we select one sensor from the unselected group whose corresponding $\hat{z}_n$ is the highest among all sensors unselected. This process goes on until the minimum eigenvalue of the Fisher information $\boldsymbol{\mathcal{F}}_{\mathrm{B}}(\boldsymbol{\theta})$ of the selected sensors is larger than the threshold $T_f$. The specific algorithm is summarized in Algorithm 1.

**Algorithm 1** Transformation of the selection vector of the relaxed optimization problem

1: **procedure**
2: Initial: Given the solution $\hat{\boldsymbol{z}} \triangleq [\hat{z}_1, \hat{z}_2, ...\hat{z}_N]$, let $\Omega$ be the set containing the elements of $\boldsymbol{z}$. Define an empty set $\mathcal{J}_z = \emptyset$
3: Step 1: $z_m = \max\{\Omega\}$.
4: Step 2: Put the corresponding sensor index of $z_m$ into $\mathcal{J}_z$, delete $z_m$ from $\Omega$.
5: Step 3: Compute $\boldsymbol{\mathcal{F}}_B(\boldsymbol{z}) = \sum_{j \in \mathcal{J}_z} \boldsymbol{\mathcal{F}}_B^{(j)}$
6: Step 4: If $\lambda_{\min}\{\boldsymbol{\mathcal{F}}_B(\boldsymbol{z})\} \geq T_f$, go to Step 6. Otherwise repeat step 1.
7: **end procedure**
8: Define an all-zero vector $\check{\boldsymbol{z}}$, and we set $\check{z}_j = 1, j \in \mathcal{J}_z$. $\check{\boldsymbol{z}}$ is the transformed solution.

### 3.2.3 Equivalence Theorem

Let the solutions of the original optimization problem (3.24) and the binary transformed solution of the relaxed optimization problem (3.25) be denoted by $\boldsymbol{z}^*$ and $\check{\boldsymbol{z}}$, respectively. Generally, $\boldsymbol{z}^*$ and $\check{\boldsymbol{z}}$ will not be equivalent, and we cannot say much about the gap $\|\boldsymbol{z}^* - \hat{\boldsymbol{z}}\|_2$. However, we can prove their equivalence under the assumptions listed below:

**Assumption 3.** The regressors $\boldsymbol{h}_i, i = 1, 2, ..., N$ satisfy the following:

$$\text{either} \quad \boldsymbol{h}_i^T \boldsymbol{h}_j = 0 \text{ or } \boldsymbol{h}_i = g_{i,j}\boldsymbol{h}_j, \ i, j = 1, 2, ..., N, \tag{3.26}$$

where $g_{i,j}$ is a scalar constant. Furthermore, there always exists at least one set of sensors $\mathcal{S}$, with size $|\mathcal{S}| = D$, whose corresponding regressors are mutually orthogonal, i.e., they satisfy $\boldsymbol{h}_i^T \boldsymbol{h}_j = 0$, for all $i, j \in \mathcal{S}$.

This assumption suggests that the $\boldsymbol{h}_n$'s are either orthogonal or linear correlated with each other, for $n = 1, 2, ..., N$, and at the same time, $\boldsymbol{H} := [\boldsymbol{h}_1, \boldsymbol{h}_2, ..., \boldsymbol{h}_N]$ is a full row rank matrix. This assumption is needed to decompose the convex problem into a linear programming problem per dimension.

It is useful to fix the ideas with a simple example. Let the number of sensors be 6 and let the dimension of $\boldsymbol{\theta}$ be $D = 3$. Suppose the first three sensors labeled $1, 2, 3$ have regressors that are mutually orthogonal, and so the second three sensors $(4, 5, 6)$. In this case, there are two sets $\mathcal{S}$, namely $\mathcal{S}_1 = \{1, 2, 3\}$ and $\mathcal{S}_2 = \{4, 5, 6\}$. In addition, we suppose that sensors 1 and 4 are linearly correlated, and so the couples 2 and 5, and 3 and 6 (note: linearly correlated means they are measuring the "same space").

**Assumption 4.** The sensors have different regressors $\boldsymbol{h}_i$ and channels, so that the product $a_i \|\boldsymbol{h}_i\|_2^2$ with

$$a_i = \mathbb{E}_{\boldsymbol{\theta}} \left\{ \frac{(1 - 2\text{Pe}_i)^2}{s_i^2(1 - s_i)^2} f_i^2(\tau_i - \boldsymbol{h}_i^T \boldsymbol{\theta}) \right\}$$

is different for each sensor.

**Assumption 5.** The pdfs of the elements of $\boldsymbol{\theta}$ are independent with each other and they are identical.

We then have the following theorem,

**Theorem 1.** *Let $\boldsymbol{z}^*$ be the optimal solution of the optimization problem* (3.24)*. This solution is not unique in general, so let $Z^*$ be the finite set of optimal solutions, i.e., $\boldsymbol{z}^* \in Z^*$.*
*Under Assumption 3, Assumption 4, and Assumption 5, the solution of the relaxed optimization problem* (3.25)*, once mapped to $\{0, 1\}$ via Algorithm 1 also belongs to the set $Z^*$.*

*Proof.* See Appendix 3.4.1

□

The theorem that we have just proven says that the relaxation and the Algorithm 1 are not completely arbitrary way to approximate the solution of the original non convex problem (3.24). In fact, under some assumptions their solution are equivalent.

**Disclaimer:** *the assumptions that we have used to prove the theorem in this section, can be considered restrictive (especially Assumption 3). These assumptions had the only purpose to help us show that our relaxation was not completely arbitrary. As such, they will not be used anywhere else in this thesis.*

### 3.2.4 Simulation

In this part, we validate the theoretical derivation and approach by numerical simulations.

We consider a group of 64 sensors deployed in a grid manner on a two-dimensional plane. The distance between two subsequent sensors is 1. There are two sources located in particular locations (Figure 3.2). The signal strength from source $d$ ($d = 1$ or 2) at sensor $n$ is $h_{n,d}\theta_d$, with

$$h_{n,d} = \exp\left(-\frac{\mathcal{D}_{n,d}}{\sigma^2}\right), \tag{3.27}$$

where $\mathcal{D}_{n,d}$ is the distance between sensor $n$ and source $d$, and $\sigma$ is a known parameter [21]. We can then generate all the regressors $\boldsymbol{h}_n, n = 1, 2, ..., N$ by this model. Let the distribution of $\boldsymbol{\theta}$ be $\mathcal{N}(3, \boldsymbol{\Sigma_\theta})$, where the covariance matrix $\boldsymbol{\Sigma_\theta}$ is a diagonal matrix and the diagonal elements are all 0.5.

The primary step for this simulation is to construct the Bayesian Fisher information presented in (3.15). Notice that there is no closed form expression for the expectation over $\boldsymbol{\theta}$, alternatively, we choose a Monte-Carlo approach to approximate the term

$$\mathbb{E}_{\boldsymbol{\theta}}\left\{\frac{(1-2\mathrm{Pe}_n)^2}{s_n(1-s_n)} f_n^2(\tau_n - \boldsymbol{h}_n^T\boldsymbol{\theta})\right\} \tag{3.28}$$

for each $n$. Specifically 100 realizations of $\boldsymbol{\theta}$ are drawn from its distribution, denoted as $\widetilde{\boldsymbol{\theta}}_i$, $i = 1, 2, ..., 100$. The estimation of this term is

$$\mathbb{E}_{\boldsymbol{\theta}}\left\{\frac{(1-2\mathrm{Pe}_n)^2}{s_n(1-s_n)} f_n^2(\tau_n - \boldsymbol{h}_n^T\boldsymbol{\theta})\right\} \approx \frac{1}{100}\sum_{i=1}^{100} \frac{(1-2\mathrm{Pe}_n)^2}{\widetilde{s}_{n,i}(1-\widetilde{s}_{n,i})} f_n^2(\tau_n - \boldsymbol{h}_n^T\widetilde{\boldsymbol{\theta}}_i), \tag{3.29}$$

where $\widetilde{s}_{n,i}$ is the $s_n$ corresponding to $\widetilde{\boldsymbol{\theta}}_i$. The threshold is set to the value $\tau_n = \boldsymbol{h}_n^T \boldsymbol{\theta}_\mu$, where $\boldsymbol{\theta}_\mu$ is the mean of $\boldsymbol{\theta}$. Anyway, one knows nothing about whether this is optimal threshold for a sensor or not, and we leave the determination of optimal threshold in this case as the future work. With this we can solve the relaxed optimization problem (3.25). To solve the relaxed optimization problem we adopt CVX [24], which is a solver for convex optimization in Matlab. We transform the solution of the relaxed optimization to a binary vector by Algorithm 1, and decide the selected sensors by the transformed solution.

To obtain an approximated Bayesian mean square error, for each $\widetilde{\theta}_i$, 500 groups of measurements and quantized bit data of the *selected* sensor are generated based on pre-defined Pe and noise distribution, and accordingly 500 MAP estimates, $\widetilde{\boldsymbol{\theta}}_{i,j}, i = 1, 2, ..., 100, j = 1, 2, ..., 500$ are produced by (3.9) which is solved by the function Fmincon in Matlab (the problem is convex but it is difficult to put it as a SDP and solve it in CVX). The corresponding approximated mean square error of the particular $\widetilde{\boldsymbol{\theta}}_i$ is then,

$$\mathrm{MSE}_i = \frac{1}{500} \sum_{j=1}^{500} \left(\widetilde{\boldsymbol{\theta}}_{i,j} - \widetilde{\theta}_i\right)^T \left(\widetilde{\boldsymbol{\theta}}_{i,j} - \widetilde{\theta}_i\right). \tag{3.30}$$

The approximated Bayesian mean square error is then the average of the 100 $\mathrm{MSE}_i$, i.e.,

$$\mathrm{BMSE} = \frac{1}{100} \sum_{i=1}^{100} \mathrm{MSE}_i. \tag{3.31}$$

In the first simulation we vary the threshold $T_f$, from 10 to 38 with an interval of 2. The variances of the noise of each sensor are set to be the same, that is 0.5. The bit error rate of each sensor is also the same. Three values of the bit error rate are considered, and they are 0, 0.1 and 0.2. Figure 3.3 depicts the selected value when $T_f = 24, \mathrm{Pe} = 0.2$, before and after the transformation, and we mark the corresponding selected sensors in Figure 3.2 with black squares. The completed performance metrics (the minimum eigenvalue of Fisher information) of the different bit error rates with respect to the threshold $T_f$ are presented in Figure 3.4. In this figure, it is clear that all curves are above the dotted line, which is the case when the minimum eigenvalue equals $T_f$. These figures confirm the validation of the selected algorithm, that is, the minimum eigenvalue of the FIM of the selected sensors is equal to or larger than $T_f$.

To compare the differences of the cases of three bit error rates, we depict the resulted numbers of selected sensors in Figure 3.5. The curve of $\mathrm{Pe} = 0.1$ is above that of $\mathrm{Pe} = 0$, and the curve $\mathrm{Pe} = 0.2$ is above the other two. This phenomenon implies that for the same $T_f$, when the bit error rate is higher, more sensors are needed to meet the same performance requirement, because the worse wireless channels deteriorate the signal from sensors to fusion center. This phenomenon can also be caused by the measurement noise. In Figure 3.6, we fix the bit error rate to be 0 for all sensors, but this time we simulate 3 cases when the noise variances of all sensors are $\sigma = 0.5, 0.65$ and 0.8, respectively.

In Figure 3.7, we plot the Bayesian mean squares error of MAP estimator versus the Tf. From it we can when the threshold $T_f$ is increasing, the Bayesian mean squares error is decreasing accrodingly.

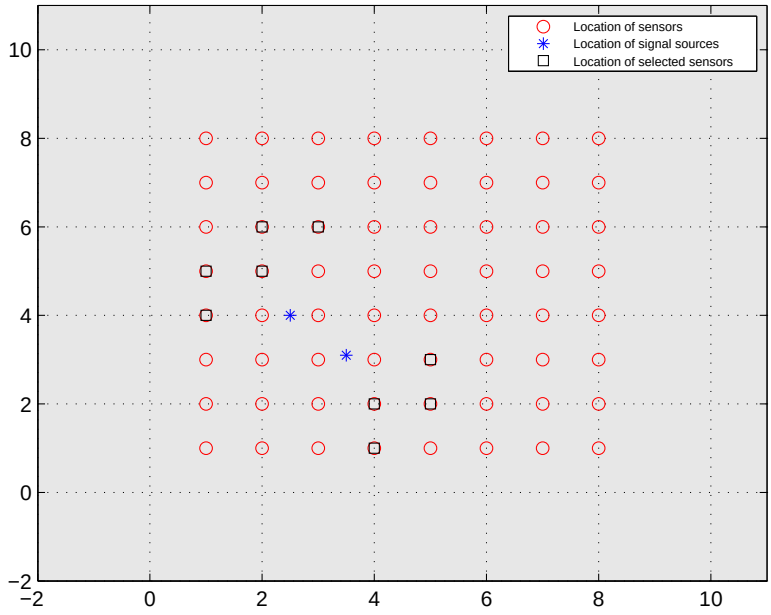


Figure 3.2: The locations of sensors and signal sources.

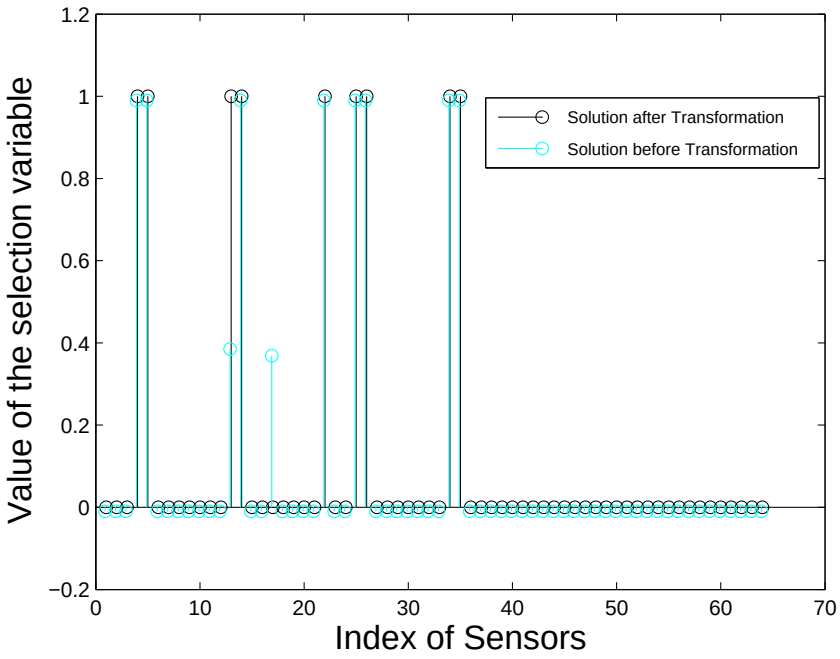


Figure 3.3: The values of the selection vector, with Pe $= 0.2, \sigma = 0.5$ for all sensors.

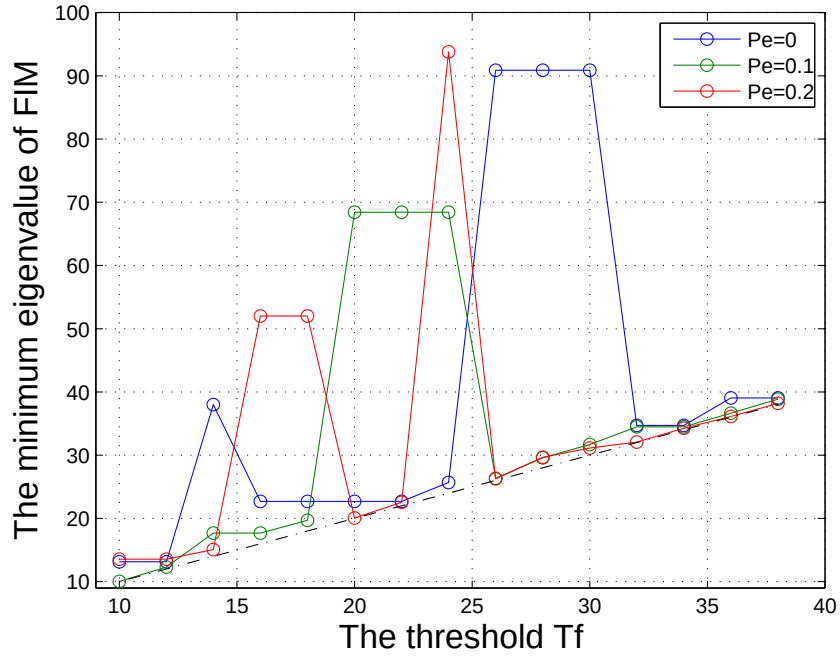


Figure 3.4: The minimum eigenvalue of the FIM with a fixed $\sigma = 0.5$ for all sensors.

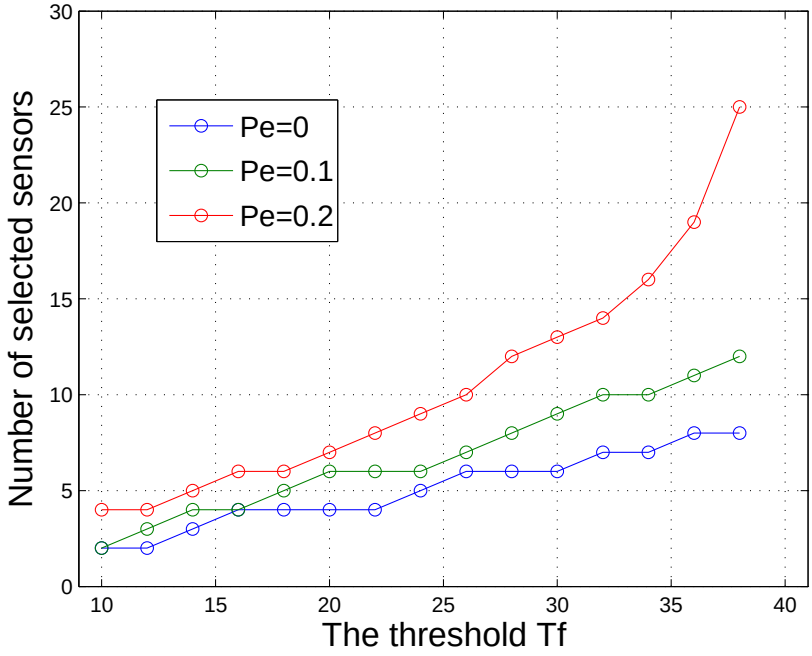


Figure 3.5: Number of selected sensors with a fixed $\sigma = 0.5$ for all sensors.

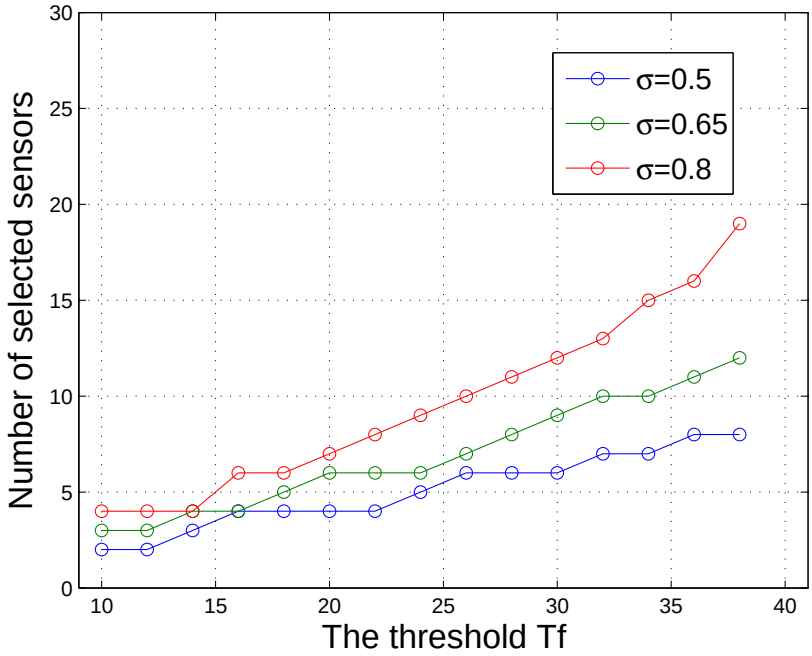


Figure 3.6: Number of selected sensors with a fixed $\mathrm{Pe} = 0$ for all sensors.

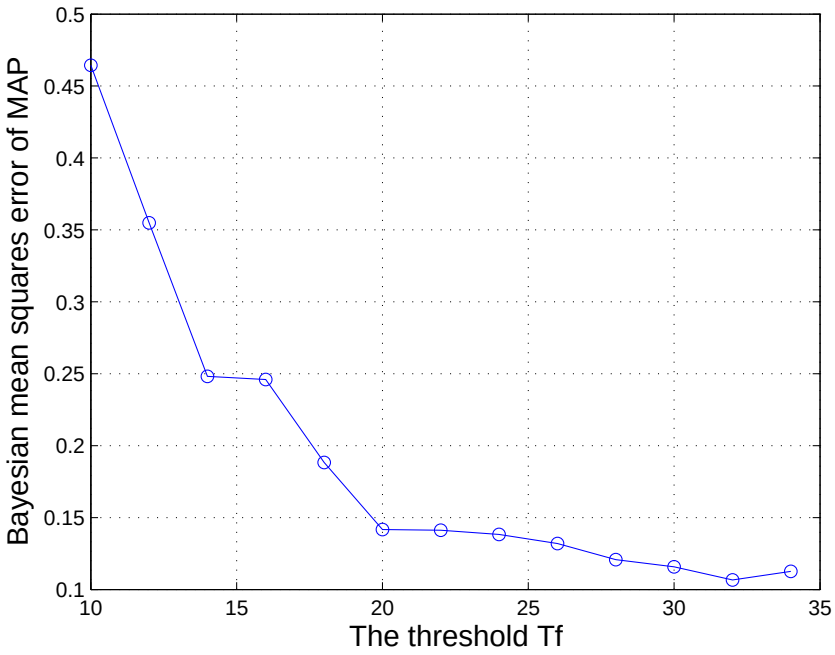


Figure 3.7: Bayesian mean squares error, with noise variances are all 0.5, and bit error rates are all 0.1

## 3.3 Conclusion

In this chapter, we have discussed a framework of WSNs using a one-bit quantization scheme, considering the measurement noise and distortion of data in the wireless channel which is modeled by a related bit error rate. We have seen how to model the sensor selection problem as a convex optimization problem, in which a relaxation technique is adopted. We further analyzed the equivalence of the solutions of the original optimization problem and the relaxed optimization problem. Simulation examples confirm the correction of the theoretical derivations and validation of the relaxed optimization problem for sensor selection.

As for future work in this direction, we propose the following sensor selection refined model.

### 3.3.1 Refined sensor selection model

The sensor selection model (3.24) selects the minimum number of sensors to meet the requirement (3.23). Generally, the optimal solution of the original optimization problem is not unique, i.e., more than one sub-set of sensors have the same minimum number of sensors and their corresponding minimum eigenvalues meet the requirement. It is quite interesting to investigate how to recognize the best one among the qualified sub-sets of sensors, i.e., its minimum eigenvalue of the Fisher information is largest among all. To this aim, we propose a refined model,

$$\{\boldsymbol{z}^*, t^*\} = \underset{\boldsymbol{z}\in\{0,1\}^N,\ t}{\operatorname{argmin}} \ \|\boldsymbol{z}\|_0 - \mu t \tag{3.32a}$$

$$\text{s.t.} \ \sum_n z_n \boldsymbol{F}_B^{(n)} - t\boldsymbol{I}_D \succeq \boldsymbol{0}, \tag{3.32b}$$

$$t \geq T_f, \tag{3.32c}$$

where $\mu$ is a constant which can be altered to change the weights on $\|\boldsymbol{z}\|_0$ and $t$. In this new model, we make a compromise between the number of sensor to activate and the performance requirement. The latter aspect is implemented by allowing the performance threshold, denoted by $t$, to be changeable and a parameter to be optimized. To guarantee a certain performance level, we impose on $t$ that it should be larger than a pre-designed threshold $T_f$. In this case, the choice of $T_f$ becomes less critical, in the sense that a comparable small $T_f$ can also lead to a high performance solution of sensor selection. As usual, we relax (3.32) such that it becomes a convex optimization problem,

$$\{\hat{\boldsymbol{z}}, \hat{t}\} = \underset{\boldsymbol{z}\in[0,1]^N,\ t}{\arg\min} \ \|\boldsymbol{z}\|_1 - \mu t \tag{3.33a}$$

$$\text{s.t.} \ \sum_n z_n \boldsymbol{F}_B^{(n)} - t\boldsymbol{I}_D \succeq \boldsymbol{0}, \tag{3.33b}$$

$$t \geq T_f, \tag{3.33c}$$

Note that the weighted factor $\mu$ is crucial, and we leave the further analysis for future studies.

## 3.4 Appendix

### 3.4.1 Proof of Theorem 1

Define:
$a_n := \mathbb{E}_{\boldsymbol{\theta}}\left\{\frac{(1-2\mathrm{Pe}_n)^2}{s_n^2(1-s_n)^2} f_n^2(\tau_n - \boldsymbol{h}_n^T\boldsymbol{\theta})\right\}$
$\boldsymbol{\mathcal{F}}_B^u := \sum_{n=1}^{N} \boldsymbol{\mathcal{F}}_B^{(n)}$

With these definitions, we have $\boldsymbol{\mathcal{F}}_B^{(n)} = a_n \boldsymbol{h}_n \boldsymbol{h}_n^T$, and $\boldsymbol{\mathcal{F}}_B = \boldsymbol{\mathcal{F}}_B^u + \boldsymbol{\mathcal{F}}_{\boldsymbol{\theta}}$ (see (3.15)). Define now the sets $\mathcal{G}_d, d = 1, 2, ..., D$, which contain the indexes of sensors whose $\boldsymbol{h}_j$ are linearly correlated. In our previous example these sets are $\mathcal{G}_1 = \{1, 4\}$, $\mathcal{G}_1 = \{2, 5\}$, and $\mathcal{G}_1 = \{3, 6\}$. The number of these sets is $D$ due to Assumption 3. Furthermore, for the same assumption for all $j \in \mathcal{G}_d$, the ratios $\frac{\boldsymbol{h}_j}{\|\boldsymbol{h}_j\|_2}$ are equivalent to each other, and we define it as,

$$\hat{\boldsymbol{h}}_d := \frac{\boldsymbol{h}_j}{\|\boldsymbol{h}_j\|_2}, \; j \in \mathcal{G}_d, \quad d = 1, 2, \ldots, D. \tag{3.34}$$

We can further show that $\hat{\boldsymbol{h}}_d$ is one of the eigenvectors of $\boldsymbol{\mathcal{F}}_B^u$. In fact, its norm is unitary, i.e., $\|\hat{\boldsymbol{h}}_d\| = 1$, and according to Assumption 3,

$$\begin{aligned}
\boldsymbol{\mathcal{F}}_B^u \hat{\boldsymbol{h}}_d &= \left[\sum_{j\in\mathcal{G}_d} a_j \boldsymbol{h}_j \boldsymbol{h}_j^T + \sum_{j\notin\mathcal{G}_d} a_j \boldsymbol{h}_j \boldsymbol{h}_j^T\right] \hat{\boldsymbol{h}}_d \\
&= \left[\sum_{j\in\mathcal{G}_d} a_j \boldsymbol{h}_j \boldsymbol{h}_j^T\right] \hat{\boldsymbol{h}}_d \\
&= \left[\sum_{j\in\mathcal{G}_d} a_j \|\boldsymbol{h}_j\|_2^2 \frac{\boldsymbol{h}_j}{\|\boldsymbol{h}_j\|_2} \frac{\boldsymbol{h}_j^T}{\|\boldsymbol{h}_j\|_2}\right] \hat{\boldsymbol{h}}_d = \left[\sum_{j\in\mathcal{G}_d} a_j \|\boldsymbol{h}_j\|_2^2 \, \hat{\boldsymbol{h}}_d \, \hat{\boldsymbol{h}}_d^T \, \hat{\boldsymbol{h}}_d\right] \\
&= \left[\sum_{j\in\mathcal{G}_d} a_j \|\boldsymbol{h}_j\|_2^2\right] \hat{\boldsymbol{h}}_d,
\end{aligned} \tag{3.35}$$

where we have used the fact that sensors in $\mathcal{G}_d$ have regressors that are orthogonal to the ones outside the set (Assumption 3), the definition of $\hat{\boldsymbol{h}}_d$ and the fact that its norm is unitary.
Therefore $\hat{\boldsymbol{h}}_d$ is one of the eigenvectors of $\boldsymbol{\mathcal{F}}_B^u$, and $\sum_{j\in\mathcal{G}_d} a_j \|\boldsymbol{h}_j\|_2^2$ is the corresponding eigenvalue. Consequently, we have the following eigenvalue decomposition of $\boldsymbol{\mathcal{F}}_B^u$,

$$\begin{aligned}
\boldsymbol{\mathcal{F}}_B^u =& [\hat{\boldsymbol{h}}_1, \hat{\boldsymbol{h}}_2, ..., \hat{\boldsymbol{h}}_D] \begin{bmatrix} \sum_{j\in\mathcal{G}_1} a_j \|\boldsymbol{h}_j\|_2^2 & & \\ & \ddots & \\ & & \sum_{j\in\mathcal{G}_D} a_j \|\boldsymbol{h}_j\|_2^2 \end{bmatrix} [\hat{\boldsymbol{h}}_1, \hat{\boldsymbol{h}}_2, ..., \hat{\boldsymbol{h}}_D]^T \\
=& \boldsymbol{U}\boldsymbol{\Lambda}\boldsymbol{U}^T,
\end{aligned} \tag{3.36}$$

where

$$\begin{aligned}\boldsymbol{U} :=&[\hat{\boldsymbol{h}}_1, \hat{\boldsymbol{h}}_2, ..., \hat{\boldsymbol{h}}_D] \\ \boldsymbol{\Lambda} :=&\begin{bmatrix} \sum\limits_{j\in\mathcal{G}_1} a_j\|\boldsymbol{h}_j\|_2^2 & & \\ & \ddots & \\ & & \sum\limits_{j\in\mathcal{G}_D} a_j\|\boldsymbol{h}_j\|_2^2 \end{bmatrix}.\end{aligned} \tag{3.37}$$

As for $\boldsymbol{\mathcal{F}_\theta}$, we have,

$$\{\boldsymbol{\mathcal{F}_\theta}\}_{i,j} = \mathbb{E}_\theta\left\{\frac{\partial \ln p(\boldsymbol{\theta})}{\partial\theta_i}\frac{\partial \ln p(\boldsymbol{\theta})}{\partial\theta_j}\right\}. \tag{3.38}$$

Based on Assumption (5) and the regularity property of $p(\boldsymbol{\theta})$, if $i \neq j$,

$$\begin{aligned}\{\boldsymbol{\mathcal{F}_\theta}\}_{i,j} =&\mathbb{E}_\theta\left\{\frac{\partial \ln p(\theta_i)}{\partial\theta_i}\frac{\partial \ln p(\theta_j)}{\partial\theta_j}\right\} \\ =&\mathbb{E}_\theta\left\{\frac{\partial \ln p(\theta_i)}{\partial\theta_i}\right\}\mathbb{E}_\theta\left\{\frac{\partial \ln p(\theta_j)}{\partial\theta_j}\right\} \\ =&0.\end{aligned} \tag{3.39}$$

Similarly, when $i = j$,

$$\begin{aligned}\{\boldsymbol{\mathcal{F}_\theta}\}_{i,j} =&\mathbb{E}_\theta\left\{\frac{\partial \ln p(\theta_i)}{\partial\theta_i}\frac{\partial \ln p(\theta_j)}{\partial\theta_j}\right\} \\ =&\mathbb{E}_\theta\left\{\left(\frac{\partial \ln p(\theta_i)}{\partial\theta_i}\right)^2\right\} \\ =:&\mathcal{F}_\theta^s.\end{aligned} \tag{3.40}$$

Therefore we have the expression for $\boldsymbol{\mathcal{F}_\theta}$,

$$\boldsymbol{\mathcal{F}_\theta} = \mathcal{F}_\theta^s\ \boldsymbol{I}_D. \tag{3.41}$$

Based on (3.36) and (3.41), $\boldsymbol{\mathcal{F}}_B$ can be re-cast as,

$$\begin{aligned}\boldsymbol{\mathcal{F}}_B =&\boldsymbol{\mathcal{F}}_B^u + \boldsymbol{\mathcal{F}_\theta} \\ =&\boldsymbol{U}\boldsymbol{\Lambda}\boldsymbol{U}^T + \mathcal{F}_\theta^s\ \boldsymbol{I}_D \\ =&\boldsymbol{U}\left(\boldsymbol{\Lambda} + \mathcal{F}_\theta^s\ \boldsymbol{I}_D\right)\boldsymbol{U}^T\end{aligned} \tag{3.42}$$

Given (3.42), (3.23) is equivalent to,

$$\boldsymbol{\Lambda} + \mathcal{F}_\theta^s\ \boldsymbol{I}_D = \begin{bmatrix} \sum\limits_{j\in\mathcal{G}_1} a_j\|\boldsymbol{h}_j\|_2^2 + \mathcal{F}_\theta^s & & \\ & \ddots & \\ & & \sum\limits_{j\in\mathcal{G}_D} a_j\|\boldsymbol{h}_j\|_2^2 + \mathcal{F}_\theta^s \end{bmatrix} \succeq T_f\boldsymbol{I}_D, \tag{3.43}$$

or,

$$\sum_{j \in \mathcal{G}_d} a_j \|\boldsymbol{h}_j\|_2^2 + \mathcal{F}_\theta^s \geq T_f, \ d = 1, 2, ..., D. \tag{3.44}$$

Based on this, the original optimization problem (3.24) becomes,

$$\underset{\boldsymbol{z} \in \{0,1\}^N}{\arg\min} \quad \|\boldsymbol{z}\|_0 \tag{3.45a}$$

$$\text{s.t.} \quad \sum_{j \in \mathcal{G}_d} z_j \ a_j \|\boldsymbol{h}_j\|_2^2 + \mathcal{F}_\theta^s \geq T_f, \ d = 1, 2, ..., D \ , \tag{3.45b}$$

and the equivalent relaxed optimization problem (3.25) is then,

$$\underset{\boldsymbol{z} \in [0,1]^N}{\arg\min} \quad \|\boldsymbol{z}\|_1 \tag{3.46a}$$

$$\text{s.t.} \quad \sum_{j \in \mathcal{G}_d} z_j \ a_j \|\boldsymbol{h}_j\|_2^2 + \mathcal{F}_\theta^s \geq T_f, \ d = 1, 2, ..., D \ . \tag{3.46b}$$

The constraints in (3.46b) are linear and they decouple across the dimension $d$. For each dimension, given that the optimization problem (3.46) is a linear program and the coefficients $a_j \|\boldsymbol{h}_j\|_2^2$ are all different among each other (Assumption 4), its solution will lay on the vertices of the polytope described by the constraints. In particular, for each $j \in \mathcal{G}_d$ the solution component $\hat{z}_j$ will be either 0, 1, or in only one case a number between 0 and 1. After Algorithm 1, the non-Boolean components will be mapped to 1.

It is not difficult to see that this mapped solution is, in addition, a solution of the optimization problem (3.45): in fact, it is feasible and it has the minimum cardinality as possible. Thus the mapped solution of (3.46) with Algorithm 1 belongs to $Z^*$.

# Wireless sensor network with Multi-Bit Quantization

# 4

In this chapter, we introduce a multi-bit quantization scheme such that the original measurements are quantized to multiple bits to be transmitted through the wireless channel. Then the important parameters of this quantization approach, like aggregated errors, Bayesian Cramer-Rao Bound and Bayesian mean square errors etc., are derived, with and without bit errors. Based on the derived Bayesian Cramer-Rao lower bound we develop the bit allocation algorithm to optimally decide the numbers of bits for each sensors to transmit. In our approach, the performance metric is expressed by defined selection vectors, and we restrict the performance metric to be larger than a threshold and minimize a defined cost function whose value is determined by the selection vectors.

Table 4.1: Definition of key variables in this Chapter

| Variables | Definition |
|---|---|
| $y_n$ | The original measurement of sensor $n$ |
| $L$ | $y_n \in (-L, L)$ |
| $x_n$ | The convert value of $y_n$, $x_n = \frac{L+y_n}{2L}$ |
| $b_{n,i}$ | The $i$-th MSB of $x_n$ |
| $\hat{x}_n$ | The quantized value of $x_n$ |
| $K_n$ | The number of MSB of $\hat{x}_n$ |
| $\hat{y}_n$ | The quantized value of $y_n$, $\hat{y}_n = 2L\hat{x}_n - L$ |
| $\varphi(.)$ | A function that relates $y_n$ and $\hat{y}_n$, $\hat{y}_n = \varphi(y_n, K_n)$ |
| $\hat{\epsilon}_n$ | The integrated error, $\hat{\epsilon}_n = \hat{y}_n - y_n$ |
| $\mathcal{S}_{K_n}$ | $\mathcal{S}_{K_n} := \{L2^{-K_n} \times 0 - L,\ L2^{-K_n} \times 1 - L,\ L2^{-K_n} \times 2 - L,$ $, ...,\ L2^{-K_n} \times (2^{K_n} - 1) - L\}$ |
| $s_{K_n}(j)$ | The $j$-th elements of $\mathcal{S}_{K_n}$ |
| $y_n^*$ | The noiseless measurement of sensor $n$, $y_n^* = \boldsymbol{h}_n^T \boldsymbol{\theta}$ |
| $\widetilde{y}_n$ | Received value of $\hat{y}_n$ at the fusion center due to bit errors |
| $\varepsilon_n^e$ | Integrated error in the case of bit errors, $\varepsilon_n^e = \widetilde{y}_n - y_n$ |

## 4.1 Multi-bit Quantization Approach

### 4.1.1 Bounded Measurement Model

To proceed with the multi-bit quantization discussion, we make a reasonable assumption on the measurement model $y_n = \boldsymbol{h}_n \boldsymbol{\theta} + w_n$.

**Assumption 6.** *The zero-mean noise $w_n$ is bounded as $(-B, B)$, where $B$ is a positive scalar, and each element of $\boldsymbol{\theta}$ and $\boldsymbol{h}_n$ are also bounded. As a result, we can always find a positive scalar $L$ for which the measurement of each sensor $y_n$ is bounded as $(-L, L)$.*

We remark that, it is quite reasonable to make such an assumption. In fact, although most noise models are unbounded, the probability for the noise to be very large is very small and (we assume here) negligible. Given this, we can set a threshold $B$ that is large enough such that the probability $p_n(w_n)$ is practically zero if $w_n \in (-\infty, -B] \bigcup [B, \infty)$. Therefore, when dealing with unbounded noise, we can truncate the pdf $p_n(w_n)$ in a way that outside $(-B, B)$, it becomes zero. To make the integral of the probability equal to 1, the probability is scaled up as

$$\overline{f}_n(w_n) = \begin{cases} \left(1 + \dfrac{F_n(-B) + 1 - F_n(B)}{F_n(B) - F_n(-B)}\right) f_n(w_n) & , \text{ if } w_n \in (-B, B) \\ 0 & , \text{ otherwise} \end{cases} \tag{4.1}$$

i.e., $f_n(w_n)$ and $F_n(w_n)$ are the pdf and cdf of the original noise, respectively, and $\overline{f}_n(w_n)$ is the truncated and scaled version of $f_n(w_n)$. By such a transformation, the integral of $\overline{f}_n(w_n)$ over $(-B, B)$ equals one.

In practice, we assume that when a sensor obtains measurements that are outside the range $(-L, L)$, a censored action is taken to abandon the "outlier", such that no out-ranged measurement will be transmitted to the fusion center [26, 27]. In what follows, we just assume that $w_n$ has a bounded pdf, as well as $y_n$ (i.e., Assumption 6 holds).

### 4.1.2 Multi-Bit Quantization When No Bit Error Occurs

We start our analysis by considering the case in which there is no bit error in the communication of the quantized measurements.

Given that the measurement $y_n$ is bounded as $y_n \in (-L, L)$ for all $n$, we can map it, at the local sensor, to a variable $x_n$ that varies between $(0, 1)$ as

$$x_n = \frac{L + y_n}{2L}. \tag{4.2}$$

Express now the mapped $x_n$ by its binary form,

$$x_n = \sum_{i=1}^{\infty} b_{n,i} 2^{-i}, \quad \text{with} \quad b_{n,i} \in \{0, 1\}, \tag{4.3}$$

where $b_{n,i}$ is defined as the $i$-th most significant bit (MSB) of $x_n$. We can form a message $\mathcal{M}_n$ that contains the first $K_n$ MSBs of $x_n$ as,

$$\mathcal{M}_n = \{b_{n,1}, b_{n,2}, ..., b_{n,K_n}\} \tag{4.4}$$

and this message is sent to the fusion center through the wireless channel. The message will be then used to reconstruct the quantized value of $x_n$ at the fusion center, by using the $K_n$ MSBs,

$$\hat{x}_n = \sum_{i=1}^{K_n} b_{n,i} 2^{-i}. \tag{4.5}$$

In this part, we assume the wireless channel to be perfect, that is: no bit error occurs during transmission; therefore the message $\mathcal{M}_n$ will be correctly received at the fusion center. We also note that the numbers of MSBs $K_n$ may be different across sensors because measurements of different sensors have different quality, (we will describe how to select the best quantization later, in the Bit Allocation Algorithm, in Section 4.2). The approximation of the measurement $y_n$ at the fusion center is consequently [Cfr. (4.2)],

$$\hat{y}_n = 2L\hat{x}_n - L. \tag{4.6}$$

We can see $\hat{y}_n$ as a function of the original measurement $y_n$ to be reconstructed and the number of MSBs $K_n$ as

$$\hat{y}_n = \varphi(y_n, K_n), \tag{4.7}$$

where $\varphi(\cdot, \cdot)$ is the nonlinear function that summarizes the steps from encoding (4.2) to reconstruction (4.6).

The framework with multi-bit transmission that we present in this part is visualized in Figure 4.1. In the figure, the measurement $y_n$ in sensor $n$ is converted to $x_n$. After quantizing $x_n$, the $K_n$ MSBs of $x_n$ are preserved to generate the quantized value $\hat{x}_n$. The $K_n$ MSBs are contained in a message $\mathcal{M}_n$, which is transmitted through the errorless wireless channel to the fusion center. At the fusion center, $\hat{x}_n$ is correctly decoded. A quantized value of the original measurement of $y_n$, is then reconstructed and it is denoted by $\hat{y}_n$.

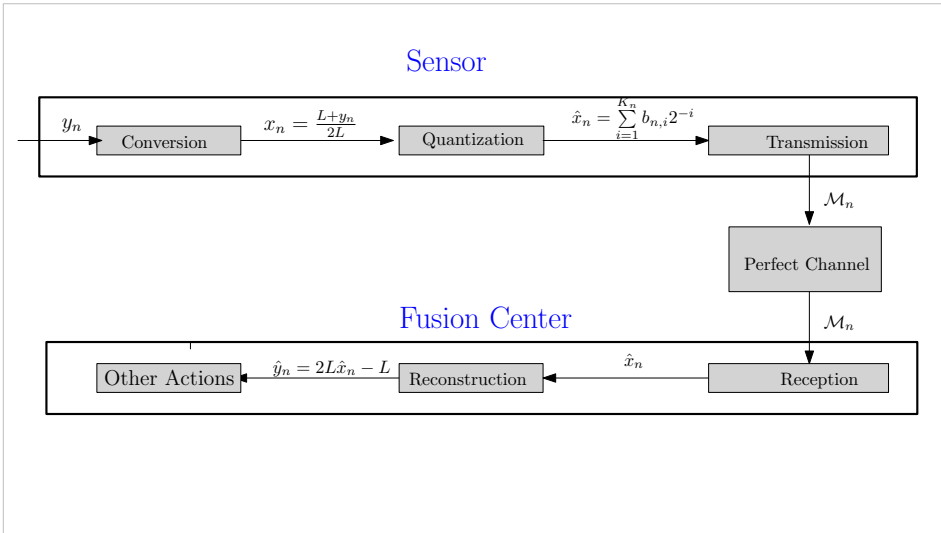


Figure 4.1: Procedure of transmission and reception by multi-bit quantization in a perfect wireless channel.

### 4.1.3 Aggregated Error in the Case of No Bit Error

When we use the multi-bit quantization scheme to send only the $K_n$ MSBs of each sensor's measurement, not only the measurement noise $w_n$ is involved, but the quanti-

zation error is introduced. The aggregated error for sensor $n$ that contains these two sources of errors is defined as,

$$\varepsilon_n = \hat{y}_n - \boldsymbol{h}_n^T \boldsymbol{\theta}. \tag{4.8}$$

An extreme case is when we send an infinite number of bits to the fusion center such that $\hat{y}_n = y_n$, and thus $\varepsilon_n$ is exactly the measurement noise $w_n$. In this case, since we have full knowledge about the pdf of $w_n$, the characteristics of it can be exploited for many purposes, such as the derivation of the MSE, or other estimates based on the knowledge of the pdf of $w_n$. Under the same philosophy, we wonder if in the general case — when a finite number of bits is sent — we can characterize the aggregated error $\varepsilon_n$, based on the fact that we already have the knowledge of the pdf of the regular noise $w_n$. In fact, we can show that $\varepsilon_n$ is a discrete distributed random parameter. Prior to this, we compute the possible values of $\hat{y}_n$, and show that they belong to a discrete set.

**Definition 1.** The set $\mathcal{S}_{K_n}$

$$\mathcal{S}_{K_n} := \{0\times L2^{-K_n+1}-L,\ 1\times L2^{-K_n+1}-L,\ 2\times L2^{-K_n+1}-L,\ ...,\ (2^{K_n}-1)\times L2^{-K_n+1}-L\} \tag{4.9}$$

is a sorted set with $2^{K_n}$ elements, and the $i$-th element is denoted as $s_{K_n}(i) = i \times L2^{-K_n+1} - L$.

**Lemma 2.** The quantized value $\hat{y}_n = \varphi(y_n, K_n)$ that is generated via the $K_n$ MSBs has a discrete possible value that belongs to the sorted set $\mathcal{S}_{K_n}$. If $\hat{y}_n = s_{K_n}(j)$ with $j$ a particular integer, then we have

$$y_n \in \Big[s_{K_n}(j)\,,\, s_{K_n}(j) + L2^{-K_n+1}\Big) = \Big[s_{K_n}(j)\,,\, s_{K_n}(j+1)\Big). \tag{4.10}$$

*Proof.* See Appendix 4.4.1. □

With this lemma, we can derive the pdf of the aggregated error $\varepsilon_n$:

**Definition 2.** We define with $y_n^*$ the noiseless measurement, i.e., $y_n^* := \boldsymbol{h}_n^T \boldsymbol{\theta}$, and with $\hat{y}_n^*$ its corresponding quantized value, i.e., $\hat{y}_n^* := \varphi(y_n^*, K_n)$.

**Theorem 3.** When the pdf of $w_n$, i.e., $f_n(w_n)$, and the corresponding cdf $F_n(w_n)$ are known, the aggregated error $\varepsilon_n$, defined in (4.8), is a discrete random parameter. Its possible values are

$$\varepsilon_n(t) = \hat{y}_n^* - y_n^* + tL2^{-K_n+1}, \tag{4.11}$$

with $t$ an integer, and their probabilities are,

$$\begin{aligned} \eta_n(t) := \mathbb{P}\mathrm{r}\big[\varepsilon_n = \varepsilon_n(t)\big] =& \mathbb{P}\mathrm{r}\big[\varepsilon_n(t) \le w_n < \varepsilon_n(t) + L2^{-K_n+1}\big] \\ =& F_n\left(\varepsilon_n(t) + L2^{-K_n+1}\right) - F_n\left(\varepsilon_n(t)\right). \end{aligned} \tag{4.12}$$

*Proof.* See Appendix 4.4.2. □

This theorem states that the aggregated noise has discrete values, and provides the probability distribution of it, which we exploit to derive the Bayesian error covariance matrix and the related Bayesian mean square error in Appendix 4.4.4. Although the Bayesian error covariance matrix has no direct use by far, but the Bayesian mean square of the least square error estimator is tighter to other mean square error than the ones by Bayesian Cramer-Rao lower bound, therefore exploiting Bayesian mean square for bit allocation is defined as our future work.

### 4.1.4 Maximum a Posteriori Estimator and Bayesian Cramer-Rao Lower Bound

Since the quantized value $\hat{y}_n$ has a gap with the original measurement $y_n$ due to quantization, that we see $\boldsymbol{\theta}$ as a random parameter. Generally, it is hard to find a closed-form solution. Therefore, the maximum a posteriori (MAP) is a good choice for the estimation of $\boldsymbol{\theta}$. It considers the prior knowledge of $\boldsymbol{\theta}$ and is easy to obtain if we have the expression of the likelihood function $p(\hat{\boldsymbol{y}}, \boldsymbol{\theta})$, with $\hat{\boldsymbol{y}} = [\hat{y}_1, \hat{y}_2, ..., \hat{y}_N]$.

According to Lemma 2, we have $\hat{y}_n \in \mathcal{S}_{K_n}$, thus we specify $p(\hat{y}_n, \boldsymbol{\theta})$ as $p(\hat{y}_n = s_{K_n}(p), \boldsymbol{\theta})$, therefore the likelihood function can also be factorized as $p(\hat{\boldsymbol{y}}, \boldsymbol{\theta}) = p(\boldsymbol{\theta}) \prod_{n=1}^{N} p(\hat{y}_n = s_{K_n}(p)|\boldsymbol{\theta})$. Since the prior $p(\boldsymbol{\theta})$ is known under Assumption 2, the remaining part is the conditional likelihood function, $p(\hat{y}_n = s_{K_n}(p)|\boldsymbol{\theta})$. In fact, based on Lemma 2, a necessary and sufficient condition for $\hat{y}_n$ to be equivalent to $s_{K_n}(p)$ is that $y_n \in \big[s_{K_n}(p), s_{K_n}(p+1)\big)$, i.e.,

$$\begin{aligned} p(\hat{y}_n = s_{K_n}(p)|\boldsymbol{\theta}) =& \Pr\{s_{K_n}(p) \leq \boldsymbol{h}_n^T\boldsymbol{\theta} + w_n < s_{K_n}(p) + L2^{-K_n+1}\} \\ =& \Pr\{s_{K_n}(p) - \boldsymbol{h}_n^T\boldsymbol{\theta} \leq w_n < s_{K_n}(p) + L2^{-K_n+1} - \boldsymbol{h}_n^T\boldsymbol{\theta}\} \\ =& \mathrm{F}_n(s_{K_n}(p) + L2^{-K_n+1} - \boldsymbol{h}_n^T\boldsymbol{\theta}) - \mathrm{F}_n(s_{K_n}(p) - \boldsymbol{h}_n^T\boldsymbol{\theta}) \end{aligned} \tag{4.13}$$

where $\mathrm{F}_n(.)$ is the cdf of $w_n$. The log-likelihood function is then,

$$L(\hat{\boldsymbol{y}}, \boldsymbol{\theta}) = \log p(\hat{\boldsymbol{y}}, \boldsymbol{\theta}) = \sum_{n=1}^{N} \log p(\hat{y}_n = s_{K_n}(p_n)|\boldsymbol{\theta}) + \log p(\boldsymbol{\theta}). \tag{4.14}$$

where $p_n$ is a particular integer. The MAP is obtained by maximizing $L(\hat{\boldsymbol{y}}, \boldsymbol{\theta})$ over $\boldsymbol{\theta}$. We can prove the concavity of $L(\hat{\boldsymbol{y}}, \boldsymbol{\theta})$ under certain conditions such that we can find out the global solution by typical convex optimization tools,

**Theorem 4.** *The logarithm likelihood function $L(\hat{\boldsymbol{y}}, \boldsymbol{\theta})$ is concave with respect to $\boldsymbol{\theta}$ if the probability functions $p(\boldsymbol{\theta})$ and $f_n(w_n)$ are log-concave for with $n = 1, 2, ..., N$.*

*Proof.* We begin the proof by first showing that $p(\hat{y}_n = s_{K_n}(p)|\boldsymbol{\theta})$ is log-concave if

$f_n(w_n)$ is log-concave. To show this, notice that,

$$\begin{aligned} p(\hat{y}_n = s_{K_n}(p)|\boldsymbol{\theta}) &= \mathrm{F}_n(s_{K_n}(p) + L2^{-K_n+1} - \boldsymbol{h}_n^T\boldsymbol{\theta}) - \mathrm{F}_n(s_{K_n}(p) - \boldsymbol{h}_n^T\boldsymbol{\theta}) \\ &= \int_{s_{K_n}(p)-\boldsymbol{h}_n^T\boldsymbol{\theta}}^{s_{K_n}(p)+L2^{-K_n+1}-\boldsymbol{h}_n^T\boldsymbol{\theta}} f_n(t)\ \mathrm{d}t \\ &= \int f_n(t)\left[u(t+\boldsymbol{h}_n^T\boldsymbol{\theta} - s_{K_n}(p)) - u(t+\boldsymbol{h}_n^T\boldsymbol{\theta} - s_{K_n}(p) + L2^{-K_n+1})\right]\ \mathrm{d}t \end{aligned} \tag{4.15}$$

where $u(.)$ is the step function. Note that the part $\left[u(t+\boldsymbol{h}_n^T\boldsymbol{\theta} - s_{K_n}(p)) - u(t+\boldsymbol{h}_n^T\boldsymbol{\theta} - s_{K_n}(p) + L2^{-K_n+1})\right]$ is a log-concave function in $t$ and $\boldsymbol{\theta}$. The product of two log-concave functions, $f_n(t)\left[u(t+\boldsymbol{h}_n^T\boldsymbol{\theta} - s_{K_n}(p)) - u(t+\boldsymbol{h}_n^T\boldsymbol{\theta} - s_{K_n}(p) + L2^{-K_n+1})\right]$, is still log-concave function, and integral over $t$ of this product function is log-concave function in $\boldsymbol{\theta}$ (see [3]). That is to say, $p(\hat{y}_n = s_{K_n}(p)|\boldsymbol{\theta})$ is log-concave, and the logarithmic of it is concave. Finally, $L(\hat{\boldsymbol{y}}, \boldsymbol{\theta})$ is a linear combination of multiple concave functions, hence it is concave.

□

We next derive the Bayesian Cramer-Rao lower bound using the likelihood function, which is an lower bound for any estimate of $\boldsymbol{\theta}$. The gradient of the local logarithm conditional likelihood with respect to $\boldsymbol{\theta}$ can be computed as,

$$\begin{aligned} \nabla_{\boldsymbol{\theta}} \ln p(\hat{y}_n = s_{K_n}(p)|\boldsymbol{\theta}) =& \nabla_{\boldsymbol{\theta}} \ln\left[\mathrm{F}_n(s_{K_n}(p) + L2^{-K_n+1} - \boldsymbol{h}_n^T\boldsymbol{\theta}) - \mathrm{F}_n(s_{K_n}(p) - \boldsymbol{h}_n^T\boldsymbol{\theta})\right] \\ \overset{(1)}{=}& \frac{\nabla_{\boldsymbol{\theta}}\left\{F_n(s_{K_n}(p) + L2^{-K_n+1} - \boldsymbol{h}_n^T\boldsymbol{\theta}) - F_n(s_{K_n}(p) - \boldsymbol{h}_n^T\boldsymbol{\theta})\right\}}{F_n(s_{K_n}(p) + L2^{-K_n+1} - \boldsymbol{h}_n^T\boldsymbol{\theta}) - F_n(s_{K_n}(p) - \boldsymbol{h}_n^T\boldsymbol{\theta})} \\ =& \frac{-f_n(s_{K_n}(p) + L2^{-K_n+1} - \boldsymbol{h}_n^T\boldsymbol{\theta}) + f_n(s_{K_n}(p) - \boldsymbol{h}_n^T\boldsymbol{\theta})}{F_n(s_{K_n}(p) + L2^{-K_n+1} - \boldsymbol{h}_n^T\boldsymbol{\theta}) - F_n(s_{K_n}(p) - \boldsymbol{h}_n^T\boldsymbol{\theta})}\boldsymbol{h}_n \end{aligned} \tag{4.16}$$

where in the equality we use the fact that the gradient of the cdf is the pdf. The local Bayesian Fisher Information is then,

$$\begin{aligned} \boldsymbol{\mathcal{F}}_n(K_n) =& \mathbb{E}_{\hat{y}_n,\boldsymbol{\theta}}\{\nabla_{\boldsymbol{\theta}} \ln p(\hat{y}_n = s_{K_n}(p)|\boldsymbol{\theta})\nabla_{\boldsymbol{\theta}}^T \ln p(\hat{y}_n = s_{K_n}(p)|\boldsymbol{\theta})\} \\ =& \mathbb{E}_{\hat{y}_n,\boldsymbol{\theta}}\left\{\left[\frac{-f_n(s_{K_n}(p) + L2^{-K_n+1} - \boldsymbol{h}_n^T\boldsymbol{\theta}) + f_n(s_{K_n}(p) - \boldsymbol{h}_n^T\boldsymbol{\theta})}{F_n(s_{K_n}(p) + L2^{-K_n+1} - \boldsymbol{h}_n^T\boldsymbol{\theta}) - F_n(s_{K_n}(p) - \boldsymbol{h}_n^T\boldsymbol{\theta})}\right]^2\right\}\boldsymbol{h}_n\boldsymbol{h}_n^T \\ \overset{(1)}{=}& \mathbb{E}_{\boldsymbol{\theta}}\left[\sum_{i=0}^{2^{K_n}-1}\left[\frac{-f_n(s_{K_n}(i) + L2^{-K_n+1} - \boldsymbol{h}_n^T\boldsymbol{\theta}) + f_n(s_{K_n}(i) - \boldsymbol{h}_n^T\boldsymbol{\theta})}{F_n(s_{K_n}(i) + L2^{-K_n+1} - \boldsymbol{h}_n^T\boldsymbol{\theta}) - F_n(s_{K_n}(i) - \boldsymbol{h}_n^T\boldsymbol{\theta})}\right]^2 \times \right. \\ & \left. p(\hat{y}_n = s_{K_n}(i)|\boldsymbol{\theta})\right]\boldsymbol{h}_n\boldsymbol{h}_n^T \\ =& \mathcal{G}(K_n)\boldsymbol{h}_n\boldsymbol{h}_n^T, \end{aligned} \tag{4.17}$$

where in equality (1) the expectation over $\hat{y}_n$ is specified exploiting the probability of $\hat{y}_n$, and we defined

$$\mathcal{G}(K_n) := \mathbb{E}_{\boldsymbol{\theta}} \left[ \sum_{i=0}^{2^{K_n}-1} \left[ \frac{-f_n(s_{K_n}(i) + L2^{-K_n+1} - \boldsymbol{h}_n^T\boldsymbol{\theta}) + f_n(s_{K_n}(i) - \boldsymbol{h}_n^T\boldsymbol{\theta})}{F_n(s_{K_n}(i) + L2^{-K_n+1} - \boldsymbol{h}_n^T\boldsymbol{\theta}) - F_n(s_{K_n}(i) - \boldsymbol{h}_n^T\boldsymbol{\theta})} \right]^2 p(\hat{y}_n = s_{K_n}(i)|\boldsymbol{\theta}) \right]. \tag{4.18}$$

Based on (3.12), and the independent property of Fisher Information, the Bayesian Fisher Information is the summation of the $N$ local Fisher information plus the Fisher Information of $\boldsymbol{\theta}$,

$$\boldsymbol{\mathcal{F}}_B = \sum_{n=1}^{N} \boldsymbol{\mathcal{F}}_n(K_n) + \boldsymbol{\mathcal{F}}_{\boldsymbol{\theta}}. \tag{4.19}$$

### 4.1.5 Remark: Without Prior Knowledge of the Unknown Parameter

In this remark, we want to discuss some aspect of quantization and the generation of unbiased estimates of least square error estimate when no prior knowledge about the unknown parameter $\boldsymbol{\theta}$ is available. This is a remark, and as such none of its derivations will be used later on.

When we have no prior knowledge about the unknown parameter $\boldsymbol{\theta}$, maximum likelihood estimate (MLE) is adopted instead. Alternatively, we can use least square error estimate (LSE) to estimate $\boldsymbol{\theta}$, which is more computational efficient than MLE. To exploit LSE, the reconstructed value $\hat{y}_n$ is seen as an estimate of the original measurement $y_n$ adding with quantized error. LSE is obtained by,

$$\begin{aligned} \hat{\boldsymbol{\theta}}_{\text{LS}} =& \arg\min_{\boldsymbol{\theta}} \sum_{n}^{N} \|\hat{y}_n - \boldsymbol{h}_n^T\boldsymbol{\theta}\|_2^2 \\ =& \arg\min_{\boldsymbol{\theta}} \|\hat{\boldsymbol{y}} - \boldsymbol{H}\boldsymbol{\theta}\|_2^2, \end{aligned} \tag{4.20}$$

with the following definitions,

$$\begin{aligned} \boldsymbol{H} &:= [\boldsymbol{h}_1, \boldsymbol{h}_2, ..., \boldsymbol{h}_N] \quad \in \mathbb{R}^{D\times N} \\ \hat{\boldsymbol{y}} &:= [\hat{y}_1, \hat{y}_2, ..., \hat{y}_N]^T \quad \in \mathbb{R}^N \\ \boldsymbol{y} &:= [y_1, y_2, ..., y_1]^T \quad \in \mathbb{R}^N \end{aligned}$$

Suppose $\boldsymbol{H}$ is a matrix with full row rank, such that $\boldsymbol{H}\boldsymbol{H}^T$ is invertible. Therefore we have the solution for (4.20) by [36],

$$\hat{\boldsymbol{\theta}}_{LS} = \left(\boldsymbol{H}\boldsymbol{H}^T\right)^{-1} \boldsymbol{H}\hat{\boldsymbol{y}}. \tag{4.21}$$

Since we abandon the bits after the $K_n$-th MSB, the quantized $\hat{x}_n$ equals or it is smaller than the original $x_n$. Since $\hat{y}_n = 2L\hat{x}_n - L$, then $\hat{y}_n$ is also smaller than or equal to $y_n$. This means that the estimated $\boldsymbol{\theta}$ (via the LSE) will be in general biased.

When $\theta$ is a scalar value, i.e., $y_n = \theta + w_n$, to make the expectation of $\hat{y}_n$ unbiased, [41] proposes to add an extra bit, the probabilistic bit to the message $\mathcal{M}_n$, $b_{n,e}$, which has a value,

$$\begin{aligned} \mathbb{P}\mathrm{r}[b_{n,e} = 1] &= 2^{K_n} \sum_{i=K_n+1}^{\infty} b_{n,i} 2^{-i} =: r_n \\ \mathbb{P}\mathrm{r}[b_{n,e} = 0] &= 1 - \mathbb{P}\mathrm{r}[b_{n,e} = 1] = 1 - r_n. \end{aligned} \tag{4.22}$$

With this probabilistic bit, $\hat{x}_n$ becomes,

$$\hat{x}_n = \sum_{i=1}^{K_n} b_{n,i} 2^{-i} + b_{n,e} 2^{-K_n}. \tag{4.23}$$

and the re-constructed quantized value of $y_n$ at the fusion center is,

$$\hat{y}_n = 2L \left( \sum_{i=1}^{K_n} b_{n,i} 2^{-i} + b_{n,e} 2^{-K_n} \right) - L. \tag{4.24}$$

In our case, $\boldsymbol{\theta}$ is not scalar, however with the probabilistic bit $b_{n,e}$, we can show that $\hat{\boldsymbol{y}} := [\hat{y}_1, \hat{y}_2, ..., \hat{y}_N]^T$ is an unbiased estimate of $\boldsymbol{y}$ with the extra probabilistic bits, and $\hat{\boldsymbol{\theta}}_{LS}$ is consequently an unbiased estimate of $\boldsymbol{\theta}$.

To prove this, we begin by making the following definitions,

$$\boldsymbol{b}_e := [\ b_{1,e}, b_{2,e}, ..., b_{N,e}\ ] \quad \in \mathbb{R}^N$$

$$\boldsymbol{r} := [\ r_1, r_2, ..., r_N\ ] \quad \in \mathbb{R}^N$$

$$\boldsymbol{c} := [\ 2^{-K_1+1} L, 2^{-K_2+1} L, ..., 2^{-K_N+1} L\ ] \quad \in \mathbb{R}^N$$

The original measurement $y_n$ at sensor $n$ can be expressed as,

$$\begin{aligned} y_n &= 2Lx_n - L \\ &= 2L \sum_{i=1}^{\infty} b_{n,i} 2^{-i} - L = 2L \left( \sum_{i=1}^{K_n} b_{n,i} 2^{-i} + \sum_{i=K_n+1}^{\infty} b_{n,i} 2^{-i} \right) - L \\ &\overset{(1)}{=} 2L(\hat{x}_n + 2^{-K_n} r_n - 2^{-K_n} b_{n,e}) - L \\ &= 2L\hat{x}_n - L + 2^{-K_n+1} L(r_n - b_{n,e}) \\ &\overset{(2)}{=} \hat{y}_n + 2^{-K_n+1} L(r_n - b_{n,e}), \end{aligned} \tag{4.25}$$

where (1) is due to the definition (4.23), while (2) is due to the definition (4.24).
Therefore, one can see that $\hat{\boldsymbol{y}} - \boldsymbol{y} = \boldsymbol{c} \odot (\boldsymbol{b}_e - \boldsymbol{r})$, with $\odot$ the Hadamard product multiplication. The expectation of $\hat{\boldsymbol{y}} - \boldsymbol{y}$ yields,

$$\mathbb{E}\{\hat{\boldsymbol{y}} - \boldsymbol{y}\} = \boldsymbol{c} \odot (\mathbb{E}\{\boldsymbol{b}_e\} - \boldsymbol{r}) \tag{4.26}$$

The definition of the elements of $\boldsymbol{r}$ in (4.22) implies that $\mathbb{E}\{\boldsymbol{b}_e\}-\boldsymbol{r}=\boldsymbol{0}$. Therefore $\mathbb{E}\{\hat{\boldsymbol{y}}-\boldsymbol{y}\}=\boldsymbol{0}$, that is $\hat{\boldsymbol{y}}$ is an unbiased estimate of $\boldsymbol{y}$. Consequently,

$$\begin{aligned}\mathbb{E}\{\hat{\boldsymbol{\theta}}_{\mathrm{LS}}\} &= \left(\boldsymbol{H}\boldsymbol{H}^T\right)^{-1}\boldsymbol{H}\ \mathbb{E}\{\hat{\boldsymbol{y}}\}\\ &= \left(\boldsymbol{H}\boldsymbol{H}^T\right)^{-1}\boldsymbol{H}\ \mathbb{E}\{\boldsymbol{y}\}\\ &= \left(\boldsymbol{H}\boldsymbol{H}^T\right)^{-1}\boldsymbol{H}\ \mathbb{E}\{\left(\boldsymbol{H}^T\boldsymbol{\theta}+\boldsymbol{w}\right)\}\\ &= \boldsymbol{\theta}+\left(\boldsymbol{H}\boldsymbol{H}^T\right)^{-1}\boldsymbol{H}\ \mathbb{E}\{\boldsymbol{w}\}\end{aligned} \tag{4.27}$$

By definition, $\boldsymbol{w}$ is zero-mean, therefore $\mathbb{E}\{\hat{\boldsymbol{\theta}}_{\mathrm{LS}}\}=\boldsymbol{\theta}$, that is $\hat{\boldsymbol{\theta}}_{\mathrm{LS}}$ is an unbiased estimate of $\boldsymbol{\theta}$.

We can see the the role of the probabilistic bit $b_{n,e}$ is to make $\boldsymbol{\theta}_{\mathrm{LS}}$ unbiased. At the same time, transmitting an extra bit increases the cost of energy of the WSN, and we cannot say much about the benefits of including the extra probabilistic bit rather than including the next MSB $b_{n,K_n+1}$. In addition, adding the bit $b_{n,e}$ makes the analysis of the multi-bit scheme significantly more involved. Given this, in what follows we will not include the extra probabilistic bit $b_{n,e}$, and we leave a thorough analysis as future research.

### 4.1.6 Multi-Bit Quantization When Bit Errors Occur

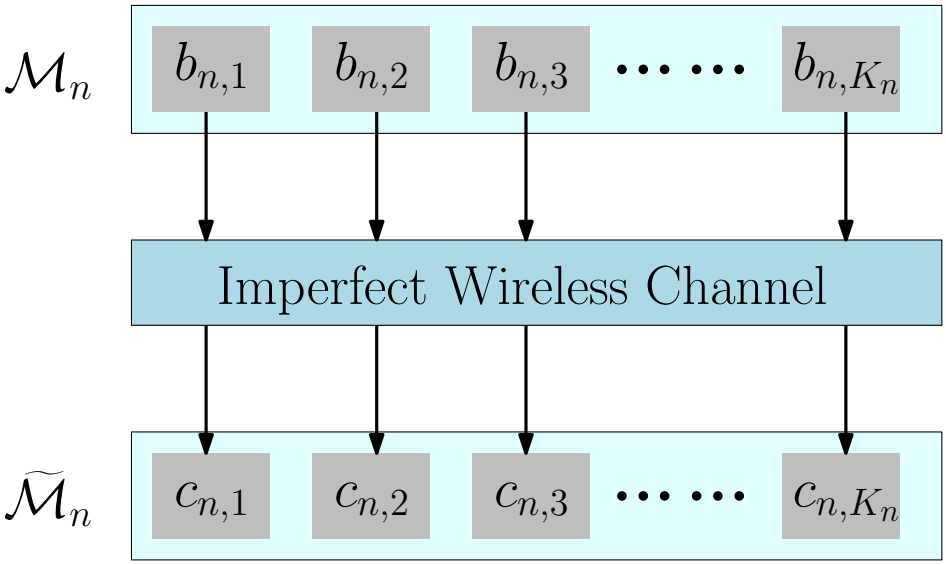


Figure 4.2: Illustration of transmission and reception of each bit over imperfect wireless channel

In the previous part, we have regarded the wireless channel as being perfect, so that the transmitted message $\mathcal{M}_n$ can be errorless received. In realistic environments, the received message, denoted as $\widetilde{\mathcal{M}}_{nn}$ may be different from the transmitted message due to bit errors in the wireless channel. We denote the bits that are contained in $\widetilde{\mathcal{M}}_n$ as $c_{n,i}, i=1,2,...,K_n$, i.e,

$$\widetilde{\mathcal{M}}_n := \{c_{n,1}, c_{n,2}, ..., c_{n,K_n}\}, \tag{4.28}$$

where $c_{n,i}$ corresponds to the original transmitted bit $b_{n,i}$ (see Figure 4.2), and we make the following assumption on the bit error process.

**Assumption 7.** *Each bit $b_{n,i}$ contained in the transmitted message $\mathcal{M}_n$ is independently affected by the wireless channel.*

This assumption indicates that for a wireless channel with bit error rate $\mathrm{Pe}_n$, a transmitted bit $b_{n,i}$ is incorrectly received with probability $\mathrm{Pe}_n$, and it may happen that $b_{n,i} \neq c_{n,i}$.

The quantized value of $y_n$ based on $\widetilde{\mathcal{M}}_n$ at the fusion center is denoted as $\widetilde{y}_n$,

$$\widetilde{y}_n = 2L \sum_{i=1}^{K_n} c_{n,i} 2^{-i} - L, \tag{4.29}$$

Notice that $\widetilde{y}_n$ can also be written as

$$\widetilde{y}_n = L2^{-K_N+1} \sum_{i=1}^{K_n} c_{n,i} 2^{K_n-i} - L, \quad c_{n,i} \in \{0,1\} \tag{4.30}$$

and as such, the possible values of $\widetilde{y}_n$ are the same as in the no bit error case, $\hat{y}_n$ (see Lemma 2), i.e., $\widetilde{y}_n$ belongs to the discrete set $\mathcal{S}_{K_n}$, which is defined in Definition 1.

The Illustration of the transmission and reception procedure with bit errors is depicted in Figure 4.3.

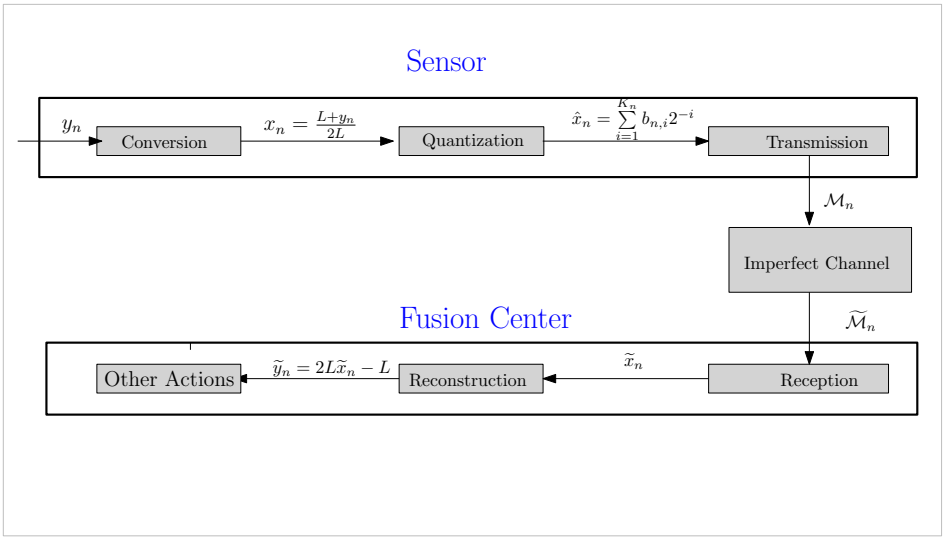


Figure 4.3: Procedure of transmission and reception by multi-bit quantization in imperfect wireless channel where bit errors occur.

#### 4.1.6.1 Distribution of The Aggregated Error With Bit Errors

We provide the distribution of the aggregated considering the bit errors. To distinguish from the case when no bit errors occur, we denote the respective aggregated error as,

$$\varepsilon_n^e = \widetilde{y}_n - y_n \tag{4.31}$$

We are interested in the distribution of $\varepsilon_n^e$. As we have discuss above, $\varepsilon_n^e$ has the same possible discrete values as the no bit error case, $\varepsilon_n(t)$. In fact, bit errors will only change the distribution of the aggregated error. In order to show this, we need some extra background and definitions. First, as said both $\widetilde{y}_n$ and $\hat{y}_n$ belong to the set $\mathcal{S}_{K_n}$. In general, we can say that $\hat{y}_n = \mathcal{S}_{K_n}(p)$, for a certain element $p$, while $\widetilde{y}_n = \mathcal{S}_{K_n}(q)$ for another element $q$. If $p = q$ then there aren't any bit error, while if $p \neq q$ then bit errors have occurred.
Since we assume that the bits of $\hat{y}_n$ are independently affected by the channel effect, we need to decompose the element $\mathcal{S}_{K_n}(p)$ in its bit decomposition as

$$s_{K_n}(p) = L2^{-K_N+1} \sum_{i=1}^{K_n} b_{n,i} 2^{K_n - i} - L = \hat{y}_n, \tag{4.32}$$

while

$$s_{K_n}(q) = L2^{-K_N+1} \sum_{i=1}^{K_n} c_{n,i} 2^{K_n - i} - L = \widetilde{y}_n. \tag{4.33}$$

Finally, the probability that the element $s_{K_n}(p)$ is transformed into $s_{K_n}(q)$ by the channel will be indicated as $\mathcal{T}(s_{K_n}(p), s_{K_n}(q))$.

We are now ready for the main result of this section.

**Theorem 5.** *When bit errors occur, the probabilities of the aggregated errors are,*

$$\begin{aligned} \eta_n^e(t) :&= \Pr\{\varepsilon_n^e = \varepsilon_n(t)\} \\ &= \sum_{i=0}^{2^{K_n}-1} \mathcal{T}(s_{K_n}(i), s_{K_n}(n_0 + t))\ \eta_n(i - n_0), \end{aligned} \tag{4.34}$$

*where $\eta_n(i - n_0)$ is defined in (4.12), $n_0$ is the value with the quantized value of the noiseless measurement $\hat{y}_n^* = \varphi(y_n^*, K_n) = s_{K_n}(n_0)$, and the probability $\mathcal{T}(s_{K_n}(p), s_{K_n}(q))$ has the expression*

$$\mathcal{T}(s_{K_n}(p), s_{K_n}(q)) = \prod_{i=1}^{K_n} (1 - \mathrm{Pe}_n)^{1-|b_{n,i}-c_{n,i}|} \mathrm{Pe}_n^{|b_{n,i}-c_{n,i}|}. \tag{4.35}$$

*Proof.* See Appendix 4.4.3. □

#### 4.1.6.2 Bayesian Cramer-Rao Lower Bound With Bit Errors

As stated above, when the fusion center receives $\widetilde{y}_n = s_{K_n}(q)$, with $q$ a particular integer, which it can be altered from all possible values of $\hat{y}_n = s_{K_n}(i), i = 0, 1, 2, ..., 2^{K_n} - 1$, and the probability of it is $\mathcal{T}(s_{K_n}(i), s_{K_n}(q))$. Therefore by the Total Probability Theorem,

$$p(\widetilde{y}_n = s_{K_n}(q)|\boldsymbol{\theta}) = \sum_{i=0}^{2^{K_n}-1} p(\hat{y}_n = s_{K_n}(i)|\boldsymbol{\theta}) \mathcal{T}(s_{K_n}(i), s_{K_n}(q)). \tag{4.36}$$

The logarithmic gradient of it is,

$$\begin{aligned}
&\nabla_{\boldsymbol{\theta}} \ln p(\widetilde{y}_n = s_{K_n}(q)|\boldsymbol{\theta}) \\
&= \sum_{i=0}^{2^{K_n}-1} \mathcal{T}(s_{K_n}(i), s_{K_n}(q)) \nabla_{\boldsymbol{\theta}} \ln p(\hat{y}_n = s_{K_n}(i)|\boldsymbol{\theta}) \\
&= \sum_{i=0}^{2^{K_n}-1} \frac{-f_n(s_{K_n}(i) + L2^{-K_n+1} - \boldsymbol{h}_n^T\boldsymbol{\theta}) + f_n(s_{K_n}(i) - \boldsymbol{h}_n^T\boldsymbol{\theta})}{F_n(s_{K_n}(i) + L2^{-K_n+1} - \boldsymbol{h}_n^T\boldsymbol{\theta}) - F_n(s_{K_n}(i) - \boldsymbol{h}_n^T\boldsymbol{\theta})} \mathcal{T}(s_{K_n}(i), s_{K_n}(q)) \boldsymbol{h}_n
\end{aligned} \tag{4.37}$$

That leads to the local Bayesian Fisher Information,

$$\begin{aligned}
&\boldsymbol{\mathcal{F}}_n(K_n) = \\
&= \mathbb{E}_{\widetilde{y}_n, \boldsymbol{\theta}} \left\{ \left[ \sum_{i=0}^{2^{K_n}-1} \frac{-f_n(s_{K_n}(i) + L2^{-K_n+1} - \boldsymbol{h}_n^T\boldsymbol{\theta}) + f_n(s_{K_n}(i) - \boldsymbol{h}_n^T\boldsymbol{\theta})}{F_n(s_{K_n}(i) + L2^{-K_n+1} - \boldsymbol{h}_n^T\boldsymbol{\theta}) - F_n(s_{K_n}(i) - \boldsymbol{h}_n^T\boldsymbol{\theta})} \mathcal{T}(s_{K_n}(i), s_{K_n}(q)) \right]^2 \right\} \boldsymbol{h}_n \boldsymbol{h}_n^T \\
&= \mathbb{E}_{\boldsymbol{\theta}} \left\{ \sum_{j=0}^{2^{K_n}-1} \mathcal{O}(K_n, j)\ p(\widetilde{y}_n = s_{K_n}(j)|\boldsymbol{\theta}) \right\} \boldsymbol{h}_n \boldsymbol{h}_n^T \\
&= \mathbb{E}_{\boldsymbol{\theta}} \left\{ \sum_{j=0}^{2^{K_n}-1} \mathcal{O}(K_n, j) \sum_{i=0}^{2^{K_n}-1} p(\hat{y}_n = s_{K_n}(i)|\boldsymbol{\theta}) \mathcal{T}(s_{K_n}(i), s_{K_n}(j)) \right\} \boldsymbol{h}_n \boldsymbol{h}_n^T \\
&\quad = \mathcal{G}_{\mathrm{Pe}}(K_n) \boldsymbol{h}_n \boldsymbol{h}_n^T
\end{aligned} \tag{4.38}$$

with

$$\mathcal{O}(K_n, j) := \left[ \sum_{i=0}^{2^{K_n}-1} \frac{-f_n(s_{K_n}(i) + L2^{-K_n+1} - \boldsymbol{h}_n^T\boldsymbol{\theta}) + f_n(s_{K_n}(i) - \boldsymbol{h}_n^T\boldsymbol{\theta})}{F_n(s_{K_n}(i) + L2^{-K_n+1} - \boldsymbol{h}_n^T\boldsymbol{\theta}) - F_n(s_{K_n}(i) - \boldsymbol{h}_n^T\boldsymbol{\theta})} \mathcal{T}(s_{K_n}(i), s_{K_n}(j)) \right]^2 . \tag{4.39}$$

And the Fisher Information can also be obtained using (4.19).

It is worth to emphasize that the expression of the local Bayesian Fisher information presented in (4.38) is a generalized version of the local Bayesian Fisher information with no bit error in (4.17). In fact, when no bit errors occur, $\mathrm{Pe}_n = 0$, for $, n = 1, 2, ..., N$, which implies $\mathcal{T}(s_{K_n}(p), s_{K_n}(q)) = 1$ iff $s_{K_n}(p)$ equals $s_{K_n}(q)$, and zero otherwise. Therefore, there is only one term in the summation in (4.38), that is exactly the equality (1) in (4.17).

#### 4.1.6.3 Maximum A Posteriori With Bit Errors

As above, we can use the maximum a posteriori to estimate $\boldsymbol{\theta}$ in the case of bit errors occur.

By (4.14) and (4.36) we can explicit write the log-likelihood function as,

$$L(\widetilde{\boldsymbol{y}}, \boldsymbol{\theta}) = \sum_{n=1} \ln \left[ \sum_{i=0}^{2^{K_n}-1} p(\hat{y}_n = s_{K_n}(i)|\boldsymbol{\theta}) \mathcal{T}(s_{K_n}(i), \widetilde{y}_n) \right] + \ln p(\boldsymbol{\theta}) \tag{4.40}$$

We can maximumize $L(\widetilde{\boldsymbol{y}}, \boldsymbol{\theta})$ with respect to $\boldsymbol{\theta}$ to obtain an MAP estimate. However, note that we cannot prove $L(\widetilde{\boldsymbol{y}}, \boldsymbol{\theta})$ is concave in $\boldsymbol{\theta}$, therefore no guarantee of optimality about the solution.

### 4.1.7 Impact of Number of Bits and Bit Error Rate to the Local Bayesian Fisher information

Two important factors in this model are the numbers of bits used to quantize the original measurements and the channel effect, the bit error rate. One may wonder how these two will affect the final estimating performance. Intuitively, more bits involved to quantize are prone to increase the accuracy to reconstruct the original measurements and consequently improve the performance, and it seems that we can always benefit from low bit error rates. To further analyze these effects, we conduct a simulation to show the relations between the two factors and the coefficient of the local Bayesian Fisher information (See (4.38) ),

$$\mathcal{G}_{\mathrm{Pe}}(K_n) := \mathbb{E}_{\boldsymbol{\theta}} \left\{ \sum_{j=0}^{2^{K_n}-1} \mathcal{O}(K_n, j)\ p(\widetilde{y}_n = s_{K_n}(j)|\boldsymbol{\theta}) \right\}. \tag{4.41}$$

This is a term related to the number of bits and the bit error rate and the value of it reflects the potential contribution of the sensor directly, therefore we adopt $\mathcal{G}_{\mathrm{Pe}}(K_n)$ to see the impact of the two factors. We consider the regressor $\boldsymbol{h}_n = [\ 0.2 \quad 0.5\ ]^T$, and let the $w_n$ to be a random value with zero-mean and variance 0.5 Gaussian noise. In Figure 4.4 we plot the value of $\mathcal{G}_{\mathrm{Pe}}(K_n)$ versus $\mathrm{Pe}_n$ and the number of bits. The surface of it presents a shape of half saddle. To see it more deeply, Figure 4.5 and Figure 4.6 extract the traverse-sections from two directions. From these two figures we can see that more bits always lead to higher value of $\mathcal{G}_{\mathrm{Pe}}(K_n)$. Particularly, Figure 4.5 shows that the increasing amount of $\mathcal{G}_{\mathrm{Pe}}(K_n)$ is significant from one bit to two bits and this metric becomes more constant with numbers of bits increasing, and when the numbers of bits reach four or higher, the curves are almost flat. That means we get no further gain in $\mathcal{G}_{\mathrm{Pe}}(K_n)$ by adding more bits. Therefore, we can see the case of four bits as approximately being equivalent to the case of analog transmission in this configuration. The curves in Figure 4.6 present a shape of symmetric valley, i.e., the values of $\mathcal{G}_{\mathrm{Pe}}(K_n)$ are the highest when $\mathrm{Pe}_n$ is near to 0 and 1 and become the lowest exactly at the 0.5. It seems to be opposite to the common sense, that higher bit error rates close to one can also bring lower $\mathcal{G}_{\mathrm{Pe}}(K_n)$, and thus the the measurement of this sensor is less informative. However, it is not difficult to explain this phenomenon: if the bit error rate is closed to 0, we know that a bit received tends to be the true value of the original transmitted bit, and on the other hand when bit error rate is closed to 1, the received bit is highly probable to have a value that is opposite to the original transmitted bit. A extreme example is that, when the bit error rate is 1, we know the bit received is absolutely opposite to the original transmitted bit. Therefore if we flip the received bit we can obtain the true value of the transmitted bit.

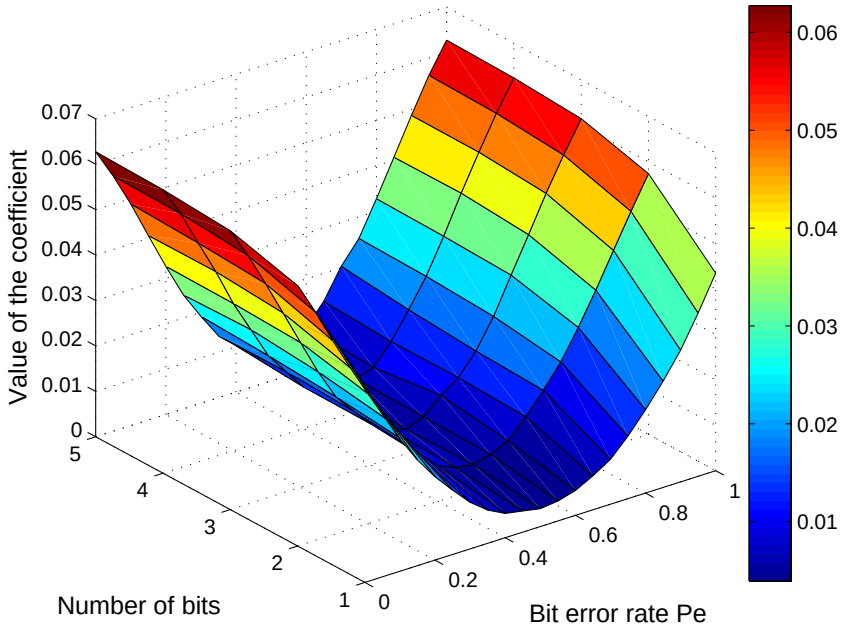


Figure 4.4: Values of the coefficient versus bit error rates and numbers of bits.

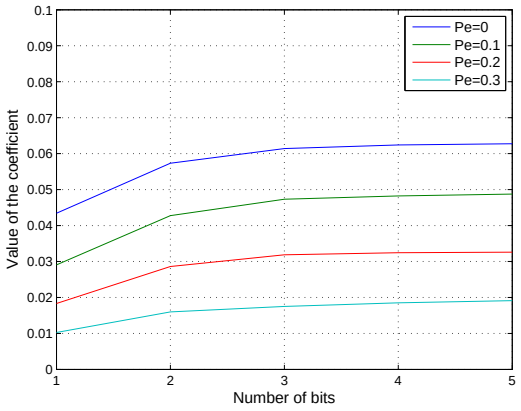


Figure 4.5: Values of the coefficient versus numbers of bits.

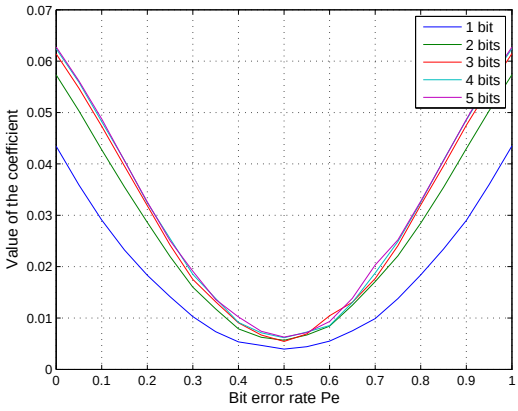


Figure 4.6: Values of the coefficient versus bit error rates.

## 4.2 Bit Allocation Algorithm

### 4.2.1 Problem Formulation

As stated above, the measurements of different sensors contribute in different ways to the final estimate at the fusion center, due to the regressor $\boldsymbol{h}_n$, noise variance and the bit error rate $\mathrm{Pe}_n$. For the one-bit quantization, we determined which subset of sensors should be enabled to transmit their measurement, according to the criterion in (3.18) which states

that the minimum eigenvalue of the BFIM should be larger than a threshold. From another perspective, this scheme is equivalent to determining which sensors should transmit one bit while the others transmit zero bits. When we extend this to the multi-bit case, one interesting problem is how can we determine the number of bits that each sensor will transmit to the fusion center.

From the simulation results in Section 4.1.7, we can see that more bits to transmit leads to a higher performance of the final estimation at the fusion center. However, it means a higher cost of resources will occur in the WSN. It is a tradeoff between estimation performance and resource management. To specify the cost, we can assign a cost parameter for each number of bits to transmit from a sensor, i.e., for a sensor to transmit $k$ bits, it will cost $C_k$. Note that $C_k$ is the same for each sensor because we assume that the cost of the same number of bits are the same for any two different sensors. As stated above, each sensor transmits $K_n$ bits, with the corresponding cost $C_{K_n}$, therefore the global cost is the summation of the cost sof all sensors,

$$C^g = \sum_{i=1}^{N} C_{K_i}. \tag{4.42}$$

For the sake of resource management, we aim at minimizing the global cost $C^g$, and at the same time, the performance of the estimate at the fusion center should be guaranteed to be above certain level. We denote the performance metric as $\mathcal{P}(\boldsymbol{K}, \boldsymbol{\theta})$, where $\boldsymbol{K} := [K_1, K_2, ..., K_N]$. This definition indicates how the number of bits and the unknown parameter $\boldsymbol{\theta}$ affect the performance metric. We restrict the choice of the number of bits $K_n$ in a finite sorted set, $\mathcal{U}_K$, and the elements in it vary from the smallest value $\mathcal{U}_{\min}$ to the largest value $\mathcal{U}_{\max}$, and we denote the size of $\mathcal{U}_K$ as $M_{\mathcal{U}} = \mathcal{U}_{max} - \mathcal{U}_{min} + 1$. It also means that the $K_n$ can be chosen from $M_{\mathcal{U}}$ candidate values plus the zero value (no bit is transmitted). With this, we can consequently state the bit allocation problem as,

$$\begin{aligned} \underset{\boldsymbol{K} \in \{\mathcal{U}_K, 0\}^N}{\arg\min} \quad & C^g = \sum_{i=1}^{N} C_{K_i} \\ \text{subject to :} \quad & \mathcal{P}(\boldsymbol{K}, \boldsymbol{\theta}) \leq T \end{aligned} \tag{4.43}$$

i.e, this optimization problem aims at finding out the optimal bit number set $\boldsymbol{K}$ that minimizes the global cost $C^g$, and at the same time, constrain the performance $\mathcal{P}(\boldsymbol{K}, \boldsymbol{\theta})$ to be smaller than a threshold $T$. Note that $\mathcal{P}(\boldsymbol{K}, \boldsymbol{\theta})$ does not have to be necessarily smaller than a threshold. For some metric, the $\mathcal{P}(\boldsymbol{K}, \boldsymbol{\theta})$ can be constrained to be larger than a threshold.

The remained problem is to define the performance metric $\mathcal{P}(\boldsymbol{K}, \boldsymbol{\theta})$. Intuitively, we can specify $\mathcal{P}(\boldsymbol{K}, \boldsymbol{\theta})$ as the Bayesian mean square error that is the trace of the Bayesian error covariance matrix derived in (4.74). However, it is intractable to handle the bit allocation with Bayesian mean square error restriction. Alternatively, we adopt the metric of the minimum eigenvalue of the corresponding Bayesian Fisher information that is used in the one-bit quantization case. The criterion is to restrict it to be larger than a threshold.

#### 4.2.1.1 Remark: Discussion About the Cost

It is worth to discuss how to determine the values of $C_j$ (the cost that a sensor transmits $j$ bits).

Generally, more bits to transmit results in a higher cost, in other words, $C_i \leq C_j$ if $i \leq j$. Intuitively, it is reasonable to set $C_j$ to be proportional to $j$, that implies one more bit to transmit requires one more unit of cost. However, in practical cases, the cost is not always increasing linearly with the number of bits to transmit for a single sensor, because to start a transmission extra information is needed to be exchanged between a sensor and the fusion center, therefore, for example, transmitting two bits for a sensor at the same time always cost less than twice the cost of transmitting one bit.

Another factor needed to be considered in designing the value of the cost is the remaining energy of a sensor. One scheme to prolong the longevity of a WSN is to consume energy of sensors in balance or evenly. In other words, it is not wise to overuse a particular sub-set of sensors than others, because by this way the energy of this sub-set of sensors will be exhausted faster than others. To solve such a problem, we can allow the cost $C_j$ to be various over different sensors and design the values of the cost considering the remaining energy of a sensor, i.e., when a sensor has less remaining energy, the costs for all numbers of bits should be set to higher values than other sensors.

### 4.2.2 Bit Allocation Based on the Minimum Eigenvalue of the Bayesian Fisher Information

We specify the performance metric $\mathcal{P}(\boldsymbol{K}, \boldsymbol{\theta})$ by the minimum eigenvalue of the Bayesian Fisher information. To begin with, we define vectors $\boldsymbol{f}_n$ that have a dimension as the same with size of the bit number candidate set $\mathcal{U}_K$. The elements of $\boldsymbol{f}_n$ is the defined as,

$$\begin{aligned}\{\boldsymbol{f}_n\}_j :=& \mathcal{G}(\mathcal{U}_K(j)) \\ =& \mathbb{E}_{\boldsymbol{\theta}} \left\{ \sum_{i=0}^{2^{\mathcal{U}_K(j)}-1} \left[ \frac{-f_n(s_{\mathcal{U}_K(j)}(i) + L2^{-\mathcal{U}_K(j)+1} - \boldsymbol{h}_n^T\boldsymbol{\theta}) + f_n(s_{\mathcal{U}_K(j)}(i) - \boldsymbol{h}_n^T\boldsymbol{\theta})}{F_n(s_{\mathcal{U}_K(j)}(i) + L2^{-\mathcal{U}(j)+1} - \boldsymbol{h}_n^T\boldsymbol{\theta}) - F_n(s_{\mathcal{U}_K(j)}(i) - \boldsymbol{h}_n^T\boldsymbol{\theta})} \right]^2 \times \right. \\ & \left. p(\hat{y}_n = s_{\mathcal{U}_K(j)}(i)|\boldsymbol{\theta}) \right\}\end{aligned} \tag{4.44}$$

where $\mathcal{U}_K(j)$ is the $j$-th element of the sorted set $\mathcal{U}_K$ (see (4.18)). We then can express the local Bayesian Fisher information matrix, when $\mathcal{U}_K(j)$ quantized bits are used, as $\{\boldsymbol{f}_n\}_j \boldsymbol{h}_n \boldsymbol{h}_n^T$ (see (4.17)), or equivalently,

$$\boldsymbol{\mathcal{F}}_n(\mathcal{U}_K(j)) := \boldsymbol{I}_{M_{\mathcal{U}}}^{(j)\,T} \boldsymbol{f_n} \boldsymbol{h}_n \boldsymbol{h}_n^T = \{\boldsymbol{f}_n\}_j \boldsymbol{h}_n \boldsymbol{h}_n^T, \tag{4.45}$$

where $\boldsymbol{I}_{M_{\mathcal{U}}}^{(j)}$ is the $j$-th column of the identity matrix with dimention $M_{\mathcal{U}}$. In bit allocation problem, we need to decide which number of bits for sensor $n$ should be used, i.e, determine the value of $j$ which ranges from 1 to the size of $\mathcal{U}_K$, $M_{\mathcal{U}}$. To this aim, we define a variable vector $\boldsymbol{v}_n$ for each sensor.

**Definition 3.** The vector $\boldsymbol{v}_n$ is a vector with dimension $M_{\mathcal{U}}$, that corresponds to sensor $n$. It is either an all-zero vector, or a vector with only one element of it is 1 and the remaining elements are all zeros. $\boldsymbol{V}$ stacks $\boldsymbol{v}_n$ for $n = 1, 2, ..., N$, $\boldsymbol{V} = [\boldsymbol{v}_1, \boldsymbol{v}_2, ..., \boldsymbol{v}_N]$.

We can also interpret the definition of $\boldsymbol{v}_n$ in a mathematical way,

$$\begin{aligned} \boldsymbol{v}_n &\in \{0, 1\}^{M_{\mathcal{U}}}, \\ \|\boldsymbol{v}_n\|_0 &\leq 1, \end{aligned} \tag{4.46}$$

The $\boldsymbol{v}_n$ can be used to express the local Bayesian Fisher information, i.e., when $\mathcal{U}_K(j)$ bits for sensor $n$ are used, we can set $\boldsymbol{v}_n$ as an all-zero vector except that the $j$-th element of it is 1, then (4.45) can be written as,

$$\boldsymbol{\mathcal{F}}_n(\mathcal{U}_K(j)) := \mathcal{G}(\mathcal{U}_K(j))\boldsymbol{h}_n\boldsymbol{h}_n^T = \boldsymbol{v}_n^T\boldsymbol{f}_n\boldsymbol{h}\boldsymbol{h}^T, \tag{4.47}$$

Since our goal is to determine the number of bits for each sensor, we see $\boldsymbol{v}_n$ as an undetermined parameter, then the corresponding global Bayesian Fisher Information that depends on $\boldsymbol{V}$ is,

$$\boldsymbol{\mathcal{F}}(\boldsymbol{V}) = \sum_{n=1}^{N} \boldsymbol{v}_n^T\boldsymbol{f}_n\boldsymbol{h}\boldsymbol{h}^T + \boldsymbol{\mathcal{F}}_{\boldsymbol{\theta}} \tag{4.48}$$

For the case when bit errors occur, we can substitute $\mathcal{G}(\mathcal{U}_K(j))$ with $\mathcal{G}_{\text{Pe}}(\mathcal{U}_K(j))$ (see (4.38)).

The minimum eigenvalue of the Bayesian Fisher Information is the matrix that we use for bit allocation, which we require to be larger than a threshold $T_f$. Since the minimum eigenvalue of the Bayesian Fisher information equals the inverse of the maximum eigenvalue of the Bayesian Cramer-Rao lower bound, the constraint in (4.43) becomes,

$$\mathcal{P}(\boldsymbol{K}, \boldsymbol{\theta}) = \max\{(\boldsymbol{\mathcal{F}})^{-1}\} \leq \frac{1}{T_f} \tag{4.49}$$

Next we construct the global cost with respect to $\boldsymbol{v}_n$. Define a cost vector, $\boldsymbol{C} := [C_{\mathcal{U}_K(1)}, C_{\mathcal{U}_K(2)}, ..., C_{\mathcal{U}_K(M_{\mathcal{U}})}]^T$. The vector $\boldsymbol{C}$ stacks all costs of the number of bits in $\mathcal{U}_K$ for a sensor to transmit. Then the local cost can be expressed as $\boldsymbol{C}^T\boldsymbol{v}_n$, i.e., when the number of bits for sensor $n$ to transmit is $\mathcal{U}_K(j)$, then the $j$-th element of $\boldsymbol{v}_n$ is 1 and the other elements of it are zero. The local cost is $C_{\mathcal{U}_K(j)}$, or equivalently, $\boldsymbol{C}^T\boldsymbol{v}_n$. The global cost is then,

$$C^g = \sum_{n=1}^{N} \boldsymbol{C}^T\boldsymbol{v}_n \tag{4.50}$$

and we can finally formulate the optimization problem to search for the optimal value of $\boldsymbol{v}_n$ (or the optimal number of bits for each sensor to transmit, $K_n$),

$$\begin{aligned} \boldsymbol{V}^* = \arg\min_{\boldsymbol{V}} \quad & C^g = \sum_{n=1}^{N} \boldsymbol{C}^T\boldsymbol{v}_n \\ \text{subject to :} \quad & \lambda_{\min}\left\{\sum_{n=1}^{N} \boldsymbol{v}_n^T\boldsymbol{f}_n\boldsymbol{h}\boldsymbol{h}^T + \boldsymbol{\mathcal{F}}_{\boldsymbol{\theta}}\right\} \geq T_f \\ & \boldsymbol{v}_n \in \{0,1\}^{M_{\mathcal{U}}}, \quad ||\boldsymbol{v}_n||_0 \leq 1, \\ & n = 1, 2, ..., N \end{aligned} \tag{4.51}$$

where $\lambda_{\min}\{\}$ denotes the minimum eigenvalue of a matrix. To make it to be solvable, we relax it to an SDP problem by allowing the values of the elements in $\boldsymbol{v}_n$ to vary between $[0, 1]$ and constrain their summation to be not larger than 1. Also, we replace the performance

constraint by, $\sum_{n=1}^{N} \boldsymbol{v}_n^T \boldsymbol{f}_n \boldsymbol{h}\boldsymbol{h}^T + \boldsymbol{\mathcal{F}}_{\boldsymbol{\theta}} \succeq T_f \boldsymbol{I}_D$. The relaxed SDP becomes,

$$\begin{aligned} \hat{\boldsymbol{V}} = \arg\min_{\boldsymbol{V}} \quad & C^g = \sum_{n=1}^{N} \boldsymbol{C}^T \boldsymbol{v}_n \\ \text{subject to :} \quad & \sum_{n=1}^{N} \boldsymbol{v}_n^T \boldsymbol{f}_n \boldsymbol{h}\boldsymbol{h}^T + \boldsymbol{\mathcal{F}}_{\boldsymbol{\theta}} \succeq T_f \boldsymbol{I}_D \\ & \boldsymbol{v}_n \in [0,1]^{M_{\mathcal{U}}}, \quad \|\boldsymbol{v}_n\|_1 \leq 1, \\ & n = 1, 2, ..., N. \end{aligned} \tag{4.52}$$

Note that the solution of (4.52) is not the one in Definition 3. It is probable that for a $\hat{\boldsymbol{v}}_n$ (the $n$-th column in $\hat{\boldsymbol{V}}$), more than one element have a non-zero value. To address this problem, we reserve only the largest element in $\hat{\boldsymbol{v}}_n$ by set it to be 1, and set the others to be zero. After we obtained the transform solution $\boldsymbol{V}^* = \{\boldsymbol{v}_1^*, \boldsymbol{v}_2^*, ..., \boldsymbol{v}_N^*\}$, the decisions of the number of bits for each sensor can be determine by $\boldsymbol{v}_n^*$, i.e., if the $j$-th element of $\boldsymbol{v}_n^*$ is 1, then the number of bits for sensor $n$, $K_n$, is $\mathcal{U}_K(j)$. The algorithm is summarized in the following.

**Algorithm 2** Transformation procedure of the solution of the relaxed problem

1: Initial: Giving the solution $\hat{\boldsymbol{V}}$, define $\boldsymbol{\Omega} := \{|\hat{\boldsymbol{v}}_1|, |\hat{\boldsymbol{v}}_2|, ..., |\hat{\boldsymbol{v}}_N|\}$, and an empty vector set $\boldsymbol{\mathcal{J}}_v$, and an empty index set $\boldsymbol{\mathcal{I}}_v$. Define an all-zero matrix $\boldsymbol{V} \in \mathbb{R}^{M_{\mathcal{U}} \times N}$
2: Step 1: Let $t$ be the index of $\max\{\boldsymbol{\Omega}\}$, and set the corresponding $\max\{\boldsymbol{\Omega}\}$ to be zero. Also let $\boldsymbol{v}_m$ be $t$-th column of $\hat{\boldsymbol{V}}^*$.
3: Step 2: Set the element of $\boldsymbol{v}_m$ with largest value to be 1, and the other elements to be 0. Put $\boldsymbol{v}_m$ in to $\boldsymbol{\mathcal{J}}_v$, $t$ into $\boldsymbol{\mathcal{I}}_v$.
4: Step 3: Set the $t$-th column of $\hat{\boldsymbol{V}}^*$ to be $\boldsymbol{v}_m$
5: Step 4: Compute $\boldsymbol{\mathcal{F}}(\boldsymbol{V}^*)$
6: Step 5: If $\lambda_{\min}\{\boldsymbol{\mathcal{F}}(\boldsymbol{V}^*)\} \geq T_f$, go to Step 6, otherwise repeat Step 1.
7: The $\boldsymbol{V}^*$ is the final transformed solution. The number of bits for each sensor can be obtained by seeing which element of $\boldsymbol{v}_n^*$ in $\boldsymbol{V}^*$ is non-zero.

### 4.2.3 Sparsity-Enhanced Iterative Algorithm

The solution of the original optimization problem presents a characteristic of sparsity. The sparsity resides on two aspects: (1). If $T_f$ is not a large number, it is likely that only a small sub-set of sensors needs to transmit a certain number of bits to meet the performance constraint, that means most $\boldsymbol{v}_n$ will be zero vectors. (2). At most one element of $\boldsymbol{v}_n$ is non-zero according to its definition.

To utilize the sparsity features, we refine the objective function of (4.51) or (4.52). The philosophy behind the refined relaxed optimization problem is based on the re-weighted $\ell_1$-norm iterative algorithm, that was proposed in [4] and is applied in [6] [35].

The specific modification is first to introduce a weight for each term of the summation in the objective function,

$$\sum_{n=1}^{N} \boldsymbol{C}^T \boldsymbol{v}_n \; q_n = \boldsymbol{C}^T \boldsymbol{V} \boldsymbol{q} \tag{4.53}$$

where $q_n \in \mathbb{R}^1$ and $\boldsymbol{q} := \left[q_1, q_2, ..., q_N\right]^T \in \mathbb{R}^N$. Unlike the original objective function, which we can see equivalently as each term in the summation has a fixed weight 1, $q_n$ is fluctuating according to the value of $\|\hat{\boldsymbol{v}}_n\|_2$ of the previous iteration, once the $\|\hat{\boldsymbol{v}}_n\|_2$ from last iteration's solution is small, $q_n$ will be set to a large value. As for the sparsity for the elements of $\boldsymbol{v}_n$, another term is adding in the new objective and the whole becomes,

$$\sum_{n=1}^{N} \quad \boldsymbol{C}^T \boldsymbol{v}_n \; q_n + \mu \; \boldsymbol{u}_n^T \boldsymbol{v}_n = \boldsymbol{C}^T \boldsymbol{V} \boldsymbol{q} + \mu \; \mathbb{T}\mathrm{r}\{\boldsymbol{U}^T \boldsymbol{V}\} \tag{4.54}$$

where $\boldsymbol{u}_n \in \mathbb{R}^{M_{\mathcal{U}}}$ is a non-negative vector corresponding to $\boldsymbol{v}_n$ and $\boldsymbol{U} := \left\{\boldsymbol{u}_1, \boldsymbol{u}_2, ..., \boldsymbol{u}_N\right\} \in \mathbb{R}^{M_{\mathcal{U}} \times N}$, with $M_{\mathcal{U}}$ the size of the bit number candidate set $\mathcal{U}_K$. It is the same with $\boldsymbol{q}$, $\boldsymbol{u}_n$ updates according to the $\hat{\boldsymbol{v}}_n$ of the solution of last iteration. The detailed algorithm is described as follow:

STEP 1) **Initialization**: $k = 0$, $\boldsymbol{q}^{(0)} = \boldsymbol{1}_N$, $\boldsymbol{U}^{(0)} = \boldsymbol{0}_{M_{\mathcal{U}}} \boldsymbol{0}_N^T$, with $\boldsymbol{0}_t$ and $\boldsymbol{1}_t$ are $t$-dimension zero and one vectors, respectively.

STEP 2) **Computation**: Solve the following optimization problem,

$$\begin{aligned} \hat{\boldsymbol{V}} = \arg\min_{\boldsymbol{V}} \quad & \boldsymbol{C}^T \boldsymbol{V} \boldsymbol{q}^{(k)} + \mu \; \mathbb{T}\mathrm{r}\{{\boldsymbol{U}^{(k)}}^T \boldsymbol{V}\} \\ \text{subject to :} \quad & \sum_{n=1}^{N} \boldsymbol{v}_n^T \boldsymbol{f}_n \boldsymbol{h} \boldsymbol{h}^T + \boldsymbol{\mathcal{F}}_{\boldsymbol{\theta}} \geq T_f \boldsymbol{I}_D \\ & \boldsymbol{v}_n \in [0,1]^{M_{\mathcal{U}}}, \quad \|\boldsymbol{v}_n\|_1 \leq 1, \\ & n = 1, 2, ..., N. \end{aligned} \tag{4.55}$$

STEP 3) **Update**: $q_n^{(k+1)} = \frac{1}{\epsilon + \|\boldsymbol{v}_n^{(k)}\|_2}$, the $i$th element of $\boldsymbol{u}_n^{(k+1)}$, $\{\boldsymbol{u}_n\}_i^{(k+1)} = \frac{1}{\epsilon + |\{\boldsymbol{v}_n^{(k)}\}_i|}$, with $n = 1, 2, ..., N$, $i = 1, 2, ...M_{\mathcal{U}}$.

STEP 4) **Judgement:** $k = k + 1$. If $k = k_{max}$ or the iteration converges, stop iteration, otherwise repeat from the computation step.

The role of the very small positive number $\epsilon$ is to prevent $\boldsymbol{q}^{(k)}$ or $\boldsymbol{U}^{(k)}$ to have elements with infinite value.

### 4.2.4 Simulation

Simulation results about the numerical analysis of the new approach are presented. This time we consider a WSN with $N = 64$ sensors and use the same model to generate $\boldsymbol{h}_n$ as in the simulation in the previous chapter. The $\boldsymbol{\theta}$ is set to be an random parameter with each element of it follows zero-mean truncated Gaussian distribution with variance $\sigma_\theta^2 = 0.2$ and bounded by 0.5. The bound $L = 1.5$ to make sure that $y_n$ is swinging between $(-L, L)$.

In the first simulation, we set the noise for each sensor to be a zero-mean truncated Gaussian distributed parameter with variance $\sigma_w^2 = 0.3$ and bounded by 0.5. To compare we consider five bits allocation schemes: The numbers of bits in the first four are fixed from 1

to 4. That is to say, if we fix the number of bits to be K then a sensor will either transmits K bits or transmits no bits. In the last scheme we let the number of bits to be flexible, that is exactly our new approach. Since from previous simulation we learn that when the number of bits reaches 4 or higher, there is no significant increasing in the Fisher information, we let the set of number of bits to be $\boldsymbol{U}_K = [1, 2, 3, 4]$. Without loss of generality, the cost $C_k$ is set to be the same with the number of bits, i.e., $C_k = k$ and $\boldsymbol{C} = [1, 2, 3, 4]$. That also means minimizing the global cost is equivalent to minimizing the total number of bits for the whole WSN.

In Figure 4.7,4.8, 4.9 we plot the values of $C^g$ versus the threshold $T_f$, with the bit error rates setting to be $0, 0.1, 0.2$, respectively. It can be seen from these figures that among all the bits allocation schemes, our approach achieves smallest cost for a particular threshold $T_f$. Especially, it is better than the case of fixed 4 bits. This has a significant meaning because the fixed 4 bits case is regarded as the case of transmitting analog signal, that is to say, by our new approach we can further reduce the cost of a WSN compared with the existing sensors selection techniques which aim to determine a sensor is to transmit analog signals or not.

We can also see that the curves of the schemes with higher fixed number of bits are in general above those with smaller fixed numbers of bits. In particular, when $T_f$ is small, the curves of the flexible number of bits are almost the same with the curves of the case of fixed one bit scheme. These phenomenons mainly result from two reasons. First, the values of the costs $C_k$ in the simulation are set to be proportional to the numbers of bits transmitted. The second reason is based on the identical values of the bit error rate and variance of noise of each sensor, with them the differences of contributions of sensors depend only on the regressors $\boldsymbol{h}_n$. In figure 4.4 we see that the gain to add one more bit to quantize the measurement is getting less and less with number of bits increasing. Therefore, the whole system benefits more by activating another sensor or adding a bit to the sensors already allocated with smaller number of bits, or in other word it gets more improvement in performance at less cost in this way. However, when $T_f$ grows large, for the fixed schemes with small number of bits, the performance requirement is not satisfied even when all sensors are activated. In practical situation, the costs of transmitting bits are usually not proportional to the numbers of bits, and bit error rates and variances of noise are most likely not identical over sensors. To verify our analysis, we do another simulation, with the cost vector to be $\boldsymbol{C} = [1\ 1.5\ 2\ 2.5]$, and the bit error rates and variance are set to be uniform random values between $[0, 0.3]$ and $[0.1, 0.5]$, respectively, and the results are plot in figure 4.10. From it we can see that the phenomenas disappear.

In Figure 4.11 the costs of different bit error rates of all sensors are compared. It can be seen that with a higher bit error rate, the cost is always higher, which implies more bits are needed to obtain the same level of performance. The phenomenon can also be seen with different noise variance (See Figure 4.12)

## 4.3 Conclusion

In this chapter, to further exploit the original measurements, multi-bit quantization approach is introduced that reserve multiple MSBs of a measurement. Based on this quantization scheme we derive the likelihood function, with and without bit errors. Based on the likelihood function, the log-likelihood function is formed, which we prove to be concave, therefore global optimality can be obtained. We also derive the Bayesian Cramer-Rao lower bound.

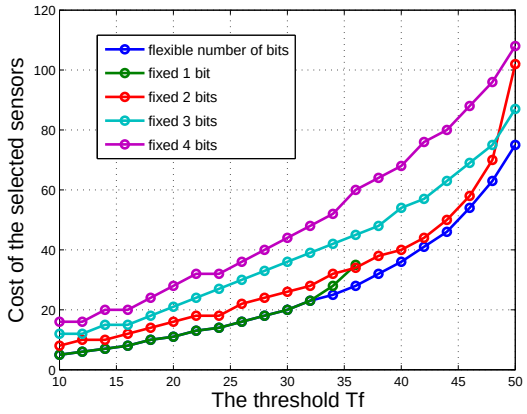


Figure 4.7: The cost versus the threshold. Bit error rates are all 0, variance of noises are all 0.5

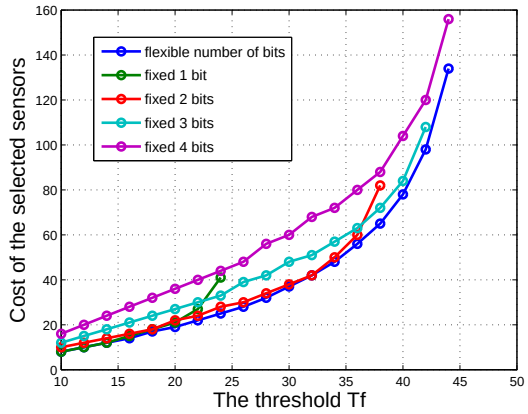


Figure 4.8: The cost versus the threshold. Bit error rates are all 0.1, variance of noises are all 0.5.

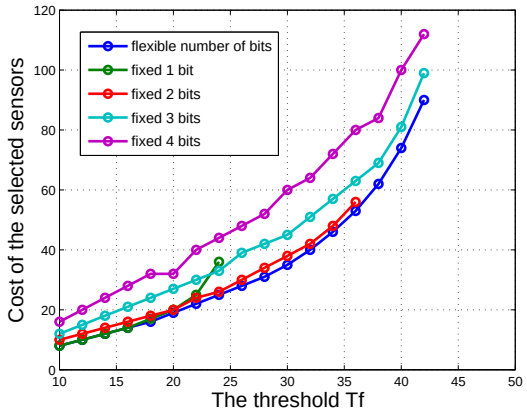


Figure 4.9: The cost versus the threshold. Bit error rates are all 0.1, variance of noises are all 0.5.

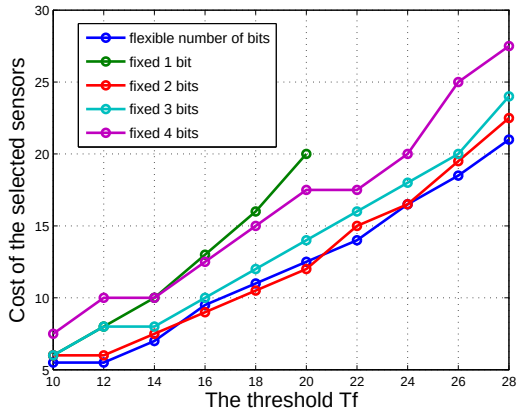


Figure 4.10: The cost versus the threshold. The bit error rates and the variance of noises are random, and the costs are not linear to the number of bits.

We propose the bit allocation algorithm, which is a generalized version of sensor selection, i.e., it decides not only which sensors should be activated, but further, the number of bits each sensors should transmit. Simulation results show that the bit allocation algorithm can further reduce the cost of a WSN compared with the sensor selection where analog data is adopted. From the simulations we can also see the effect of wireless channel, i.e., when all wireless channels have bad quality, more sensors or more bits are needed to obtain a certain level of estimation performance.

We adjust the sparsity enhance algorithm to improve the sparsity of the solution of our approach. Since the result of the bit allocation without the sparsity enhance operation is good enough, therefore we did not validate the efficiency of sparsity enhance algorithm by simulation, but in other WSN configuration, the solutions may not sparse enough, therefore

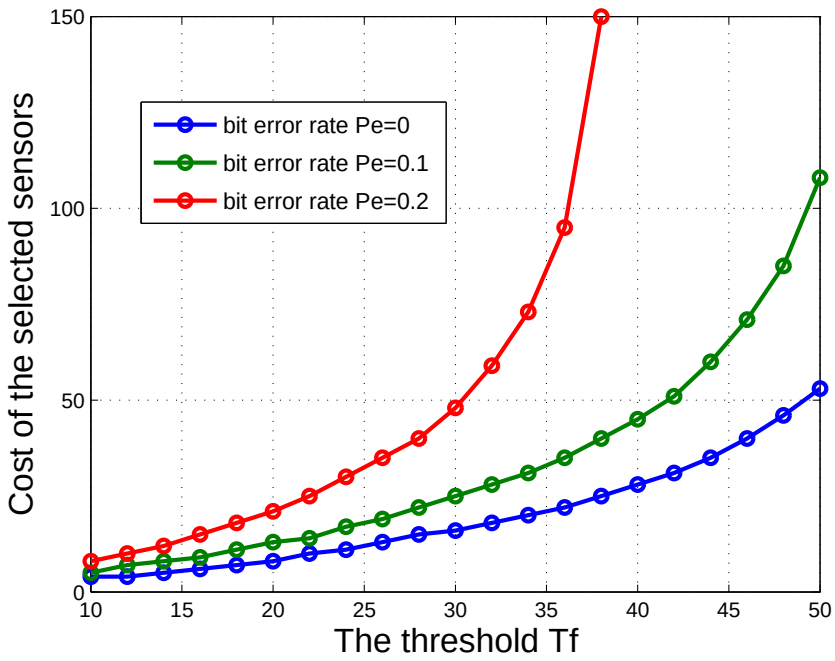


Figure 4.11: The cost versus the threshold, variances of noise are all 0.2

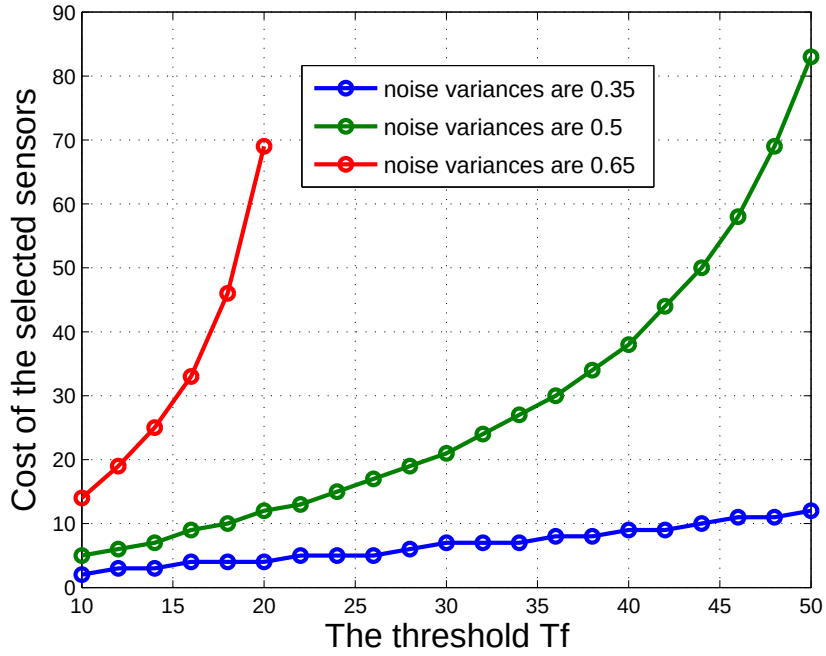


Figure 4.12: The cost versus the threshold, bit error rates are all 0.

the sparsity enhance algorithm will be of use.

We also define the aggregate error and based on it the Bayesian mean square error of the least square error estimate is derived. Since it is intractable to exploit the Bayesian mean square error for bit allocation, therefore we define it as our future work.

## 4.4 Appendix

### 4.4.1 Proof of Lemma 2

Rewrite $\hat{y}_n$ as,

$$\begin{aligned}\hat{y}_n =& 2L\hat{x}_n - L \\ \overset{(1)}{=}& 2L\sum_{i=1}^{K_n} b_{n,i}2^{-i} - L \\ =& 2L2^{-K_n}\sum_{i=1}^{K_n} b_{n,i}2^{K_n-i} - L \\ \overset{(2)}{=}& L2^{-K_n+1}B - L,\end{aligned} \tag{4.56}$$

In equality (1) we expand $\hat{x}_n$ by its binary form (see (4.5)), and in equality (2), $B := \sum_{i=1}^{K_n} b_{n,i}2^{K_n-i}$. Note that $B \in \{0, 1, ..., 2^{K_n} - 1\}$, therefore $\hat{y}_n \in \mathcal{S}_{K_n}$

Rewrite now the original measurement $y_n$ as,

$$\begin{aligned}y_n =& 2Lx_n - L \\ \overset{(1)}{=}& 2L\sum_{i=1}^{\infty} b_{n,i}2^{-i} - L \\ \overset{(2)}{=}& 2L\sum_{i=1}^{K_n} b_{n,i}2^{-i} + 2L\sum_{i=K_n+1}^{\infty} b_{n,i}2^{-i} - L \\ \overset{(3)}{=}& \hat{y}_n + 2L\sum_{i=K_n+1}^{\infty} b_{n,i}2^{-i}.\end{aligned} \tag{4.57}$$

where in equality (1), $x_n$ is expanded by its binary form (see (4.3)). In equality (2), we separate the summation of bits into two parts, one is from 1 to $K_n$ and the other is from $K_n + 1$ to infinity. Note that $\hat{y}_n = 2L\sum_{i=1}^{K_n} b_{n,i}2^{-i} - L$, thus we reach equality (3), and based on it we have the expression of the aggregated error

$$\varepsilon_n = \hat{y}_n - y_n = -2L\sum_{i=K_n+1}^{\infty} b_{n,i}2^{-i}, \tag{4.58}$$

which is bounded as,

$$0 \geq \varepsilon_n = -2L\sum_{i=K_n+1}^{\infty} b_{n,i}2^{-i} > -2L2^{-K_n} = -L2^{-K_n+1}, \tag{4.59}$$

which implies

$$\hat{y}_n \leq y_n < \hat{y}_n + L2^{-K_n+1}, \tag{4.60}$$

or $s_{K_n}(j) \leq y_n < s_{K_n}(j) + L2^{-K_n+1} = s_{K_n}(j) + s_{K_n}(j+1)$

### 4.4.2 Proof of Theorem 3

We start by considering the noiseless case

$$\begin{aligned} y^* =& \boldsymbol{h}_n^T \boldsymbol{\theta} \\ \hat{y}_n^* =& \varphi(y^*, K_n) \\ \varepsilon_n^* =& \hat{y}_n^* - y_n^*. \end{aligned} \tag{4.61}$$

In this case, $\varepsilon_n^*$ is exactly the quantization error because no measurement noise is involved. Suppose $y_n^* \in [s_{K_n}(n_0), s_{K_n}(n_0+1))$, with $n_0$ a particular integer, such that $\hat{y}_n^* = s_{K_n}(n_0)$. Equivalently, we can see $\hat{y}_n^*$ as $y_n^*$ adding a noise, and the value of the noise is $\varepsilon_n^*$ with probability 1,

$$\hat{y}_n^* = \boldsymbol{h}_n^T \boldsymbol{\theta} + \varepsilon^*. \tag{4.62}$$

Then, we add measurement noise to $y_n^*$, as $y_n = y_n^* + w_n$. We first consider the special case when the quantized value $\hat{y}_n = \varphi(y_n, K_n)$ equals the one of the noiseless one, i.e., $\hat{y}_n = \hat{y}_n^* = s_{K_n}(n_0)$. In fact, for this case

$$y_n \in \big[s_{K_n}(n_0), s_{K_n}(n_0+1)\big), \tag{4.63}$$

that means that the noise

$$w_n \in \big[\ \hat{y}_n^* - y_n^*, \hat{y}_n^* - y_n^* + L2^{-K_n+1}\big) \tag{4.64}$$

and the aggregated error in this case is $\varepsilon_n(0) = \varepsilon_n^* = \hat{y}_n^* - y_n^*$ with probability,

$$\begin{aligned} \Pr\big[\varepsilon_n = \varepsilon_n(0)\big] &= \Pr\big[w_n \in [\ \hat{y}_n^* - y_n^*, \hat{y}_n^* - y_n^* + L2^{-K_n+1}\ )\ \big] \\ &= F_n\left(\hat{y}_n^* - y_n^* + L2^{-K_n+1}\right) - F_n\left(\hat{y}_n^* - y_n^*\right). \end{aligned} \tag{4.65}$$

In the general case, for $\hat{y}_n = s_{K_n}(n_0 + t)$ with $t$ an integer, then from Lemma 2, the original measurement $y_n \in \big[s_{K_n}(n_0+t), s_{K_n}(n_0+t+1)\big)$, and the aggregated error becomes

$$\varepsilon_n = \varepsilon_n(t) = \hat{y}_n^* - y_n^* + tL2^{-K_n+1}, \tag{4.66}$$

with probability,

$$\begin{aligned} \eta_n(t) := \Pr\big[\varepsilon_n = \varepsilon_n(t)\big] = \\ \Pr\big[\ \hat{y}_n^* - y_n^* + tL2^{-K_n+1} \le w_n < \hat{y}_n^* - y_n^* + (t+1)L2^{-K_n+1}\ )\ \big] \\ = F_n\left(\hat{y}_n^* - y_n^* + (t+1)L2^{-K_n+1}\right) - F_n\left(\hat{y}_n^* - y_n^* + tL2^{-K_n+1}\right) \\ = F_n\left(\varepsilon_n(t) + L2^{-K_n+1}\right) - F_n\left(\varepsilon_n(t)\right). \end{aligned} \tag{4.67}$$

### 4.4.3 Proof of Theorem 5

We begin by proving the expression of $\mathcal{T}(s_{K_n}(p), s_{K_n}(q))$. Since we assume that the bits of $\hat{y}_n$ are independently affected by the channel effect, we only need to analyze the bits separately.

The probability for a bit $b_{n,i}$ to be correctly received, i.e, $b_{n,i} = c_{n,i}$, is $(1 - \mathrm{Pe}_n)$, or equivalently $(1 - \mathrm{Pe}_n)^{1-|b_{n,i}-c_{n,i}|}$, because $|b_{n,i} - c_{n,i}| = 0$ when being correctly received.

On the other hand, the probability of being incorrectly received is $\mathrm{Pe}_n$, or equivalently $\mathrm{Pe}_n^{|b_{n,i}-c_{n,i}|}$, due to the fact that $|b_{n,i} - c_{n,i}| = 1$. Note that whether being correctly received or not, the probabilities can both be expressed as

$$(1 - \mathrm{Pe}_n)^{1-|b_{n,i}-c_{n,i}|}\mathrm{Pe}_n^{|b_{n,i}-c_{n,i}|}. \tag{4.68}$$

Because of independent transmissions of each bit, the probability is then the product of the single probabilities, i.e.,

$$\mathcal{T}(s_{K_n}(p), s_{K_n}(q)) = \prod_{i=1}^{K_n}(1 - \mathrm{Pe}_n)^{1-|b_{n,i}-c_{n,i}|}\mathrm{Pe}_n^{|b_{n,i}-c_{n,i}|}, \tag{4.69}$$

which was what we needed to prove.

We move now on the aggregated error probability. When the aggregated error $\varepsilon_n^e = \varepsilon_n(t)$, it implies $\widetilde{y}_n = s_{K_n}(n_0 + t)$, where $n_0$ is the value with the quantized value of the noiseless measurement $\hat{y}_n^* = \varphi(y_n^*, K_n) = s_{K_n}(n_0)$ and $y_n^* = \boldsymbol{h}_n^T\boldsymbol{\theta}$. In fact, for a quantized value $s_{K_n}(n_0 + t)$ at the fusion center, it can be altered from all possible values of the quantized values from the sensor $\hat{y}_n = s_{K_n}(i), i = 0, 1, 2, ..., 2^{K_n} - 1$. When $\hat{y}_n = s_{K_n}(i)$, the aggregated error is $\varepsilon_n(i - n_0)$, which has a probability $\eta_n(i - n_0)$ provided in (4.67), therefore by the Total Probability rule we have the expression of $\eta_n^e(t)$ shown above.

### 4.4.4 Derivations of Bayesian Error Covariance Matrix and Bayesian Mean Square Error

The Bayesian mean square error of the least squares estimate is an important metric to evaluate the performance of the estimation. It equals the trace of the Bayesian error covariance matrix, which is defined as,

$$\boldsymbol{\mathcal{C}} := \mathbb{E}_{\boldsymbol{\theta},\hat{\boldsymbol{y}}}\left\{\left(\hat{\boldsymbol{\theta}}_{\mathrm{LS}} - \boldsymbol{\theta}\right)\left(\hat{\boldsymbol{\theta}}_{\mathrm{LS}} - \boldsymbol{\theta}\right)^T\right\} \tag{4.70}$$

In this part we derive the Bayesian error covariance from its definition. Since we can decompose the received signal $\hat{y}_n$ from sensor $n$ by $\hat{y}_n = \boldsymbol{h}^T\boldsymbol{\theta} + \varepsilon_n$, which comprises the certain part $\boldsymbol{h}^T\boldsymbol{\theta}$ and the uncertain (noisy) part $\varepsilon_n$. Therefore we can recast the received signal vector $\hat{\boldsymbol{y}} := [\hat{y}_1, \hat{y}_2, ..., \hat{y}_N]^T$ as,

$$\hat{\boldsymbol{y}} = \boldsymbol{H}^T\boldsymbol{\theta} + \boldsymbol{\varepsilon}, \tag{4.71}$$

where $\varepsilon := [\varepsilon_1, \varepsilon_2, ..., \varepsilon_N]^T$. Plugging this into the expression of $\hat{\boldsymbol{\theta}}_{\mathrm{LS}}$ in (4.21) yields

$$\hat{\boldsymbol{\theta}}_{\mathrm{LS}} = \left(\boldsymbol{H}\boldsymbol{H}^T\right)^{-1}\boldsymbol{H}\hat{\boldsymbol{y}} = \boldsymbol{\theta} + \left(\boldsymbol{H}\boldsymbol{H}^T\right)^{-1}\boldsymbol{H}\boldsymbol{\varepsilon}. \tag{4.72}$$

Expand (4.70) and substitute $\hat{\boldsymbol{\theta}}_{\mathrm{LS}}$ with (4.72). Then, we have

$$\begin{aligned}\boldsymbol{\mathcal{C}} :=& \mathbb{E}_{\boldsymbol{\theta},\hat{\boldsymbol{y}}}\left\{\left(\hat{\boldsymbol{\theta}}_{\mathrm{LS}}-\boldsymbol{\theta}\right)\left(\hat{\boldsymbol{\theta}}_{\mathrm{LS}}-\boldsymbol{\theta}\right)^{T}\right\}\\ =& \mathbb{E}_{\boldsymbol{\theta},\boldsymbol{\varepsilon}}\left\{\left[\left(\boldsymbol{H}\boldsymbol{H}^{T}\right)^{-1}\boldsymbol{H}\boldsymbol{\varepsilon}\right]\left[\left(\boldsymbol{H}\boldsymbol{H}^{T}\right)^{-1}\boldsymbol{H}\boldsymbol{\varepsilon}\right]^{T}\right\}\\ =& \left[\left(\boldsymbol{H}\boldsymbol{H}^{T}\right)^{-1}\boldsymbol{H}\right]\mathbb{E}_{\boldsymbol{\theta},\boldsymbol{\varepsilon}}\left\{\boldsymbol{\varepsilon}\boldsymbol{\varepsilon}^{T}\right\}\left[\left(\boldsymbol{H}\boldsymbol{H}^{T}\right)^{-1}\boldsymbol{H}\right]^{T}\\ =& \left[\left(\boldsymbol{H}\boldsymbol{H}^{T}\right)^{-1}\boldsymbol{H}\right]\boldsymbol{\mathcal{C}}_{\varepsilon}\left[\left(\boldsymbol{H}\boldsymbol{H}^{T}\right)^{-1}\boldsymbol{H}\right]^{T},\end{aligned} \tag{4.73}$$

where from the second equation the expectation is taking over $\boldsymbol{\varepsilon}$ instead of $\hat{\boldsymbol{y}}$, and $\boldsymbol{\mathcal{C}}_{\varepsilon} := \mathbb{E}_{\boldsymbol{\theta},\boldsymbol{\varepsilon}}\left\{\boldsymbol{\varepsilon}\boldsymbol{\varepsilon}^{T}\right\}$. Take two times the pseudo-inverse of the expression of $\boldsymbol{\mathcal{C}}$ in (4.73) and apply the product property of pseudo inverse [1] , we have

$$\begin{aligned}\boldsymbol{\mathcal{C}} &= \left[\left(\boldsymbol{H}\boldsymbol{H}^{T}\right)^{-1}\boldsymbol{H}\right]\boldsymbol{\mathcal{C}}_{\varepsilon}\left[\left(\boldsymbol{H}\boldsymbol{H}^{T}\right)^{-1}\boldsymbol{H}\right]^{T}\\ &= \left\{\left\{\left[\left(\boldsymbol{H}\boldsymbol{H}^{T}\right)^{-1}\boldsymbol{H}\right]\boldsymbol{\mathcal{C}}_{\varepsilon}\left[\left(\boldsymbol{H}\boldsymbol{H}^{T}\right)^{-1}\boldsymbol{H}\right]^{T}\right\}^{\dagger}\right\}^{\dagger}\\ &= \left\{\left[\left[\left(\boldsymbol{H}\boldsymbol{H}^{T}\right)^{-1}\boldsymbol{H}\right]^{T}\right]^{\dagger}\boldsymbol{\mathcal{C}}_{\varepsilon}^{\dagger}\left[\left(\boldsymbol{H}\boldsymbol{H}^{T}\right)^{-1}\boldsymbol{H}\right]^{\dagger}\right\}^{\dagger}\\ &\overset{(1)}{=} \left(\boldsymbol{H}\boldsymbol{\mathcal{C}}_{\varepsilon}^{\dagger}\boldsymbol{H}^{T}\right)^{\dagger}\\ &\overset{(2)}{=} \left(\boldsymbol{H}\boldsymbol{\mathcal{C}}_{\varepsilon}^{-1}\boldsymbol{H}^{T}\right)^{-1}.\end{aligned} \tag{4.74}$$

In equality (1), we use the fact that the pseudo-inverse of $\left[\left(\boldsymbol{H}\boldsymbol{H}^{T}\right)^{-1}\boldsymbol{H}\right]$ is $\boldsymbol{H}^{T}$. In equality (2), the pseudo-inverses are changes to regular inverse because the pseudo-inverse of an full rank square matrix is equivalent to the regular inverse. Notice $\mathcal{C}_{\varepsilon}$ is generally not a diagonal matrix because the $\boldsymbol{\varepsilon}$ is not a zero mean vector, although the elements of it is uncorrelated. The Bayesian mean square error is explicitly,

$$\mathrm{BMSE} := \mathbb{T}\mathrm{r}\left\{\left(\boldsymbol{H}\mathcal{C}_{\varepsilon}^{-1}\boldsymbol{H}^{T}\right)^{-1}\right\}. \tag{4.75}$$

# 5 Conclusion and Future Work

In this thesis, we consider the sensor selection problems (it extends to bit allocation in multi-bit quantization case) in two practical scenarios − one bit quantization and multi-bit quantization. We propose to involve the consideration of the effects of realistic wireless channel, in which the transmitted bits from sensors to the fusion center may be flipped into their opposite values, and we characterize them as bit error rate.

In one bit quantization, the likelihood function and the related Bayesian Cramer-Rao lower bound are derived, and we maximize the log-concave log-likelihood function to obtain the maximum a posteriori estimate. The sensor selection problem is formulated and convex relaxation is adopted to solve it. An equivalence theorem is also proposed that states the equivalence relation between the solution from the convex relaxation problem and the optimal one from exhaustive searching, under some assumptions. The numerical simulation results verify the correction of the established model by showing that when the bit error rates or variance of noise are higher, more sensors are needed to meet a certain level of performance. It is also shown that when the performance metric, the minimum eigenvalue of the Bayesian Fisher information is higher, the Bayesian mean squares error of the maximum a posteriori estimator is accordingly smaller.

In multi-bit quantization, the properties of an quantization scheme are investigated, and based on them, the likelihood functions, Bayesian Cramer-Rao lower bounds are derived and maximum a posterior estimators are provided, with and without the occurrence of bit errors. A novel approach for bit allocation is proposed. In the new approach, the number of bits for each is indicated by a selection vector, and the cost of the number of bits for the WSN is presented by the cost vector. Leveraging the selection vectors and the cost vector a optimization problem is formed and convex relaxation is applied to it. The simulation results show the validation of this new approach. To further emphasize the sparsity of the selection vector, the traditional sparsity enhanced approach is adapted to our case. By numerical examples, it can be seen that the new bit allocation approach can further reduce the cost compared with the existing solution of sensor selection where analog data model is assumed. In addition, we consider the case when no prior knowledge of $\boldsymbol{\theta}$ is available, in which case the least squares error estimator is investigated and based on it and the defined aggregated error the Bayesian error covariance matrix and the related Bayesian mean squares error are derived.

As for the future work, we suggest the following directions:

- We consider a WSN with one-hop communication from sensors to the fusion center. Multi-hop communication pattern is also prevalent in the operation of WSNs, in which the sensors remote from the fusion center will leverage their neighboring sensors as the relaying node to transmit data to the fusion center. In this scenario, how to select which sensors to activate is a challenging task, because we not only need to consider the performance constraint, but also the connectivity of the whole WSN [13, 43, 5].
- Investigate the configuration of the cost vector $\boldsymbol{C}$, such that the value of it not only

considers the number of bits, but it can also be adjusted according to the amount of remained energy in a sensor. By this way the remained energy will be balanced over each sensor in the long run of the WSN.

- We consider the measurement noise as being uncorrelated over sensors. When two sensors are near to each other, it is likely that the measurement noises are correlated. In this case the covariance noise will not be diagonal. We can try to develop the sensors selection and bit allocation approach with correlated noise. However, this is also a challenging task, because it needs the expression of joint cdf of noise, that is not available yet by now as we know.

- Investigate the new proposed model of sensor selection presented in Section 3.3.1.

- Investigate the multi-bit quantization scheme with the probabilistic extra bit that makes the least squares error estimator unbiased.

- Extend our work in a time-variant context, i.e., the unknown parameter $\boldsymbol{\theta}$ is changing over time. In this case, we can substitute the Bayesian Cramer-Rao lower bound with the Conditional posterior Cramer-Rao lower bound (Conditional-PCRLB) [45, 44]. The Conditional-PCRLB depends on the previous realized data and provides a tighter lower bound for the error covariance matrix.

- Develop a bit allocation algorithm based on the Bayesian error covariance matrix of the least squares error estimator. Although the least squares error estimator does not include the consideration of the prior knowledge of $\boldsymbol{\theta}$, but the related Bayesian error covariance matrix will in general be tighter to other error covariance matrix, compared with Bayesian Cramer-Rao lower bound. The challenge in it lies in the fact that $\boldsymbol{\mathcal{C}}_{\varepsilon}$ defined in 4.73 is not a diagonal matrix. In sensor selection problems, we only to decide which sensors to be activated, but in bit allocation the problem is generalized to deciding the number of bits for each sensors. In this sense, it is very difficult to handle the Bayesian error covariance matrix if $\boldsymbol{\mathcal{C}}_{\varepsilon}$ is not diagonal.

# Bibliography


[1] Moorepenrose pseudoinverse. https://en.wikipedia.org/wiki/MoorePenrose_pseudoinverse. Accessed: 2010-09-30.

[2] Tuncer Can Aysal and Kenneth E Barner. Constrained decentralized estimation over noisy channels for sensor networks. *Signal Processing, IEEE Transactions on*, 56(4):1398–1410, 2008.

[3] Stephen Boyd and Lieven Vandenberghe. *Convex optimization*. Cambridge university press, 2004.

[4] Emmanuel J Candes, Michael B Wakin, and Stephen P Boyd. Enhancing sparsity by reweighted ? 1 minimization. *Journal of Fourier analysis and applications*, 14(5-6):877–905, 2008.

[5] Nikolaos Chatzipanagiotis, Darinka Dentcheva, and Michael M Zavlanos. Approximate augmented lagrangians for distributed network optimization. In *Decision and Control (CDC), 2012 IEEE 51st Annual Conference on*, pages 5840–5845. IEEE, 2012.

[6] Sundeep Prabhakar Chepuri and Geert Leus. Sparsity-promoting sensor selection for non-linear measurement models. 2013.

[7] Sundeep Prabhakar Chepuri and Geert Leus. Sensor selection for estimation, filtering, and detection. In *Signal Processing and Communications (SPCOM), 2014 International Conference on*, pages 1–5. IEEE, 2014.

[8] Sundeep Prabhakar Chepuri and Geert Leus. Sparsity-promoting adaptive sensor selection for non-linear filtering. In *Acoustics, Speech and Signal Processing (ICASSP), 2014 IEEE International Conference on*, pages 5080–5084. IEEE, 2014.

[9] Sundeep Prabhakar Chepuri and Geert Leus. Sparsity-promoting sensor selection for non-linear measurement models. *Signal Processing, IEEE Transactions on*, 63(3):684–698, 2015.

[10] Thomas M Cover and Joy A Thomas. *Elements of information theory*. John Wiley & Sons, 2012.

[11] Haskell B Curry. The method of steepest descent for nonlinear minimization problems. *Quart. Appl. Math*, 2(3):250–261, 1944.

[12] Michael Elad. Map versus mmse estimation. In *Sparse and Redundant Representations*, pages 201–225. Springer, 2010.

[13] Jonathan Fink, Alejandro Ribeiro, and Vipin Kumar. Robust control of mobility and communications in autonomous robot teams. *Access, IEEE*, 1:290–309, 2013.

[14] Alfred Olivier Hero, David Castanon, Doug Cochran, and Keith Kastella. *Foundations and applications of sensor management*. Springer Science & Business Media, 2007.

[15] Gabriel M Hoffmann and Claire J Tomlin. Mobile sensor network control using mutual information methods and particle filters. *Automatic Control, IEEE Transactions on*, 55(1):32–47, 2010.

[16] Hadi Jamali-Rad, Andrea Simonetto, and Geert Leus. Sparsity-aware sensor selection: Centralized and distributed algorithms. *Signal Processing Letters, IEEE*, 21(2):217–220, 2014.

[17] Hadi Jamali-Rad, Andrea Simonetto, Xiaoli Ma, and Geert Leus. Distributed sparsity-aware sensor selection. 2015.

[18] Siddharth Joshi and Stephen Boyd. Sensor selection via convex optimization. *Signal Processing, IEEE Transactions on*, 57(2):451–462, 2009.

[19] Vassilis Kekatos, Georgios Giannakis, and Bruce Wollenberg. Optimal placement of phasor measurement units via convex relaxation. *Power Systems, IEEE Transactions on*, 27(3):1521–1530, 2012.

[20] Andreas Krause, Ajit Singh, and Carlos Guestrin. Near-optimal sensor placements in gaussian processes: Theory, efficient algorithms and empirical studies. *The Journal of Machine Learning Research*, 9:235–284, 2008.

[21] Qing Ling and Zhi Tian. Decentralized sparse signal recovery for compressive sleeping wireless sensor networks. *Signal Processing, IEEE Transactions on*, 58(7):3816–3827, 2010.

[22] Sijia Liu, Sundeep Prabhakar Chepuri, Makan Fardad, Engin Masazade, Geert Leus, and Pramod K Varshney. Sensor selection for estimation with correlated measurement noise. *arXiv preprint arXiv:1508.03690*, 2015.

[23] Sijia Liu, Engin Masazade, Makan Fardad, and Pramod K Varshney. Sensor selection with correlated measurements for target tracking in wireless sensor networks.

[24] Johan Löfberg. Yalmip: A toolbox for modeling and optimization in matlab. In *Computer Aided Control Systems Design, 2004 IEEE International Symposium on*, pages 284–289. IEEE, 2004.

[25] Engin Masazade, Ruixin Niu, and Pramod K Varshney. Dynamic bit allocation for object tracking in wireless sensor networks. *Signal Processing, IEEE Transactions on*, 60(10):5048–5063, 2012.

[26] Eric J Msechu and Georgios B Giannakis. Decentralized data selection for map estimation: A censoring and quantization approach. In *Information Fusion (FUSION), 2011 Proceedings of the 14th International Conference on*, pages 1–8. IEEE, 2011.

[27] Eric J Msechu and Georgios B Giannakis. Sensor-centric data reduction for estimation with wsns via censoring and quantization. *Signal Processing, IEEE Transactions on*, 60(1):400–414, 2012.

[28] George L Nemhauser, Laurence A Wolsey, and Marshall L Fisher. An analysis of approximations for maximizing submodular set functionsi. *Mathematical Programming*, 14(1):265–294, 1978.

[29] Omur Ozdemir, Ruixin Niu, and Pramod K Varshney. Dynamic bit allocation for target tracking in sensor networks with quantized measurements. In *Acoustics Speech and Signal Processing (ICASSP), 2010 IEEE International Conference on*, pages 2906–2909. IEEE, 2010.

[30] Juri Ranieri, Amina Chebira, and Martin Vetterli. Near-optimal sensor placement for linear inverse problems. *Signal Processing, IEEE Transactions on*, 62(5):1135–1146, 2014.

[31] Shilpa Rao. Sparse arrays: Vector sensors and design algorithms, 2015.

[32] Theodore S Rappaport et al. *Wireless communications: principles and practice*, volume 2. prentice hall PTR New Jersey, 1996.

[33] Alejandro Ribeiro and Georgios B Giannakis. Bandwidth-constrained distributed estimation for wireless sensor networks-part i: Gaussian case. *Signal Processing, IEEE Transactions on*, 54(3):1131–1143, 2006.

[34] Erik Rigtorp. Sensor selection with correlated noise, 2010.

[35] Venkat Roy, Sundeep Prabhakar Chepuri, and Geert Leus. Sparsity-enforcing sensor selection for doa estimation. In *Computational Advances in Multi-Sensor Adaptive Processing (CAMSAP), 2013 IEEE 5th International Workshop on*, pages 340–343. IEEE, 2013.

[36] Sailes K Sengijpta. Fundamentals of statistical signal processing: Estimation theory. *Technometrics*, 37(4):465–466, 1995.

[37] Manohar Shamaiah, Siddhartha Banerjee, and Haris Vikalo. Greedy sensor selection: Leveraging submodularity. In *Decision and Control (CDC), 2010 49th IEEE Conference on*, pages 2572–2577. IEEE, 2010.

[38] Xiaojing Shen and Pramod K Varshney. Sensor selection based on generalized information gain for target tracking in large sensor networks. *Signal Processing, IEEE Transactions on*, 62(2):363–375, 2014.

[39] Rajeev Shorey, A Ananda, Mun Choon Chan, and Wei Tsang Ooi. *Mobile, wireless, and sensor networks: technology, applications, and future directions*. John Wiley & Sons, 2006.

[40] Tao Wang, Geert Leus, and Li Huang. Ranging energy optimization for robust sensor positioning based on semidefinite programming. *Signal Processing, IEEE Transactions on*, 57(12):4777–4787, 2009.

[41] Jin-Jun Xiao and Zhi-Quan Luo. Decentralized estimation in an inhomogeneous sensing environment. *Information Theory, IEEE Transactions on*, 51(10):3564–3575, 2005.

[42] Jin-Jun Xiao, Alejandro Ribeiro, Zhi-Quan Luo, and Georgios B Giannakis. Distributed compression-estimation using wireless sensor networks. *Signal Processing Magazine, IEEE*, 23(4):27–41, 2006.

[43] Michael M Zavlanos, Alejandro Ribeiro, and George J Pappas. Network integrity in mobile robotic networks. *Automatic Control, IEEE Transactions on*, 58(1):3–18, 2013.

[44] Long Zuo. Conditional posterior cramer-rao lower bound and distributed target tracking in sensor networks. 2011.

[45] Long Zuo, Ruixin Niu, and Pramod K Varshney. Conditional posterior cramér–rao lower bounds for nonlinear sequential bayesian estimation. *Signal Processing, IEEE Transactions on*, 59(1):1–14, 2011.